2013-05-10

Determination of Low Molecular Weight Acids in Mist Chamber Extracts by Capillary Electrophoresis and Ion Chromatography

Zhou, Xueting

UNIVERSITY OF CALGARY

Determination of Low Molecular Weight Acids in Mist Chamber Extracts by Capillary Electrophoresis and Ion Chromatography

by

Xueting Zhou

A THESIS

SUBMITTED TO THE FACULTY OF GRADUATE STUDIES

IN PARTIAL FULFILMENT OF THE REQUIREMENTS FOR THE

DEGREE OF MASTER OF SCIENCE

DEPARTMENT OF CHEMISTRY

CALGARY, ALBERTA

MAY, 2013

Abstract

Acidic gases are important trace components of the troposphere because they contribute to particle formation and acid deposition. Here, a mist chamber (MIST) was used to collect acidic gases into aqueous solutions, which were analyzed by ion chromatography (IC) or capillary electrophoresis (CE). A CE method was developed, in which anions were separated in either a didodecyldimethylammonium or dimethyldioctadecylammonium bromide modified capillary at pH 5.86 and detected by indirect UV absorbance using naphthalenedisulfonate as probe with detection limits of 10 to 20 µM. The MIST collection efficiency (COE) was determined by chemical ionization mass spectrometry using acetate reagent ion. For HCOOH, the COE was < 80% when deionized water was used as trapping solution. The mass spectrometer was calibrated by MIST – IC and was superior with respect to response time (1 s versus 10 min), detection limit (< 100 ppt versus ~6 ppb), and near-absence of inlet memory effects.

Acknowledgements

Foremost, I would like to express my sincere gratitude to my supervisor Hans D. Osthoff. Thanks him for giving me a great chance to join the group and work in this exciting project. His patience and immerse knowledge has guided me through many difficulties in my research and study. His enthusiasm to research has always being a great inspiration and encouragement for me. He is a knowledgeable, dedicated and approachable supervisor. He is also a humorous and supportive friend to us all. I would never be able to complete this work without his guidance, engagement and support.

I warmly thank my thesis committee, Dr. Ann-Lise Norman, Dr. Kevin B. Thurbide and Dr. Jürgen Gailer for their insightful comments and valuable advice. I would like to especially thank Dr. Thurbide for his help with my course study which has provided good basis for my research work. His constant support and encouragement have helped me a lot.

I specially thank Dr. Raghav Yamdagni, who gave me for constant help for my course study and research. Dr. Yamdagni has spent large amount of time helping me with my study in mass spectrometry. And he also has been providing me sources to improve my research and giving me lots of wonderful comments on my thesis writing.

My special gratitude also goes to Gregg Symonds for his support and technical assistance to the ion chromatography analysis.

I thank my fellow labmates in Osthoff group for their support and unforgotten friendship. I would like to thank Dr.Levi H. Mielke, my labmate and very dear friend, who helped me with my writing and course study. His precious friendship has helped me through lots of difficulties and gave a lot of wonderful memory. I would like to thank Amanda Furgeson for her care and all the great moments we have been spend together. I would also like to thank Charles Odame-

Ankrah, Youssef Taha, Dr. Otman Abida for their support and help. They have provided such a fun filled environment during my stay in our group.

I thank all the stuffs in chemistry store electronics, machine and glass shop for their diligent work. Thanks Bonnie King and Janice Crawford for their help. I also thank Dr. Kal Mahadev, Dr. Vivian Mozol and Dr. Julie Lefebvre for their help and support for my teaching. I have really enjoyed working with them. And I have learned a lot from them.

I am also extremely thankful to my wonderful friends, Daniel, Brenda and Joshua Crowell, Bruce and Kerstin Littlejohn, Allen Zheng, Jimmy Cai, Jack Kan, Masashi Goto, Jansen Chua, Brian Sinclair, Emily Poffenroth. They and their family have given me great support, care and love. Thank you for your constant encouragement. Thank you all for the indelible moment we have spent together!

My very sincere thanks go to Keith & Pat Taylor for their parent-like support and care during my stay in Calgary. Their love and continuously support have given me so much courage and happiness.

Last but not least, I would like to thank my family: my beloved parents Wei Zhou and Mingxiu Dai, my dearest grandparents Guohua Zou and Farong Zeng for their great support and countless love!

Table of Contents

List of Tables

List of Figures and Illustrations

List of Abbreviations

Acronym/abbreviation	Definition
2, 5-PDC	2, 5–pyridinedicarboxylic acid
2-NAP	2–naphthoic acid
a.u.	Arbitrary units
BGE	Background electrolyte
BSTFA	*N, O*–bis(trimethylsilyl)-trifluoroacetamide
CDC	Collision dissociation chamber
CE	Capillary electrophoresis
CIMS	Chemical ionization mass spectrometry
CMC	Critical micelle concentration
COE	Collection efficiency
CZE	Capillary zone electrophoresis
DDAB	Didodecyldimethylammonium bromide
DEA	Diethanolamine
DMSO	Dimethylsulfoxide
DODAB	Dimethyldioctadecylammonium bromide
DR	Dynamic reserve
EK	Electrokinetic injection
EOF	Electroosmotic flow
EPA	Environmental Protection Agency
ESI	Electrospray ionization
FASS	Field-amplified sample stacking
FIA	Flow injection analysis
FID	Flame ionization detection
FTICR-MS	Fourier transform ion cyclotron resonance mass spectrometry
GC	Gas chromatography
GC-MS	Gas chromatography coupled to mass spectrometry
HD	Hydrodynamic injection
HPLC	High performance liquid chromatography
I.D.	Inner diameter
IC	Ion chromatography
IT-MS	Ion-trap mass spectrometry
ITP	Isotachophoresis
LIF	Laser-induced fluorescence
LMW	Low molecular weight
LOD	Detection limit
MA	Methacrolein
MFC	Mass flow controller
MIST	Mist chamber
MS	Mass spectrometry
MVK	Methyl vinyl ketone
n/a	not available/not applicable
NDS	2,5-naphthalenedisulfonic acid tetraahydrate

NI-PT-CIMS	Negative ion proton transfer chemical ionization mass spectrometry
O.D.	Outer diameter
ppb	Parts per billion by volume
ppt	Parts per trillion by volume
PT-CIMS	Proton transfer chemical ionization mass spectrometry
PTR-MS	Proton transfer reaction mass spectrometry
Q-MS	Quadrupole mass spectrometry
RSD	Relative standard deviation
slpm	Standard liter per minute
SOA	Secondary organic aerosol
SPE	Solid phase extraction
SRS	Self-regenerating suppressor
SVOC	Semivolatile organic compounds
TCD	Thermal conductivity detection
TOF-MS	Time-of-flight mass spectrometry
TR	Transfer ratio
TTAB	Trimethyl(tetradecyl)ammonium bromide
UTC	Coordinated universal time
UV-vis	Ultraviolet-visible
VOC	Volatile organic compounds
WAD	Wet-annular denuder

Chapter One: **INTRODUCTION**

1.1 Importance of acidic gases in the atmosphere

Acidic gases are important trace components in the troposphere, the lowest layer of the atmosphere (0 to ~12 km altitude). Inorganic acids such as nitric acid (HNO_3) or sulfuric acid (H_2SO_4) are the main components of acid rain [1]. Carboxylic acids, e.g., formic acid (HCOOH) or acetic acid (CH_3COOH), also can play a significant role in acid deposition [2]. The deposition of acids to the Earth is of concern because it can cause ecosystem acidification with adverse effects on soil, aquatic systems, plants, animals, and human health [3]. For example, in the Fort McMurray region in Alberta, ~300 tons of nitrogen oxides (NO_x = NO + NO_2) and ~300 tons of SO_2 were produced daily in 2008 [4]; the major fate of the emitted NO_x and SO_2 is oxidation to HNO_3 and H_2SO_4, respectively, leading to regionally elevated acid deposition rates [5]. In addition, acidic gases contribute to the formation and growth of aerosols (e.g., by acid-base reactions with NH_3), which can reduce visibility, harm human health, and alter the radiation balance of the Earth [6].

The formation of acidic gases constitutes an important sink for many atmospheric species, such as HO_x (OH + HO_2), NO_x and ozone (O_3). HNO_3, for example, is produced from the oxidation of NO_2 by OH radicals during the day [7] and relatively rapidly removed by dry or wet deposition. Hence, its formation can be viewed as a net sink of HO_x and NO_x. Since both HO_x and NO_x are needed to photochemically produce O_3 in the troposphere, their removal reduces the rate of O_3 formation and, ultimately, tropospheric O_3 concentrations [7].

Because of their importance to the environment and human health, it is essential to monitor acidic gases to assess their role in the atmosphere. However, the accurate measurement of atmospheric acids remains a challenge. In the troposphere, acids are usually present at only

the parts-per-billion (10^{-9}, ppb) to parts-per-trillion (10^{-12}, ppt) level (Table 1-1), which poses analytical challenges. In addition, one needs to differentiate between acids in the gas phase from those in the particle phase, as acids partition between the gas and particle phases. The partitioning of trace gases can (to first approximation) be described using Henry's law (Table 1-2). Furthermore, to reduce inlet memory effects (caused by slow adsorption and desorption rates of acids on the inner walls of the inlet tubing), inlets are usually heated. This in turn can result in erroneous measurements, because acids partition from the particle to the gas phase at elevated temperature [8-11].

The goal of this thesis was to develop a novel acidic gas measurement technique, mist chamber - capillary electrophoresis (MIST-CE), and to evaluate if this method is suitable (in terms of time resolution, selectivity, and sensitivity) for quantification of acidic gases, in particular the inorganic acids H_2SO_4 and HNO_3 and the carboxylic acids HCOOH and propionic acid (C_2H_5COOH), in ambient air.

Table 1-1 Typical abundances of selected LMW acids in the troposphere

Compound	Typical aerosol phase mixing ratios	Typical gas phase mixing ratios
HCOOH	8 – 160 ppt [12]	0.1 - 45 ppb [13]
CH_3COOH	6 – 180 ppt [12]	0.2 - 21 ppb [13]
C_2H_5COOH	n/a	0.02 - 0.66 ppb [13]
HNO_3	7 – 131 ppt [14]	0.01 - 5 ppb [15]
H_2SO_4	10 – 750 ppt [16]	~0.002 ppb [17]

Table 1-2 Selected physical properties of atmospheric acids at 298 K.

Compound	Solubility in water (mol/kg)[a]	Vapor pressure (mm Hg)	Henry`s law constant ($mol \cdot L^{-1} \cdot atm^{-1}$)	K_a
HCOOH	1.38×10^{-4} [18]	42.6 [13]	$(5.5\pm0.3)\times10^{3}$ [19]	(1.8×10^{-4}) [20, 21]
CH_3COOH	1.56×10^{-5} [18]	15.7 [13]	$(5.5\pm0.3)\times10^{3}$ [19]	(1.8×10^{-5}) [22]
C_2H_5COOH	1.31×10^{-5} [18]	3.7 [13]	$(5.7\pm0.3)\times10^{3}$ [19]	(1.3×10^{-5}) [23]
HNO_3	n/a	6.2 [24]	2.1×10^{5} [20]	(15.4) [20]
H_2SO_4	n/a	5×10^{-4} [25]	1.0×10^{11} [25]	(10^{3}) [26]

[a] solubility was calculated at equilibrium with partial pressure pHa=1×10^{-10} atm and pH=5.

1.1.1 Sulfuric acid

In the atmosphere, H_2SO_4 is primarily formed from the oxidation of SO_2, which is released during fossil fuel combustion, from volcanoes, or from oceanic phytoplankton (via release and oxidation of dimethyl sulfide) [17, 27, 28].

$$SO_2 + OH + M \longrightarrow HSO_3 + M \qquad \textbf{1-1}$$

$$HSO_3 + O_2 \longrightarrow SO_3 + HO_2 \qquad \textbf{1-2}$$

$$SO_3 + H_2O + M \longrightarrow H_2SO_4 \qquad \textbf{1-3}$$

In reaction 1-1, M is a so-called "third body", which carries off excess energy during the reaction. Because OH is predominantly a daytime species, a clear diurnal variation in H_2SO_4 concentration is usually observed [17]. In the marine boundary layer, H_2SO_4 can also be produced through the oxidation of dimethyl sulfide [29]. Recently, it has been observed that the

reaction between SO_2 and Criegee biradicals (a carbonyl oxide with two free radical sites produced during the ozonolysis of alkenes) can produce H_2SO_4 [30, 31]. This process can affect H_2SO_4 production rates in forested areas.

Because of its low vapor pressure, H_2SO_4 readily condenses onto surfaces and can form sulfate aerosol particles [32]. Its lifetime in the gas phase is therefore short (< 30 min; Table 1-3). It has also been observed that the H_2SO_4 concentration controls the rate of ultrafine particles (diameter < 100 nm) growing to cloud condensation nuclei (diameter > 100 nm) [33-35].

Table 1-3 Typical lifetimes of LMW acids in the troposphere

Compound	**Lifetime**
HCOOH	3-4 days [36]
C_2H_5COOH	gas phase: 7-10 days [37]
HNO_3	gas phase: half a day; particle phase: around a week [7]
H_2SO_4	gas phase: < 30 min [38]; particle phase: a few days [39]

1.1.2 Nitric acid

During the daytime, HNO_3 is produced from the reaction of NO_2 with OH [15, 40]:

$$OH + NO_2 + M \longrightarrow HNO_3 + M \qquad \textbf{1-4}$$

At night, HNO_3 is produced mainly via heterogeneous hydrolysis of N_2O_5 [41]:

$$N_2O_5 + H_2O \rightarrow 2HNO_3 \qquad \textbf{1-5}$$

HNO_3 can also be produced from NO_3 through reactions with hydrocarbons or reduced sulfur compounds (e.g., CH_3SCH_3, H_2S, CH_3SH) [42].

Gas-phase HNO_3 only slowly degrades photochemically with a lifetime of several weeks (Table 1-3) [15]. However, HNO_3 is highly soluble and rapidly taken up by cloud or rain droplets [43]. The primary sink of HNO_3 in the troposphere is therefore dry or wet deposition [44]. Deposition of HNO_3 to the ground introduces nitrogen back to the terrestrial and aquatic ecosystems [45], such that it plays a significant role in the global nitrogen cycle [45]. A number of experiments have shown that HNO_3 can increase the formation of secondary organic aerosol (SOA) through acid-catalyzed heterogeneous reactions [46-48].

1.1.3 Carboxylic acids

Carboxylic acids originate from both primary and secondary sources (either anthropogenic or biogenic) [49]. Primary emissions can be attributed to vehicular exhaust, biomass combustion, and especially biogenic emissions [50, 51][36]. However, carboxylic acids also originate from secondary sources, i.e., the oxidation of biogenic compounds, for example oxidation of alkenes by O_3 [52, 53] and reaction between formaldehyde and HO_2 [54-56]:

a. Ozonolysis of alkenes [52]:

$$C_2H_4 + O_3 \rightarrow HCHO + HC \bullet HOO \bullet \qquad \textbf{1-6}$$

$$HC \bullet HOO \bullet \longrightarrow 0.04HCOOH + 0.3(H_2O + CO) + other \qquad \textbf{1-7}$$

b. Isoprene oxidation [54] :

$$Isoprene + OH + NO + 2O_2 \longrightarrow MVK + MA + HCHO + NO_2 + HO_2 \qquad \textbf{1-8}$$

Methyl vinyl ketone (MVK) and methacrolein (MA) can also be sources of acids [54].

c. Reaction between formaldehyde and HO_2 [54] :

$$CH_2O + 2HO_2 \longrightarrow HCOOH + H_2O + O_2 \qquad \textbf{1-9}$$

Archibald et al. [50] have recently proposed a novel mechanism of carboxylic acid formation by the oxidation of ethenol, which accounted for 50% of formic acid production in an urban area. The possible sources of ethenol are combustion [50] or photo-tautomerization of a keto-enol [57].

Formic acid is the most important carboxylic acid in the atmosphere [2, 58]. Typically, over 80% of total HCOOH is present in the gas phase [13] at mixing ratios of a few ppb (Table 1-1). It is observed at lower concentrations in remote areas and in higher concentrations in urban areas [59, 60]. For example, along the California south coast, the mixing ratio of HCOOH was observed to be in the range of 1 to 13 ppb [61]. In western Canada and Alaska, HCOOH was measured at a maximum mixing ratio of 0.843 ppb in summer [62]. Formic acid can be removed by reaction with OH, for example [63]:

$$OH + HCOOH \xrightarrow{O_2} H_2O + CO_2 + HO_2 \qquad \textbf{1-10}$$

In cloud-free regions, the lifetime of HCOOH with respect to reaction with OH is several weeks [64]. However, the reaction of HCOOH with OH is 3 orders of magnitude faster in the aqueous phase than in the gas phase [64]. *Stavrakou et al.* [36] estimated that OH oxidation accounts for 27% of the global removal of HCOOH.

The absorption spectra of simple monocarboxylic acids have maxima in the 180–220 nm range and do not overlap with the actinic spectrum [52]. Consequently, photolysis of monocarboxylic acids in the gas phase is negligible. Because HCOOH and C_2H_5COOH are long lived with respect to gas-phase reactions, they are mainly removed by wet and dry deposition [2, 65]. The overall lifetime of carboxylic acids ranges from several hours to a few days, which is determined by the frequency of precipitation [56]. The scavenging of carboxylic acids by cloud droplets can contribute to the acidity of rain. A number of studies have shown that HCOOH

accounts for 60 – 80% of rain acidity in the Amazonia area, and up to 30 – 50% over the US during summer time [36]. Unlike H_2SO_4 or HNO_3, the negative environmental impact of rain acidified by HCOOH can be lowered by its rapid degradation by microbes in the soil [66]. However, the presence of formic acid in aerosol and cloud droplets may affect pH-dependent heterogeneous reactions [20, 56, 67].

In general, diurnal and seasonal patterns can be observed for carboxylic acids. The concentrations of the gas and particle phases typically reach their lowest levels prior to sunrise, gradually increase to maxima after solar maximum, and decrease by late evening [47, 68, 69]. The diurnal pattern is consistent with photochemical reactions as the main source of acids [70, 71]. There are also seasonal patterns: For example, carboxylic acids are more abundant during the growing season (May - August), which can be attributed to biogenic emissions [69].

1.2 Sampling and analysis: offline techniques

In offline techniques, air samples are collected in the field and analyzed usually in the laboratory by wet-chemical techniques. Common sample methods include collection by adsorption on solid matrices (i.e., filters or sorbents) or by extraction into liquids (i.e., bubblers or mist chambers) [72]. After sample collection, most samples are recovered by solvent or thermal desorption [73] and analyzed. Because a variety of analytical methods can be used, offline techniques can provide detailed structure and concentration information for a wide range of molecules.

1.2.1 Offline sampling techniques

1.2.1.1 Whole air sampling

Whole air sampling is a simple way to collect gas samples in a container. Commonly used containers are steel canisters, sample bags (made from Teflon or aluminized Tedlar), syringes, or glass bulbs [74]. The air sample is drawn into the container by pressure difference. Whole air sampling is commonly used to collect volatile organic compounds (VOCs), non-reactive gases, and reduced sulfur compounds, but is not well suited for acid sampling. One of the challenges is to remove water vapour, which may cause loss of acids in water droplets [75].

1.2.1.2 Sorbent sampling

Here, a sorbent is used to trap compounds, usually by drawing the air sample through a tube which is filled with one of a variety of solid adsorbent materials. Sorbent sampling is usually used to collect non-polar and nonreactive compounds. Sorbent materials include silica gel, activated charcoal, porous polymers, Tenax TA, and multi-bed tubes [76]. After sampling, the trapped compounds are recovered by solvent extraction or thermal desorption.

For acidic gases, high-purity silica gel is commonly used for its high surface activity [76]. Typically, the sample is recovered by solvent (water) extraction and analyzed by IC [77]. To remove particles from the gas sample, a pre-filter is usually added onto the sorbent [77]. However, target compounds may be lost on the filter, causing negative interference.

The sorbent material can be saturated at high sample concentrations and be degraded when exposed to oxidants (e.g., O_3, NO_2, NO or SO_2), which may cause difficulties in the interpretation of results. *Clausen et al*. [78] reported that Tenax TA sorbent could degrade and produce semivolatile organic compounds when exposed to O_3. In addition, compounds adsorbed

on the sorbent may also undergo transformation by reacting with O_3 or nitrogen oxides [79]. Thus, careful determination of sorbent properties (e.g., sorbent lifetime, capacity) is critical to successful sorbent sampling.

1.2.1.3 Filter and Denuder Sampling

Filters have been widely used to sample atmospheric acids. Dual filter sampling was introduced to separate particles from gas phase samples. For example, *Talbot et al.* [10] employed a Teflon-Nylon sequential filter to sample HNO_3 in the atmosphere followed by solution extraction. Particles were retained on the Teflon prefilter, and HNO_3 vapour was trapped on the Nylon filter. Similar sampling methods have also been utilized by other researchers. *Okita et al.* [80] employed a Teflon prefilter and a NaCl impregnated filter to collect particulate and gaseous HNO_3. The previously mentioned filtration technique is easy to operate, and it can selectively collect particles and gaseous acids. However, there are potential artefacts from the loss of gas phase acids on the prefilter. Evaporation of compounds from particles on the prefilter may also cause interference to gas phase determination [81].

To compensate for the bias introduced by filtration method, denuder techniques are used for air sampling in the presence of aerosols. Typically, the denuder tube is coated with a suitable adsorbent to retain the gas compounds of interest. When the sample air is driven through the tube, target gas phase compounds are adsorbed on the surface coating, while particles pass through. A filter downstream from the tube will collect the remaining particles. Based on differences in gas-phase diffusion coefficients, gas and particle phase species are discriminated and collected separately [82, 83]. This property makes denuder sampling a suitable technique to study the distribution of semivolatile organic compounds (SVOC) in different phases [84].

Various denuders have been developed and utilized for acid analysis, such as annular denuders [59] and parallel plate diffusion denuders [85, 86]. *Trebs et al*. utilized a wet-annular denuder (WAD) combined with a Steam-Jet Aerosol Collector (SJAC) followed by IC and ammonium flow injection analysis (FIA) to measure HNO_3 and particle-phase nitrate continuously [87]. *Takeuchi et al*. applied a hydrophilic membrane-based parallel-plate denuder to sample acidic gases (HCOOH, CH_3COOH, HNO_2, HNO_3, HCl and SO_2). This efficient sampling method enabled the near-real-time detection of trace acids in IC [88]. But defusing denuders also have some potential artefacts: (1) Highly volatile compounds cannot be well retained on the denuders and may lead to underestimation of sample concentration [89]. (2) For the gas phase measurement, a positive artefact may be caused by the loss of fine particles to the surface of the denuder tube, or the adsorption of compounds evaporating from particles during passage through the tube. (3) For the particle phase measurement, a breakthrough of volatile compounds to the downstream sorbent can cause higher concentrations in the particle phase [84]. Comparing 18 instruments for the measurements of HNO_3, *Hering et al.* [90] found that filtration techniques reported the highest concentrations of HNO_3, and denuders reported lower concentrations.

1.2.1.4 Solution Sampling

Gases can also be sampled by extracting them into solutions. By choosing trapping solutions, compounds can be selectively collected. In solution sampling, there are two types of gas-liquid absorption: physical absorption and chemical absorption. Physical absorption is the process by which the gas compounds dissolve in trapping solution, which is usually reversible. The extraction efficiency of physical absorption is dependent on the vapour pressure of the gas and its solubility in the liquid solution (which can be described using Henry`s law, Table 1-2).

Chemical absorption involves the reaction between gaseous compounds and the liquid compounds. Its extraction efficiency is affected by not only Henry`s law constant of reactants and products, but also the reactivity.

In solution sampling, the sample extraction efficiency is a function of (1) the physical and chemical properties of sample compounds and solvent, and (2) the characteristics of the sampling device. A number of devices have been designed for gas sampling, such as fritted bubblers [91], impingers [92], glass tubes [93] and mist chambers [1, 10, 94]. Among them, the mist chamber is commonly used for its high speed (up to 30 L/min) and extraction efficiency (up to 90% for most species [95, 96]).

Compared to sorbent and filter sampling, solution sampling has the advantage of large sample capacity. Thus, compound breakthrough (i.e., saturation) is less likely to occur. However, in long sampling times, solution sampling may have the problem of evaporation. This problem can be countered by using a less volatile solution or a hydrophobic filter. Another problem with solution sampling is that aerosols are only partially collected [97]. Usually, a prefilter is added to prevent aerosols from dissolving in the trapping solution. However, compounds evaporating from aerosols collected on the filter may result in positive interferences.

Solution sampling is most often used for compounds from stationary sources and conditions where other techniques are not as suitable, such as high humidity or temperature.

1.2.2 Analytical methods used with offline sampling

1.2.2.1 Chromatography

The extraction of air samples into solution is usually followed by ion chromatography (IC) [10, 95, 98, 99] or gas chromatography (GC) coupled with solid phase extraction. In

principle, high-performance liquid chromatography (HPLC) can be used to analyze ambient air extracts, but rarely is in practice. In recent years, capillary electrophoresis (CE) [100-105] is also frequently utilized in environmental analysis. It is fast, economic and sensitive. CE has to date mainly been applied to analyze extracts from filter samples [105, 106].

Gas chromatography is one of the most frequently used techniques for the analysis of organic compounds (e.g., hydrocarbons, halogenated compounds) in environmental samples [107, 108]. GC is a reliable separation method, in which sample components are separated effectively based on their vapour pressure. GC detection is mostly coupled with flame ionization detection (FID) [109], thermal conductivity detection (TCD) or mass spectrometry (MS) [110]. FID and TCD are universal techniques and can be used for most target compounds. However, their detection limits are several mg/L, which is not low enough for air analysis [111, 112]. Comparing to FID and TCD, MS is well suited for trace level determination (< µg/L detection limit) [113]. In MS, the target compounds are (often unambiguously) identified by their characteristic ions (if a soft ionization method is used) or ion fragments. For example, *Fraser et al.* [114] utilized GC-MS to quantify 47 carboxylic acids in the atmosphere over the Los Angeles area. In general, GC-MS is well-suited to identify complex components and determine their trace concentrations in air samples [115].

However, GC also has some limitations. In GC, separation times are typically on the order of 10 to 60 min [116], which is time-consuming, and in situ analyses using GC can be logistically challenging. Furthermore, compounds with strong polarity may interact with the GC column, especially at low concentrations (< 1 mmol L^{-1}) [117, 118]. Thus, LMW acids are not commonly analyzed by GC. To overcome the problem of high polarity, pre-column derivatization is often used to decrease the volatility [110, 119, 120]. The most common used

derivatization methods for acids are esterification by BF_3/alcohol and silylation by *N,O*-bis(trimethylsilyl)-trifluoroacetamide (BSTFA) [113]. The use of derivatization technique extends the application of GC, but limits its automation.

IC is a powerful analytical technique for the separation and determination of either anions or cations in the liquid phase. Hence, acids can be analyzed directly (as their conjugate anions) in IC without complex pre-treatment. This makes it possible to monitor acidic gases on-line. For example, *Lee et al*. [121] combined a parallel plate diffusion scrubber with IC and succeeded to monitor the diurnal changes of HCOOH, CH_3COOH and C_2H_5COOH in ambient air. For the detection of cations, atomic absorption or inductively coupled atomic emission MS are preferred over the usually deployed conductivity detector [122]. However, co-elution may hamper the analysis of some ions, such as between sodium and ammonium [122], acetate and glycolate [123], or sulfate and oxalate [124].

Typical detection limits of IC are in the nM range [125], which corresponds to a gas-phase mixing ratio of ~1 ppt for a 125 L air sampling volume totally extracted into 5 mL water. For the determination of HCOOH, the IC method can be used directly. However, to determine the concentration of C_2H_5COOH and HNO_3, which are present at lower levels, pre-concentration is required prior to IC analysis to improve the detection limit to sub-ppt level [126]. Commonly, an ion exchange pre-column concentrator (e.g., Dionex TAC-LP1 [127, 128], TAC-2 [129] or TCC-LP1 [128]) is used to enrich sample concentrations. Compared to pre-column concentration, post-column concentration is less commonly used. *Takeuchi et al*. [130] have developed a membrane tube to concentrate non-volatile compounds by removing solvent prior to the detector. The sensitivity of perchlorate in IC has been improved to as low as 0.35 ng m^{-3} corresponding to 0.095 ppt.

1.2.2.2 Capillary Electrophoresis

Capillary electrophoresis, also known as capillary zone electrophoresis (CZE), is a relatively modern analytical method. It enjoys tremendous advantages such as (relatively) short analysis times (<15 min) [103, 131], low sample consumption (μL), low waste generation, high separation efficiency (10^5 - 10^6 plates per meter), and high resolution [123, 132, 133]. For example, *Noblitt et al*. [106] reported quantification of 8 inorganic and 38 organic anions (extracted from aerosol samples) within 8 min.

In CE, ions are separated in a fused-silica capillary with a typical internal diameter (I.D.) of 50 or 75 μm on the basis of their relative velocities in electric field. The migration of ions is driven by two processes: electrophoretic flow, which results from the charge of the sample ions, and electroosmotic flow (EOF), which arises from the charge of the capillary inner wall. In an applied electric field, anions are attracted to the anode, and cations are attracted to the cathode. The inner wall of fused silica capillary is covered with silanol groups (–SiOH), which deprotonate over a pH range of between 2 and 9 [134]. Cations are paired to the $–SiO^-$ groups and form an electrical double layer, whose thickness is inversely proportional to ionic strength. When a high voltage is applied to the capillary, the inner cationic layer is stationary and the outer layer of cations moves along the capillary wall to the cathode and drags the bulk solution. This flow of bulk solution is called EOF [135, 136]. Usually, the EOF rate is so strong that all analyte molecules will move to the cathode [137]. In this way, the electrophoretic flow velocity (v_{ep}) of cations has the same direction of EOF velocity (v_{eo}). The apparent velocity (v_{app}**)** of cations to cathode is expressed as:

$$V_{app} = V_{eo} + V_{ep} \qquad \textbf{1-11}$$

For anions, the direction of v_{ep} is opposite to that of v_{eo}. Thus, the apparent velocity of anions is:

$$V_{app} = V_{eo} - V_{ep} \quad \textbf{1-12}$$

The magnitudes and signs of both v_{ep} and v_{eo} can be altered simply by changing the composition of the running buffer. Thus CE has the ability to separate anions, cations and neutral molecules, sometimes even at the same time [138].

For the detection of sample ions in CE, various detection methods have been applied, including ultraviolet-visible (UV-Vis) spectroscopy [139], fluorescence microscopy [140], conductivity [137], electrochemical detection, MS [133, 141-144], and laser-induced fluorescence (LIF) [100]. MS is the most powerful detection method for CE. CE can be directly connected to MS through electrospray ionization (ESI). In ESI, the liquid sample is sprayed out of a needle at high potential, forming charged droplets. Ion molecules are formed by extensive solvent evaporation. ESI is a soft ionization method, and particularly useful to produce limited fragment ions of macromolecules [142]. Mass analyzers that have been used include quadrupole (Q-MS) [141, 143], ion-trap (IT-MS) [133, 144], time-of-flight (TOF-MS) [133], Fourier transform ion cyclotron resonance (FT-ICRMS) [143]. Q-MS is most frequently used for its good reproducibility [141, 143].

UV detection is more commonly used in commercial CE instrument for its low cost and simplicity. For small ions without strong UV absorption bands (such as the conjugate anions of LMW acids found in the troposphere), indirect UV detection is used [145]. In this mode, a strongly UV-absorbing probe ion is added into the background electrolyte, providing a strong background absorbance. Analyte ions with low absorbance displace the probe, resulting in a decrease of absorbance. Once the analyte ions pass though the detection region, the signal returns to the original intensity.

CE also has some limitations such as poor concentration sensitivity [139, 145, 146]. The small I.D. of the capillary limits the sample injection volume and light path length in UV detection, which results in poor sample sensitivity (10^{-5} to 10^{-6} M) [147]. CE also has relatively poor reproducibility. Molecule migration time may drift with the change of background electrolyte property or capillary inner wall conditions [148-152]. During CE separation, the pH of electrolyte can be changed due to electrode reactions [153]. Instability of running buffer pH can alter the ionization of analytes and the charge of the capillary inner wall, affecting the EOF and electrophoretic mobilities of the sample ions. In addition, interactions between analyte and the inner walls of the capillary can also affect the CE performance. Once ions are binding to the surface, it can cause analyte loss and EOF change, resulting in variable migration time and peak area [154]. In addition, the use of high voltage can increase the temperature of background electrolyte, called Joule heating effects. The change of temperature will result in variations of electrolyte viscosity, which leads to the changes of ion mobility and peak shapes [155]. All those factors generally limit the reproducibility of CE.

1.3 Sampling and analysis: online techniques

On-line techniques such as proton transfer reaction-mass spectrometry (PTR-MS) [156] and proton transfer chemical ionization mass spectrometry (PT-CIMS) [157-159] are relatively novel techniques that can provide real-time analysis of air samples. These on-line detection methods have advantages of fast response, high sensitivity, low detection limit and do not require complex sample preparation, which is a considerable advantage as it is less labor-intensive and generally more accurate. For example, *Veres et al*. reported that the sensitivity of negative ion proton transfer chemical ionization mass spectrometry (NI-PT-CIMS) to formic acid could reach

21 ± 4 counts per second per ppt with a detection limit of 80-90 ppt at 1-second time resolution [157]. However, these instruments are expensive ($150,000–$500,000) and require an experienced operator. Another drawback of PTR-MS and NI-PT-CIMS are the need for reliable calibration methods, which is a challenge for sticky compounds such as HNO_3 [160].

1.4 Project Overview

To address the need to improve the monitoring of ambient acids, my research focused on developing a method to combine a high capacity sampling method — mist chamber — with a highly efficient separation method — capillary electrophoresis (MIST-CE). The objective of this project was to investigate if CE can be used as an alternative (or complement) to the normally used IC analysis. In the context of atmospheric science, CE has to date only been applied to the analysis of acids on filter extracts (e.g., humic substances [161], C_2-C_5 dicarboxylic acids [162]) or of water-soluble components of aerosol samples [106], but not to the analysis of mist chamber samples.

Chapter 2 describes the specific techniques and apparatuses used in my research, such as CE, IC and CIMS. Chapter 3 discusses the development of new CE analysis method, in which an EOF modifier was used to decrease analysis time and analyte loss on the inner walls of the CE capillary, and indirect UV detection was used to quantify conjugate anions of LMW acids. In Chapter 4, the collection efficiency of the mist chamber was determined by CIMS. In Chapter 5, CIMS response factors to acidic gases were determined using MIST-IC. Chapter 6 contains the thesis conclusions.

Chapter Two: **METHODS**

2.1 Capillary electrophoresis

2.1.1 Setup

In my research, CE analysis was carried out in a custom-built CE instrument (Figure 2-1). It was equipped with a fused silica capillary (Polymicro Technologies), a high voltage power supply (Spellman, CZE1000R), a Deuterium UV-Vis light source (Ocean Optics Mikropack, D2000), a miniature fiber optic spectrometer, which has a wavelength range of 195–520 nm and resolution of 0.35 nm (Ocean Optics, Inc., USB2000+), two optical fibers (Ocean Optics, Inc.) and a PEEK interface cross (Ocean Optics, Inc.).

Ocean Optics's SpectraSuite spectroscopy software was used to control the spectrometer and collect data. Once sample was injected into CE, the data acquisition was initiated. An intensity spectrum would display in real time. Results of the collecting data can be controlled by integration time (time period of detection; typically 30 ms), scans to average (average number of spectral acquisitions; typically 5) and boxcar width (average of adjacent data points; typically 6). After data collection, Origin Lab's ORIGIN® and Wavemetric's IGOR® software were used for data analysis and calculations. Migration time, peak height, peak areas were the primary data determined.

Two sizes of fused silica capillaries were used: (1) 73 µm I.D. and 364 µm outer diameter (O.D.) (Polymicro Technologies, part number: 2000019), or (2) 30 µm I.D. and 360 µm O.D. (Polymicro Technologies, part number: 1068150013). A ~1 cm detection window was obtained by burning off the polyimide coating. The interface cross effectively limits the detection window to 500 µm.

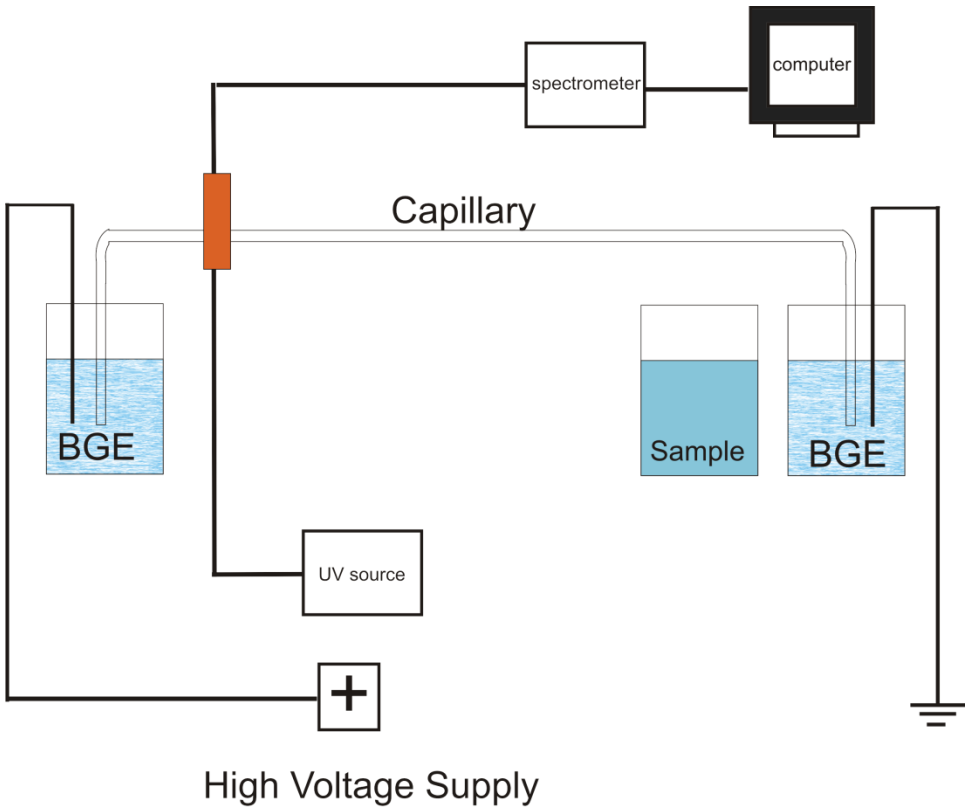

Figure 2-1 Schematic of custom CE instrument

Table 2-1 Components of CE setup

Component Name	**Producer**	**Details**
fused silica capillary	Polymicro Technologies	73 µm I.D.(2000019) 30 µm I.D. (1068150013)
high voltage power supply	Spellman	CZE1000R
UV-Vis light source	Ocean Optics Mikropack	D2000
miniature fiber optic spectrometer	Ocean Optics, Inc.	USB 2000+
optical fiber	Ocean Optics, Inc.	300 µm I.D.
PEEK interface cross	Ocean Optics, Inc.	~500 µm detection window

2.1.2 Operation

New capillaries (typical length ~55 cm) were conditioned using ~0.1 M NaOH overnight to activate the silanol groups on the inner surface and flushed with H_2O prior to use. At the beginning of each experiment, the capillary was filled with background electrolyte (BGE) using a syringe, and the capillary outlet and inlet were placed into vials containing BGE. Then, a high voltage (+ 15 kV to 30 kV) was applied to the capillary outlet (the inlet was grounded). The voltage chosen in each case to limit the current through the capillary to 30 μA; at higher currents, Joule heating can occur, which causes band broadening [163, 164].

Samples were injected by electrokinetic injection (EK). During sample injection, the vial containing BGE at the capillary inlet was replaced by one containing the sample. The high voltage applied drove sample solution into the capillary. Once sample injection was finished, the sample vial was replaced with one containing only BGE, and data collection was initiated. All separations were performed at room temperature (~22°C).

2.1.3 Co-electroosmotic CE

In my research, co-electroosmotic CE was chosen for analyzing the conjugate anions of the acids. In co-electroosmotic CE, the EOF direction is reversed using an EOF modifier such that the flow of the EOF has the same direction as the electrophoretic flow of the analytes. Reversing the EOF increases the apparent mobility of anions and allows for rapid separation [136, 165]. The magnitude of the reversed EOF is affected by the surfactant properties, concentration and coating method [166].

There are several ways to modify the EOF, including application of an external voltage field [167, 168], wall coating [166, 169] or ionic strength control [170, 171]. In my research, a

dynamic surfactant-based coating was chosen because of its simplicity and ease of implementation [136]. The coating was applied by flushing deionized water containing the EOF modifier through the capillary for 15 min. In my study, a positively charged surfactant was adsorbed on the negatively charged capillary wall by electrostatic attraction (Figure 2-2), resulting in a reversal of the surface charge from negative to positive. The exact structure of the dynamic wall coating is not known with absolute certainty; however, it is known that certain surfactants (e.g., dimethyldioctadecylammonium or didodecyldimethylammonium bromide, DDAB or DODAB) form cationic double layers (Figure 2-2, left-hand-side), whereas other surfactants (e.g., trimethyl(tetradecyl) ammonium bromide, TTAB) form micellar structures [172, 173]. The EOF reverses because now anions are in the diffuse region, such that when an electric field is applied to the capillary, the mobile anions in the diffuse region move to the anode [174, 175].

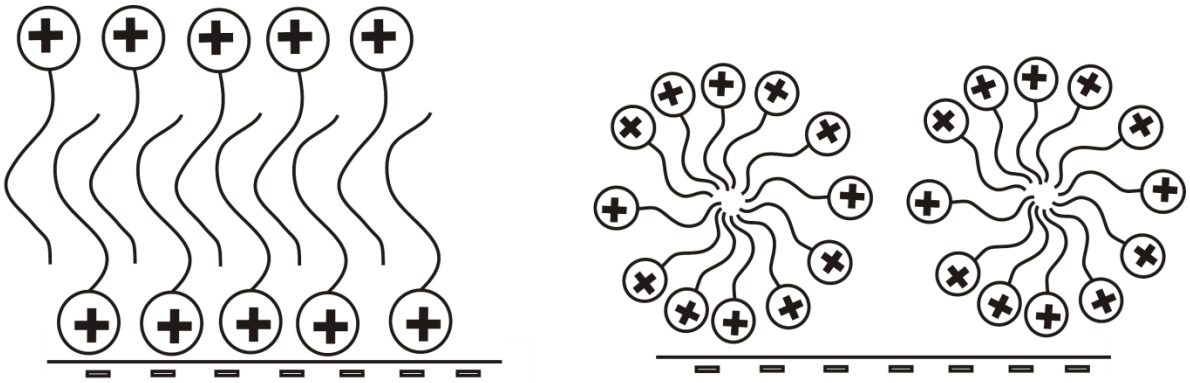

Figure 2-2 Schematic of cationic surfactant coating on the capillary. (**left**) Cationic double layer observed with DDAB or DDOAB. (**right**) Micellar structures observed with TTAB [173]

2.2 Commercial Instruments

2.2.1 Ion chromatography

2.2.1.1 Setup and operation

A Dionex DX-100 IC (Figure 2-3) equipped with a self-regenerating suppressor (SRS) and conductivity detector was used. Anions were separated on a HPIC-AS4A anion exchange column using an eluent containing 2.2 mM $NaHCO_3$ and 2.4 mM Na_2CO_3. The column was operated at an inlet pressure of 500 psi and flow rate of 2.0 mL/min. Before entering the detector cell, the eluent passed through the SRS, in which H_2SO_4 titrated the eluent to reduce the background during detection, which enhances sensitivity. The detector output voltage was digitized using a data logger board (OM-USB-1408FS) connected to a computer running LABVIEW (National Instruments). Data were analyzed by Origin Lab's ORIGIN® and Wavemetric's IGOR® software.

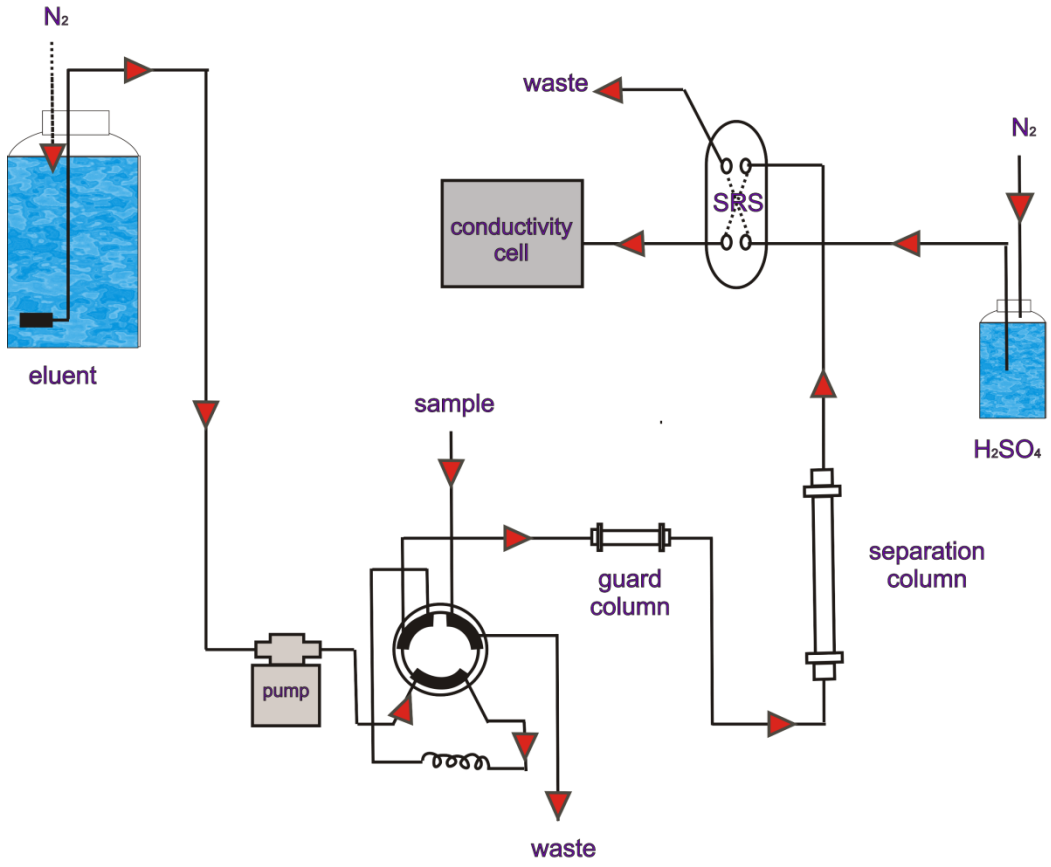

Figure 2-3 Schematic of DX-100 IC instrument [176]

2.2.1.2 Calibration

In IC detection, calibrations were carried using standard solutions prepared from HCOOK, C_2H_5COONa, and KNO_3 in deionized H_2O, respectively.

The calibration curve for propionate is shown in Figure 2-4. It is linear in the range from the detection limit to 168 µM (r^2 = 0.98). The linear regression equation was

$$A = (0.029 \pm 0.001)X - (0.12 \pm 0.07) \qquad \textbf{2-1}$$

where A is the peak area (µS·min), and X is standard concentration (µM).

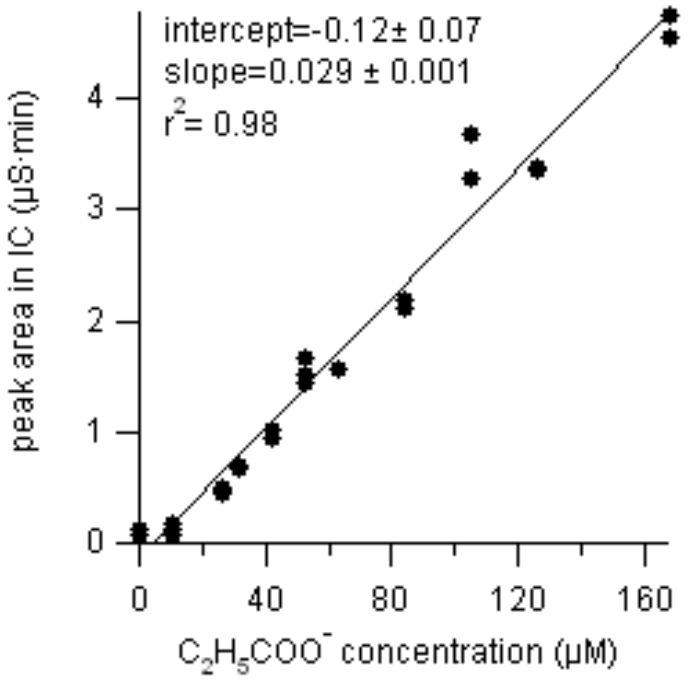

Figure 2-4 IC calibration curve of propionate

Harris describes a method for determining the limit of detection (LOD) in a chromatography experiment using the standard deviation (σ) of measurements near the LOD [177]. In this method, the LOD is estimated from an average of 3 times the average standard deviations (3σ) of measurements close to the detection limit.

The propionate data are summarized in Table 2-2. The LOD of propionate was 1.2 µM.

Table 2-2 Determination of the detection limit of propionate ion in IC

Propionate (µM)	**n**	**RSD (%)**	**σ (µM)**	**3σ (µM)**
10.5	5	5.0	0.53	1.6
26.3	4	1.5	0.39	1.2
31.6	3	1.0	0.31	0.9
			average of 3σ (µM)	1.2

The calibration curve of $HCOO^-$ in IC is linear ($r^2 = 0.98$) in the range from the detection limit to 162 µM (Figure 2-5) with LOD of 2.0 µM. The linear regression equation was:

$$A = ((2.66 \pm 0.09) \times 10^{-4})X - (1.5 \pm 0.8) \times 10^{-3} \qquad \textbf{2-2}$$

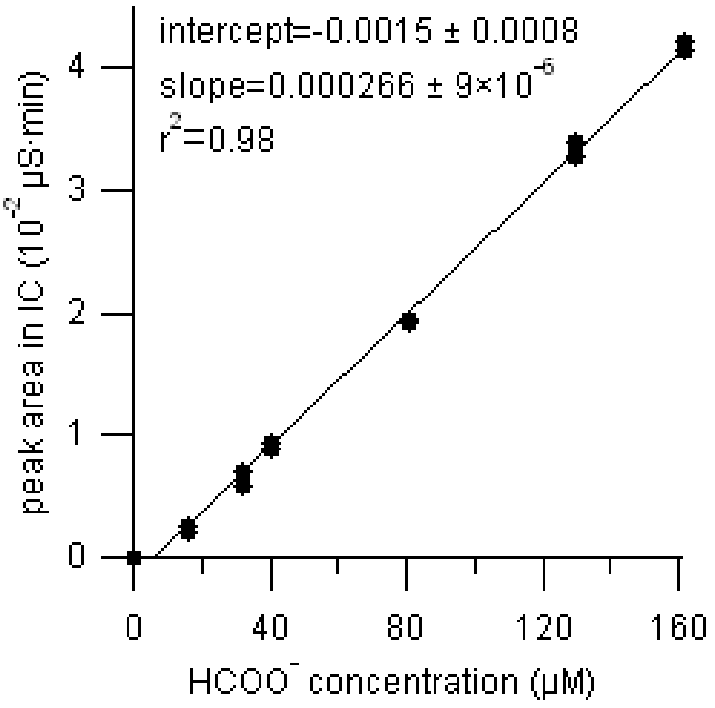

Figure 2-5 IC calibration curve of formate

The calibration graph of NO_3^- is linear between 1.8 and 44.8 µM (r^2 = 0.99, Figure 2-6) with LOD of 1.0 µM. The linear regression equation was:

$$A = (0.00164 \pm 0.00002)X - (0.0028 \pm 0.0005) \quad \textbf{2-3}$$

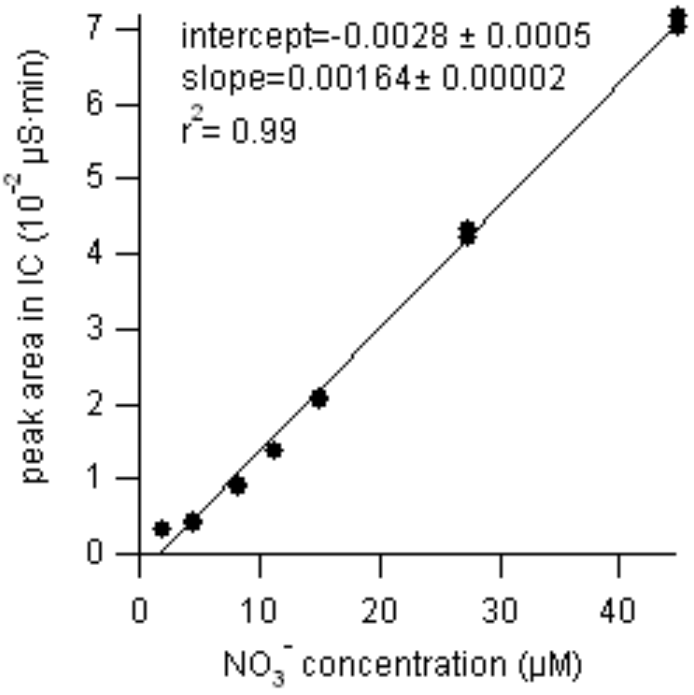

Figure 2-6 IC Calibration curve of nitrate

2.2.2 Chemical ionization mass spectrometry

Detailed descriptions of the CIMS and its operation have been given by *Mielke et al.* [178]. In this work, analyte ions are ionized using either acetate or iodide reagent ion (denoted R). Observed analyte ion counts ($[A^-]$) are expressed as the following equation [158]:

$$[A^-] = [R] \times k[HA]t \qquad \textbf{2-4}$$

Here, [R] and [HA] are reagent ion concentration and analyte gas concentration, respectively, k is the rate of ionization reaction, and t is reaction time. Equation 2-4 shows that ion counts are proportional to analyte concentration.

In my study, HCOOH and C_2H_5COOH were ionized via proton exchange with CH_3COO^- reagent ion:

$$CH_3COO^- + RCOOH \rightleftharpoons CH_3COOH + RCOO^- \qquad \textbf{2-5}$$

Most acids have lower gas-phase acidity than CH_3COOH (as judged from the relative Gibbs Free Energy changes for the deprotonation of the acids: $\Delta G(CH_3COOH)$ =341.5 kcal/mol, $\Delta G(HNO_3)$=317.8 kcal/mol, $\Delta G(HCOOH)$=338.2 kcal/mol, $\Delta G(C_2H_5COOH)$=340.1 kcal/mol) [157] and thus the equilibrium favors ionization of the analyte acids. Acetate reagent ions were produced from the dissociative electron attachment reactions of glacial acetic acid (Aldrich).

HCOOH and C_2H_5COOH were sampled by the CIMS through a 1/4" O.D. Teflon tube, and mixed with CH_3COO^- reagent ions. In the mass spectrum, peaks at m/z 45 and m/z 73 are associated with formate and propionate, respectively.

Acetate was not suitable for HNO_3 analysis because of its high ionization efficiency and elevated background counts. When too many ions are produced, the CIMS response becomes nonlinear. To monitor HNO_3, iodide reagent ion (generated by passing methyl iodide through a

^{210}Po ion source [178]) was used instead. The ionization of HNO_3 took place via a clustering reaction as follows:

$$HNO_3 + I^- \xrightarrow{H_2O} HNO_3 \cdot I^- \qquad \textbf{2-6}$$

Hence, HNO_3 was monitored at m/z 190.

During CIMS detection, the concentration of reagent ion ([R]) can change, for example because of pressure changes. This affects the rate of analyte ionization (equation 2-4), but can be effectively dealt with through normalization [158]:

$$[A^-]_{nor} = \frac{[A^-]_{det}}{[R]_{det}} \times 10^6 \qquad \textbf{2-7}$$

MS is a sensitive technique for acid analysis. However, acid compound amount is characterized by counts in CIMS, which cannot show the exact concentration. Thus, other analysis methods, such as IC and CE, were used to calibrate CIMS response here.

2.2.3 Permeation Devices

Permeation devices are commonly used to generate ppb to ppm mixing ratios of gases [179]. Compared to gas cylinders, permeation devices are more portable, cost less, and offer the advantage of tunable emission rates. For acids in particular, the generated gases generally contain fewer impurities than gas cylinders [180, 181]. Permeation devices are generally composed of a permeation tube inside a temperature-controlled permeation chamber. Permeation tubes are small capsules made of permeable membrane with liquid or solid compound sealed inside. The compound can slowly permeate through the wall creating a flow of analyte vapour. Controlling the temperature controls the effusion rate of the analyte vapour from the permeation tube (higher temperature, higher gas concentration).

Permeation tubes containing HCOOH and C_2H_5COOH were purchased from KIN-TEK. A HNO_3 permeation tube was purchased from VICI Metronics Inc. They were inserted in a commercial permeation device, a dyna-calibrator Model 120 (VICI). When the dyna-calibrator was connected to the mist chamber sampler, N_2 (Praxair) was added to increase the dilute the analyte gas. The gas mixtures were transported to the instruments through a 2 m long 1/4" O.D. Teflon tube (Saint-Gobain Performance Plastics) (Figure 2-7).

Usually, the dyna-calibrator pump flow rate was set to 0.25 standard liters per minute (slpm), and the external N_2 was set to 9.25 slpm. Concentrations of analyte were varied by simply changing the set temperature of the dyna-calibrator (range 40°C to 100°C).

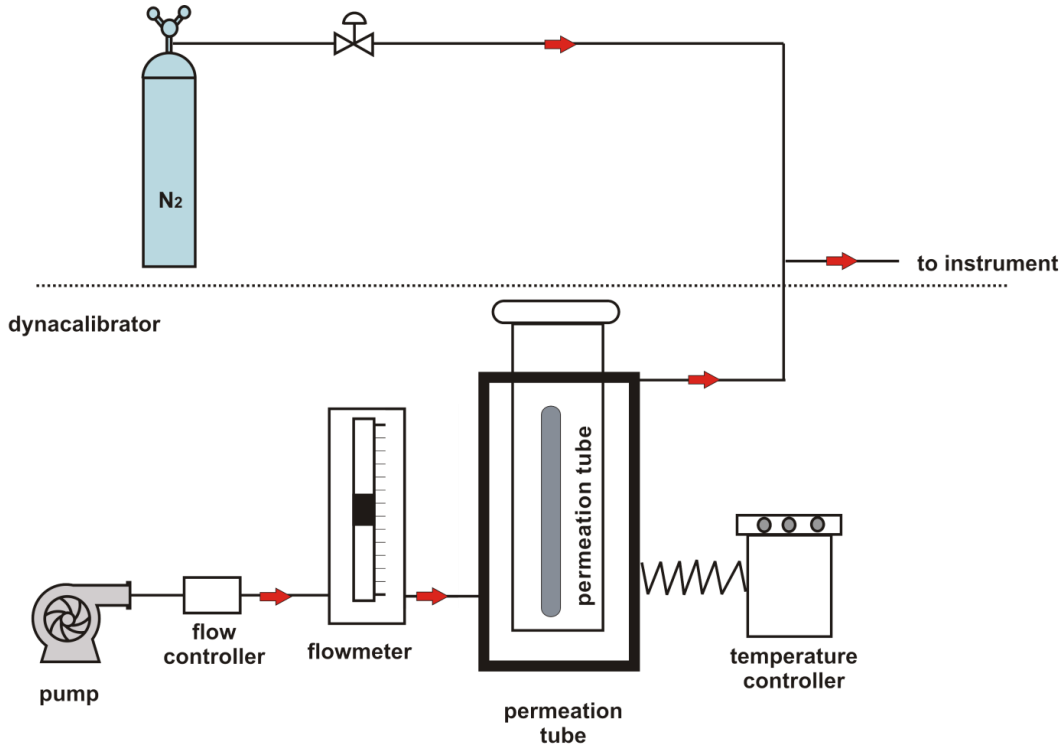

Figure 2-7 Schematic of Dyna-calibrator Model 100

2.3 pH

A VWR sympHony SB70P pH meter and a Thermo Scientific Orion® 9102SC combination pH electrode were used to measure the pH of the generated solutions. The pH meter was calibrated daily, prior to pH measurements, using Thermo Scientific Orion® pH buffer solutions (pH = 4.00, 7.00, and 10.00, certified to ± 0.01 pH units at 25 °C).

2.4 Chemicals

All chemicals were of analytical reagent grade. 1,5-Naphthalenendisulfonic acid tetraahydrate (NDS), potassium formate, potassium nitrate, piperazine (anhydrous), sodium propionate, trans-cinnamic acid, tris(hydroxymethy)aminomethane (Tris), sodium chromate, 2-naphthoic acid (2-NAP), 2, 5-pyridinedicarboxylic acid (2, 5-PDC), $NaH_2PO_4 \cdot H_2O$ and Na_2HPO_4, didodecyldimethylammonium bromide (DDAB),dimethyldioctadecylammonium bromide (DODAB), sodium phosphate monobasic monohydratesodium phosphate dibasic, and trimethyl (tetradecyl) ammonium bromide (TTAB) were purchased from Sigma-Aldrich. Sodium benzoate was purchased from Fluka. All the solutions were prepared in 18 MΩ deionised water (Thermo Scientific Barnstead Nanopure) and sonicated for at least 10 minutes.

Chapter Three: **EVALUATION OF ELECTROPHORETIC METHODS TO QUANTIFY ANIONS**

3.1 Introduction

The separation and quantification of LMW acids is of importance in several fields, including the analysis of soil [182], food and beverages [183], natural water [184] and ambient air [185] where LMW acids are ubiquitous. Accurate characterization of LMW acid abundances in ambient air (in both the particle and the gas phase) will improve the understanding of their sources, production mechanisms, transformation processes, geographical variability, and health effects [186]. As the acids originate from diverse sources and can undergo a variety of reactions, their composition can be quite complex in the atmosphere and their concentrations are usually low [133]. In general, the main conjugate anions are sulfate, nitrate and organic acids [106]. In urban areas such as Los Angeles, formic and propionic acid are usually the dominant species of the (C_1-C_{10}) organic acids [58].

IC, GC and HPLC are commonly used to analyze LMW acids. A GC, when combined with MS, can achieve high selectivity and good sensitivity [187]. However, polar compounds, such as acids, must be derivatised to increase their volatility, which prolongs the analysis time of GC-MS and increases the risk of sample loss [133]. IC and HPLC are both powerful tools for the analysis of acids in environmental samples [188]. IC is the recommended method by the U.S. Environmental Protection Agency (EPA) for the determination of inorganic anions [189]. However, they generally require large sample volumes and generate large amounts of waste [190]. Also, they lack of adequate resolution for some compounds and matrices [102, 191].

CE is an attractive alternative for the determination of acids in environmental samples. It has high separation efficiency, short analysis time and low solution consumption [163]. For the

analysis of LMW acids, indirect UV detection is the most commonly used detection method in CE, due to the lack of chromophores (structure that can absorb light) in the analytes [192]. A strong UV absorbing ion, which is called probe, is added into the BGE. The displacement of probe by analyte ions will lead to a quantifiable decrease in the background absorbance [193]. This allows the identification (from the elution time) and quantification (from the peak area) of analyte ions. Indirect UV detection is a unrestricted method, which can be applied to any ion as long as its absorption properties are different from that of the BGE. Co-electroosmotic conditions are usually used for the analysis of anions, because the high analyte mobility enables rapid analyses and good separation [136, 194].

The aim of the research described in this chapter is to develop a co-electroosmotic CE method with indirect UV detection to separate and determine the LMW acids HNO_3, H_2SO_4, HCOOH and C_2H_5COOH. Here a detailed study of probe, buffer and EOF modifiers is presented. The developed CE system allows for the sensitive and accurate determination of LMW acids.

3.2 Experimental procedure

New fused silica capillaries were pretreated with overnight incubation of 0.1 M NaOH, followed by a 30 minutes flush with 18 MΩ H_2O. To reverse the EOF, an EOF modifier (TTAB, DDAB, or DODAB) was injected into the capillary and allowed to equilibrate over a 10 min time period. Excess modifier was then flushed away with BGE (typically containing ~5 mM NDS, ~7 mM piperazine). Pre-run treatment before each sample analysis consisted of a 3 min rinse with BGE. All rinses were performed by manual syringe injection.

After the treatment of the capillary, sample or standard was introduced by EK injection. Briefly, the sample vial was placed at the capillary inlet for 10 to 60 s with high voltage applied. After a set amount of time, the BGE vial was switched back to replace the sample vial. Because the voltage was not turned off during vial switching, the separation was initiated right away. Ions were separated in the capillary based on their different mobilities and indirectly detected by UV/Vis absorption. Negative peaks indicate the displacement of probe by analyte ions. An internal standard (IS) was added to sample solution to improve the quantification (see 3.3.2.3). Trans-cinnamic acid is usually not expected to be present in real air samples. Thus, it is chosen as IS (typically 0.1 - 2 mM were added to the sample vial). Trans-cinnamate was usually the only positive peak in the electropherograms.

3.3 Results

3.3.1 Background electrolyte development

3.3.1.1 Selection of indirect detection probe

Indirect UV detection is based on the change of absorption by ion displacement of BGE by analyte ions [145]. Selecting a suitable UV probe is very critical to achieve good measurements in indirect detection. Various probes have been used for the analysis of LMW acids, including chromate [192], naphthalenesulfonate [195], 2,6-pyridinedicarboxylic acid [132], phthalate [139] or phthalic acid [196]. *Foret et al.* have discussed important criteria in the probe selection for indirect detection in CZE [197]. They concluded that the best sensitivity can be obtained by using a probe which has strong absorption and mobility similar to that of the sample ions.

In this work, the sample ions were nitrate, sulfate, formate and propionate, which cover a wide range of ion mobilities. *Noblitt et al.* reported the mobilities of nitrate and sulfate to be -6.66×10^{-4} cm^2 V^{-1} s^{-1} and -5.46×10^{-4} cm^2 V^{-1} s^{-1} respectively. In the same analysis condition, formate, propionate and trans-cinnamate have lower mobility, -5.12×10^{-4} cm^2 V^{-1} s^{-1}, -2.98×10^{-4} cm^2 V^{-1} s^{-1} and -2.4×10^{-4} cm^2 V^{-1} s^{-1} [106].

Doble et al. [196] pointed out that the mobility of the probe is the foremost aspect for the successful analysis in indirect detection. If an analyte with a higher mobility than the probe is analyzed, its constitute concentration will diffuse at the front, resulting in a fronting analyte peak. On the other hand, an analyte with lower mobility than that of the probe will appear as a tailing peak. To obtain Gaussian concentration distribution, the mobility of sample and probe should be close to each other [198, 199]. The analytes in this work have a wide range of mobilities, making it challenging to find a suitable probe. *Doble et al*. [196] and *Forte et al.* [197] pointed out that the absorption of probe could significantly affect the detection sensitivity. As in indirect UV detection, higher UV absorbance results in larger analyte peak area. Thus, probes with various mobilities and absorbance were evaluated in this work.

Another important parameter is the choice of BGE pH, which can greatly affect the separation by changing the extent of ionization of the analyte ions and silanol groups on the capillary inner wall. The ionization of silanol groups increase with the increase of pH (from 2 to 9). A basic BGE (pH > 7) can gradually absorb CO_2 and produce carbonate, resulting in competitive replacement of probe [200]. Thus, a pH in the range of 2 to 7 was preferred.

Chromate was the first probe evaluated because it has a good UV absorbance over a wide range of wavelengths [201]. It is also the most commonly used probe for highly mobile ions, such as nitrate and sulfate [201, 202]. Therefore, the less mobile formate and propionate were

used to evaluate the performance of chromate as a universal probe. In a test experiment, 10 mM sodium chromate at pH of 8.72 was used as BGE. This BGE composition was chosen because it was applied to separate nitrate and oxalate by *Trevaski* [203]. At this pH, all analytes are fully ionized. Test samples containing 600 µM HCOOK and 610 µM C_2H_5COONa were injected, but there was no peak in the electropherogram (data not shown) for reasons that are not entirely clear. The lack of peaks suggests that the carboxylate ions were not, or not very efficiently, injected into the capillary. It is also possible that the sample ion bands were diluted (on-column) by the more mobile chromate ions, and that the concentrations passing by the detector were ultimately too small to be detected. Be it as it may, because no peaks were observed, chromate was not used as a probe in my study.

Next, aromatic carboxylates (which are less mobile than chromate) were evaluated as indirect probes, including benzoate, 2-naphthoic acid (2-NAP), 2, 5-pyridinedicarboxylic acid (2, 5-PDC) and 2, 5-naphthalenedisulfonic acid tetraahydrate (NDS).

At first, a BGE containing 10 mM sodium benzoate at pH 6.1 was used. This BGE composition was chosen because it had been used to analyze several inorganic and organic acids by *Romano et al.* [102]. Figure 3-1 shows the results.

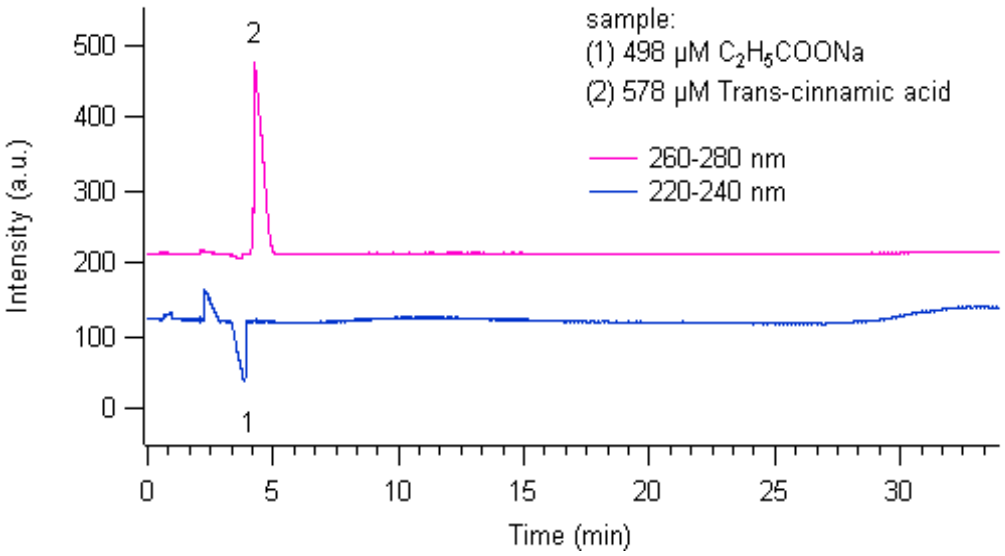

Figure 3-1 CE analysis in 10 mM benzoate. The electropherogram shows the analysis of a solution containing 498 µM sodium propionate and 578 µM trans-cinnamic acid. Conditions: applied voltage, 20 kV; sample injection, 20 kV for 30 s; BGE: 10 mM sodium benzoate, pH 6.1; capillary, I.D. 73 µm, total length 54.35 cm, effective length 34.20 cm; capillary was coated with 1.0 mM DDAB.

Figure 3-1 shows that there was good separation for propionate and IS. The propionate peak is most easily observed in the 220 to 240 nm wavelength range, whereas trans-cinnamate has maximum absorbance between 260 and 280 nm. The blue trace in Figure 3-1 (between 5 and 30 min run time) shows that the intensity of the absorption is not particularly stable.

When 200 µM KCOOH was analyzed in the same BGE (not shown), a broad and fronting peak (migration time 4.0 to 13.1 min) was observed. Hence, a more suitable probe was needed.

2-NAP was evaluated next. It has very strong absorbance (absorption coefficients of 10^3 to $10^{4.5}$ M^{-1} cm^{-1} in the 220 – 240 nm range) [204, 205]. 1 mM 2-NAP at a pH of 7.1 was used as probe to detect formate and nitrate in separate experiments. *Buchberger et al*. [206] investigated how to optimize the detection sensitivity in indirect UV detection in CE. They found that to achieve high sensitivity, the detection wavelength should be in the region where the analyte ion and BGE have the highest absorption difference. For 2-NAP, the maximum sensitivity was observed in the 260 - 290 nm range; therefore, that wavelength range was monitored.. Figure 3-2 shows the electropherograms of formate (in blue) and nitrate (in magenta). They had similar migration times, around 2.5 min. Moreover, the IS peak did not show in the electropherograms, because its UV absorbance is close to that of the 2-NAP. Thus, it was concluded that 2-NAP was unsuitable for this study.

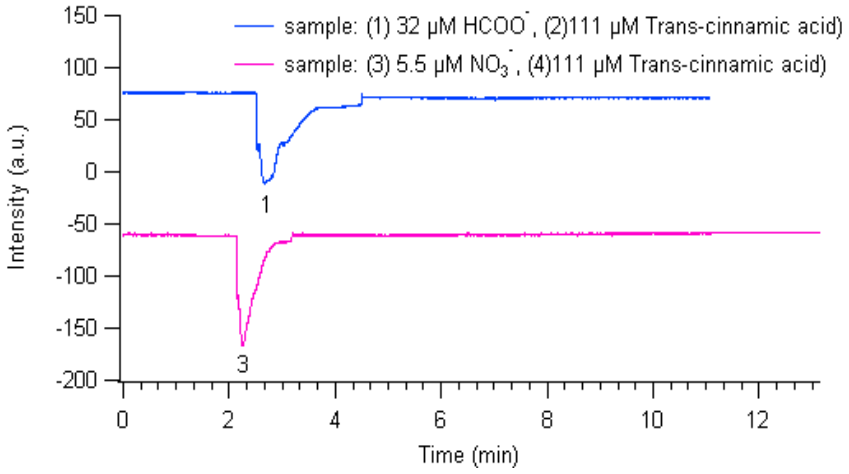

Figure 3-2 CE analysis in 1 mM 2-NAP. Conditions: applied voltage, 25 kV; UV detection, 260 – 290 nm; sample injection, 25 kV for 20 s; buffer, 1 mM 2 - NAP, pH 10.36; capillary, I.D.73 µm, total length 54.35 cm, effective length 34.20 cm; capillary was coated with 1.0 mM DDAB.

2,6-PDC is typically used at 20 mM at pH 4.5 to 7, and excellent separation of inorganic and organic acids has been demonstrated with this probe [207, 208] Here, 2,5-PDC was used as probe. Because of its limited solubility in H_2O (7.1 mM at 25°C) [209], a concentration of 2 mM 2,5-PDC at pH of 7.1 was used to separate formate, propionate and IS (Figure 3-3). However, under these conditions, the electropherogram had unstable background signal. The poor solubility of 2,5-PDC in water [206] may have contributed to this instability. Thus, 2,5-PDC was not chosen as probe.

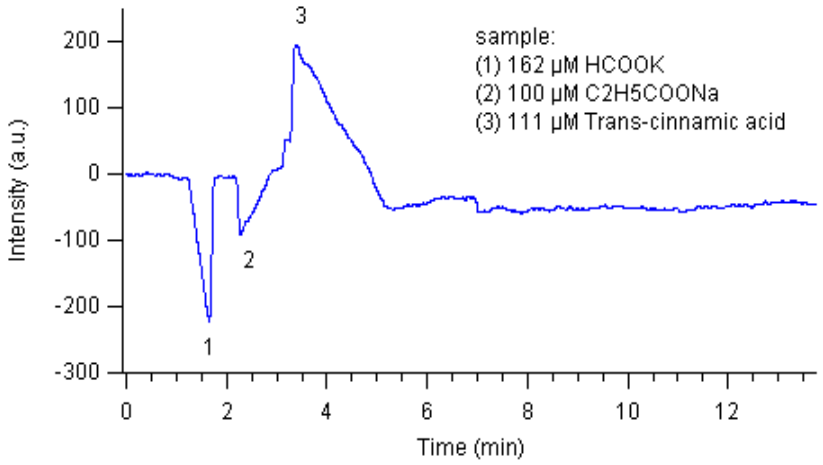

Figure 3-3. CE analysis in 1.90 mM 2,5-PDC. Conditions: applied voltage, 25 kV; UV detection, 260 - 280 nm; sample injection, 25 kV for 20 s; BGE: 1.90 mM 2,5-PDC, pH 7.1; capillary, I.D. 73 µm, total length 54.35 cm, effective length 34.20 cm; capillary was coated with 1.0 mM DDAB.

Next, NDS was evaluated as probe. NDS has been used as probe for the separation of inorganic anions, organic acids and aliphatic anionic surfactants [210]. Here, inorganic and organic ions were separated in 5.5 mM NDS with pH of 5.78, similar to the conditions used by *Noblitt et al.* [106]. The electropherograms are shown in Figure 3-4 (A) and (B), respectively.

In Figure 3-4 (A), sulfate was well resolved from the other peaks, while chloride co-eluted with nitrate ion. In Figure 3-4 (B), formate, propionate and trans-cinnamate were well separated. Since sulfate and formate exhibited fronting peaks and IS showed a tailing peak (Figure 3-4), it can be concluded that NDS has an intermediate mobility among the analyte ions. Based on the results shown above, NDS is good candidate as probe in the analysis of inorganic and organic acids.

The UV intensity spectrums of BGE and sample (containing the same concentration of formate, propionate and trans-cinnamate) are shown in Figure 3-5. They were detected with high voltage (+20 kV) applied to the capillary (I.D. 73 μm). The maximum UV intensity of BGE (4.9 mM NDS, 5.6 mM piperazine, pH 5.86) is observed at 250 nm and 328 nm. The UV intensity differences between BGE and formate, propionate or trans-cinnamate were shown in Figure 3-5. The highest difference was observed at the region of 265-285 nm. Thus, samples were detected in this wavelength region.

(A)

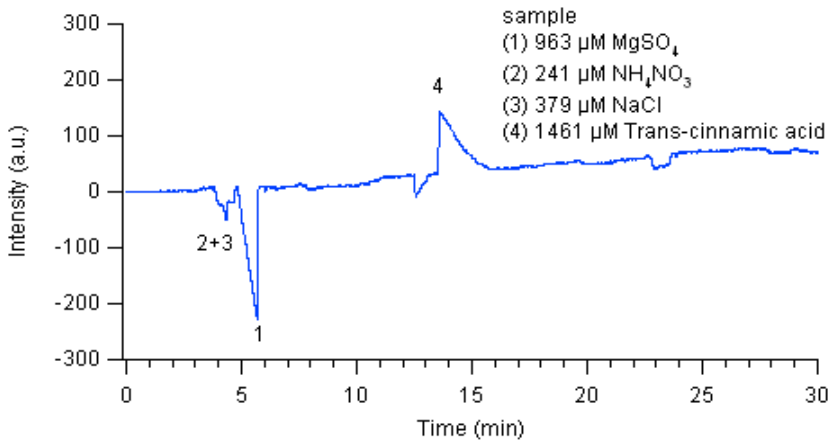

(B)

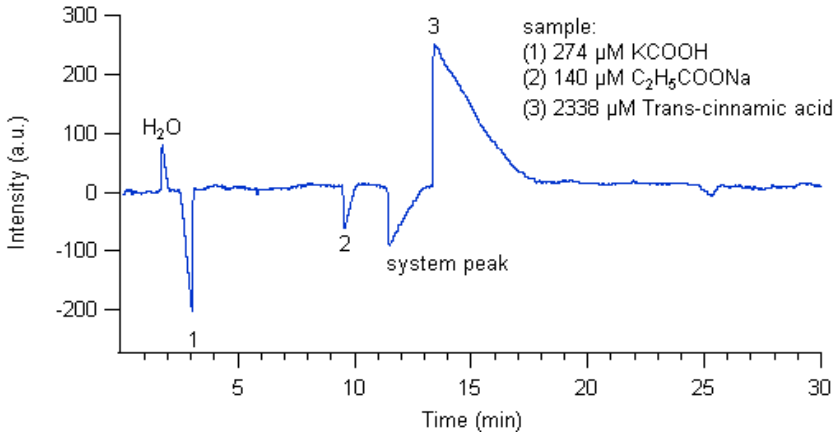

Figure 3-4. Electropherograms of inorganic (A) and organic ions (B) in 5.5 mM NDS. Conditions: applied voltage, 25 kV; UV detection, 265 – 285 nm; sample injection, 25 kV for 10 s; pH 5.78; capillary, I.D. 73 μm, total length 54.35 cm, effective length 34.20 cm; capillary was coated with 1.0 mM DDAB.

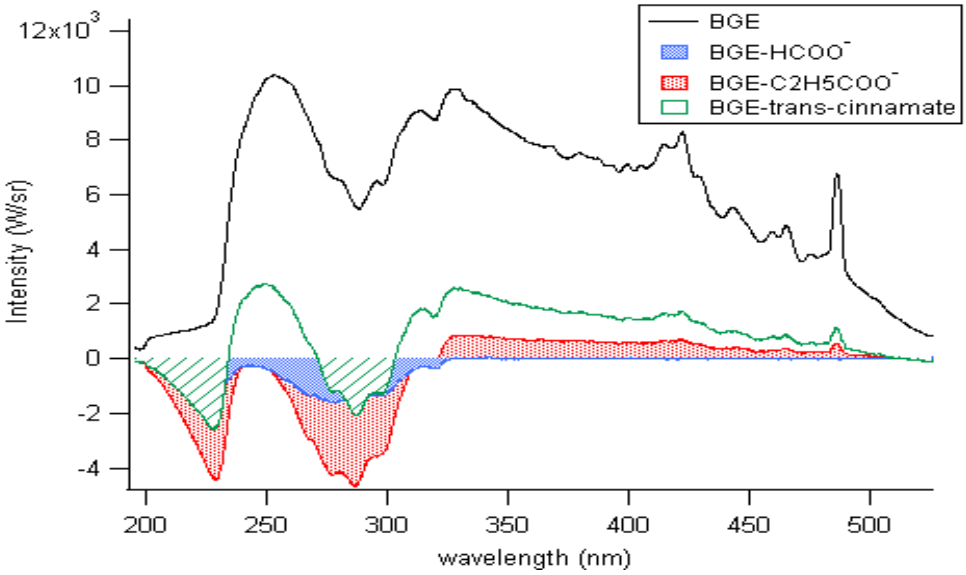

Figure 3-5. UV intensity spectrum of BGE and intensity differences between BGE and sample ions. Conditions: applied voltage, 20 kV; sample injection, 20 kV for 20 s; BGE, 4.9 mM NDS, 5.6 mM piperazine, pH 5.86; sample, 100 µM HCOOK, 100 µM C_2H_5COONa, 111 µM trans-cinnamic acid; capillary, I.D. 73 µm, total length 54.35 cm, effective length 34.20 cm.

3.3.1.2 Buffer selection

It is important that the BGE is buffered because during a CE separation in unbuffered BGE, the pH can change up to 2.5 pH units [211]. The BGE pH alters the charge of ions and therefore it can affect the electrophoretic mobilities. [212] In addition, the pH can also change the charge density on the capillary surface [213], which has a strong effect on electroosmotic mobilities [214, 215]. The variation of mobilities may affect peak`s shapes, migration time and separation efficiency [216]. For example, *Kenndler et al.* [217] reported that a minute pH deviation as small as 0.03 pH units could cause the loss of resolution between benzoic acid and

3, 5-dimethoxybenzoic acid. Therefore, selection of proper buffer and pH value is very important for the selectivity and reproducibility in CE.

One of four types of buffers can be used in indirect UV detection of anions: (1) the probe itself, (2) an anionic buffer, (3) a cationic buffer, or (4) an ampholyte [196]. The probe used in this work (NDS) is acidic (at a concentration of 5.59 mM, a pH of 2.12 was measured). The pK_a values of the analyte (HNO_3, H_2SO_4, HCOOH and C_2H_5COOH) are in the range of -2 (HNO_3) to 4.87 (RCOOH). Thus, the expected optimum separation pH is higher than pH 2.12. Addition of an extra buffer component is required to adjust and maintain the pH of BGE.

An easy approach is to use an ampholyte, which are molecules that contain both acidic and basic groups. Buffers made from ampholytes generally have low conductivity, which allows high electric field strengths and, therefore, efficient separation [218]. However, there are few ampholytes with sufficient buffer capacity at pH values near their isoelectric points (pI; the pH at which a molecule net charge equals zero and conductivity is low), because the pI is usually far from the pK_a values of the basic and acidic groups [200, 219]. Histidine is a classical ampholyte-based buffer used in CE [218]. However, it has very low buffer capacity near its pI of 7.7, and it cannot be used for high sample concentrations [220].

Another approach, which does not produce interference system peaks, is to use a cationic buffer. Tris(hydroxymethyl)aminoethane (Tris; pK_a 8.5) [211, 221] and diethanolamine (DEA; pK_a 9.2) [221] have been widely used. As a BGE pH in the neutral to acidic region is desirable [200], neither Tris nor DEA are suitable buffers and were not chosen in this work.

Piperazine is a weak base with pK_a of 5.33 and effective pH range 5 to 6 [106]. Buffers made from piperazine have been reported to have good buffer capacity at neutral pH and be able to stabilize phospholipid coating on capillaries [222]. *Varjo et al.* [223] also found small

diamines had the similar effect as piperazine-based buffer. They deduced that those profound effects might be caused by the interaction between the positively charged amines and capillary surfaces. Moreover, *Noblitt et al.* [106] observed that piperazine buffer could improve the resolution between sulfate and nitrate. Consequently, piperazine was chosen as buffer in this work.

3.3.1.3 Selection of EOF modifier

To minimize the analysis time, anions were separated in co-electroosmotic mode, in which anions are moving in the same direction as the EOF (towards the anode). The reversal of EOF direction was achieved by using surfactants to modify the inner surface of the capillary. The performances of three cationic surfactants (TTAB, DDAB and DODAB) were compared in this work. The characterization of EOF modifier is based on the stability of the coating and the effectiveness of the EOF reversal, which is commonly evaluated by measuring the EOF of a neutral marker [134, 224]. However, neutral markers are not efficiently sampled in EK injection. Furthermore, it is hard to detect neutral markers, because indirect UV detection only works for ions. Thus, EOF was not characterized using a neutral marker. Instead, the apparent mobility of ions was used to evaluate the performance of the surfactant coating. The apparent mobility can be calculated from the electropherograms using the equation [225]

$$\mu_{app} = \frac{l * L}{t_M * V} \qquad \textbf{3-1}$$

where l is the length of capillary from the inlet to the detection window (in meters), L is the total length of the capillary column (in meters), t_M is the analyte ion migration time (in seconds) and V is the applied voltage (in Volts).

Baryla et al. [172] reported that single-chained surfactants form spherical aggregates on the capillary surface, while the two-chained surfactants form bilayers [173] (Figure 2-2). TTAB is a single-chained surfactant with 15 carbons (Figure 3-6 A). When the capillary was modified with TTAB, it showed good resolution for chloride, nitrate and sulfate. However, it had poor baseline stability, and the capillary needed to be recoated after each sample injection. The poor stability of TTAB supported the finding that single-chained surfactants form dynamic coatings on the capillary surface [173]. Moreover, the mobilities of ions were very low (Figure 3-7, green trace), which indicated that TTAB did not reverse EOF effectively.

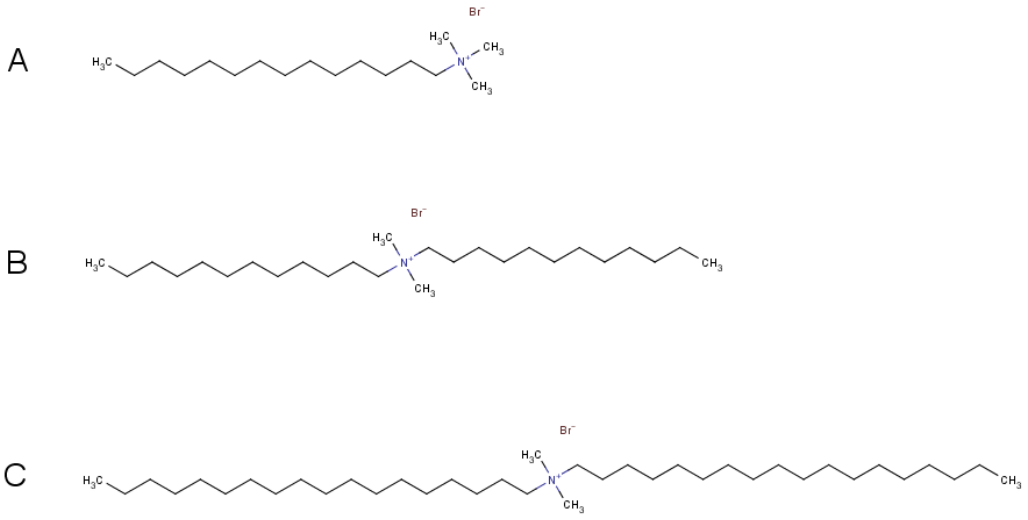

Figure 3-6 Cationic surfactants used as EOF modifier in CE. (A) trimethyl (tetradecyl) ammonium bromide (TTAB); (B) didodecyldimethylammonium bromide (DDAB); (C) dimethyldioctadecylammonium bromide (DODAB).

Yassine et al. [152] pointed out that the best coating stability can be achieved by choosing surfactant with small critical micelle concentration (CMC). DDAB is a two-chained surfactant (Figure 3-6 B), which has a lower CMC (0.035 mM in water) than that of TTAB (0.15 mM) [173]. It also produced more stable coating than TTAB, as the baseline signal was pretty stable with relative standard deviation (RSD) equals 6.9% after 5 samples had been consecutively injected. In DDAB modified capillary, the analyte separation was much faster than in TTAB modified capillary (5 min vs 22 min).

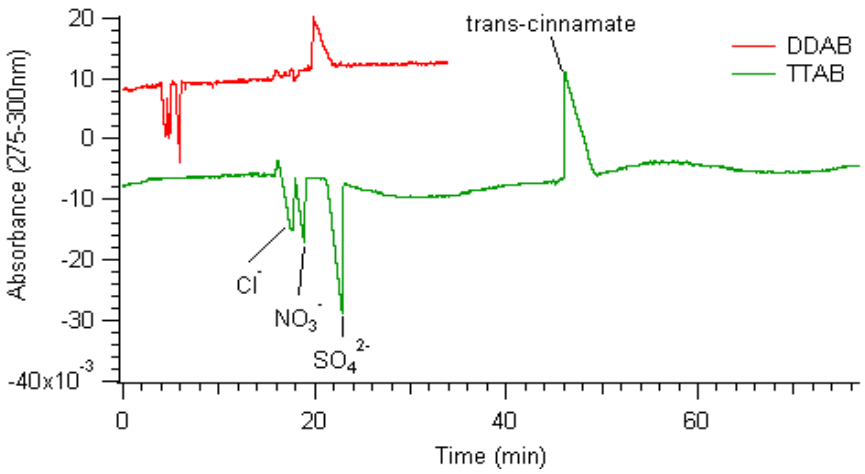

Figure 3-7 Electropherograms of ions analyzed in DDAB or TTAB modified capillary. Conditions: applied voltage, 14 kV; UV detection, 265 – 285 nm; sample injection: 124 µM KCl, 104 µM $(NH_4)_2SO_4$, 89 µM $NaNO_3$ and 277 µM trans-cinnamic acid at 14 kV for 10 s; BGE: 5.46 mM NDS, 7.72 mM piperazine; capillary, I.D.73 µm, total length 55.00 cm, effective length 34.71 cm; capillary was coated with 0.16 mM TTAB (in green) and 0.16 mM DDAB (in red).

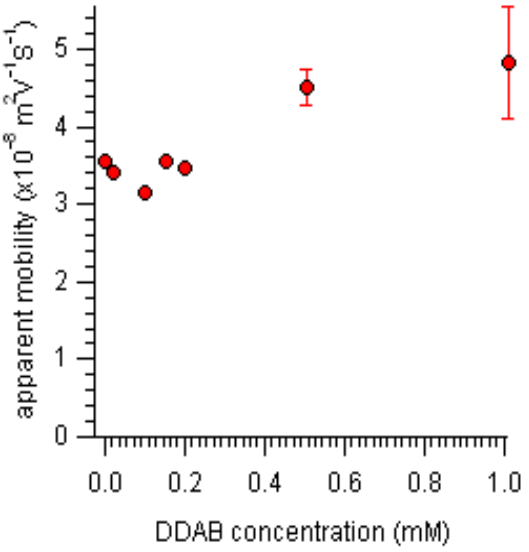

Figure 3-8 Influence of surfactant concentrations on the apparent mobility of formate. Conditions: applied voltage, 20 kV; sample injection: 101 µM KCOOH and 505 µM trans-cinnamic acid,20 kV for 20 s; BGE: 5.60 mM NDS, 7.55 mM Piperazine; capillary, I.D.73 µm, total length 54.40 cm, effective length 34.95 cm; EOF modifier: DDAB in the range of 0.021 to 1.012 mM.

The effect of DDAB concentration (varying from 0.021 to 1.012 mM) on apparent mobility was evaluated. Figure 3-8 shows that as the DDAB concentration increases, the apparent mobility of formate ions increases. When DDAB concentration reached ~0.5 mM, the mobility was relatively constant. It indicated that the capillary surface was saturated with surfactants. The optimized concentration of DDAB was therefore 0.5 mM.

To achieve good coating stability, an EOF modifier with lower CMC was used. It was found that increasing the hydrophobicity of the surfactant (such as increasing the carbon number of the surfactant chains) can decrease CMC [225]. Thus, a longer chained surfactant (such as

DODAB) is expected to have lower CMC (0.0037 μM) [226] and form more stable coatings. DODAB is mostly used at the concentration of 0.1 mM [175, 227]. As it has very low solubility in water, the concentration of DODAB was tested in the range of 0.05 to 0.303 mM. DODAB at the concentration of 0.303 mM showed effective EOF reversal and excellent stability.

Table 3-1 Anion analysis in EOF modified capillary

EOF modifier	μ ($HCOO^-$) (10^{-8} m^2 s^{-1} v^{-1})	μ (IS) (10^{-8} m^2 s^{-1} v^{-1})	N (×10^3 plates) $HCOO^-$	N (×10^3 plates) IS
0.506 mM DDAB	4.7 (± 3.5%)	2.2 (± 6.1%)	3.8 (± 18%)	0.4 (± 11%)
0.303 mM DODAB	3.6 (± 3.3%)	1.2 (± 2.6%)	1.0 (± 12%)	0.5 (± 33%)

The effect of DDAB and DODAB on EOF is shown by the apparent mobility of analyte, calculated by Equation 3-2. Sample, containing 200 μM KCOOH and 170 μM trans-cinnamic acid was analyzed in BGE (5.6 mM NDS, 7.55 mM piperazine). The optimum concentration of DODAB was ~0.3 mM, which was used to compare with ~0.5 mM DDAB. The magnitude of analyte mobility and plate number are higher in the DDAB modified capillary (Table 3-1). Plate number (N) was calculated using [228]:

$$N = 41.7\frac{(t_R / W_{0.1})^2}{(A/B + 1.25)} \qquad \textbf{3-2}$$

Here, t is the ion migration time, $W_{0.1}$ is width at 10% of peak height, B is the width from the peak midpoint to the tailing edge (10% of peak height), and A is the width from the midpoint to the fronting edge (10% of peak height). The μ and N suggest that 0.5 mM DDAB can reverse the EOF more efficiently and achieve higher separation efficiency.

Measurements of the apparent mobility under continuous sample injection can be used to test the stability of the EOF modifier on the capillary [173]. In a typical experiment, the capillary was rinsed with deionized water containing 0.506 mM DDAB or 0.303 mM DODAB for 10 min, followed by a second rinse with BGE (5.6 mM NDS, 7.55 mM piperazine) to flush out excess EOF modifier. Sample (200 μM KCOOH, 170 μM trans-cinnamic acid) was injected continuously at 20 kV for 15 s. In the DDAB-modified capillary, a slight decline of apparent mobility was observed after 5 successive injections (RSD = 3.5%, Figure 3-9, blue circles). However, after 5 runs, peak broadening made it impossible to quantify the analyte. In the DODAB-coated capillary in contrast, excellent stability was observed for 15 injections. The apparent mobility only changed 4.3% (Figure 3-9, in red). The results indicated that DODAB formed the most uniform and stable coating of the three surfactants tested. The observation was also in agreement with the theory that increasing the hydrophobicity of the surfactant increases the stability of coating [149].

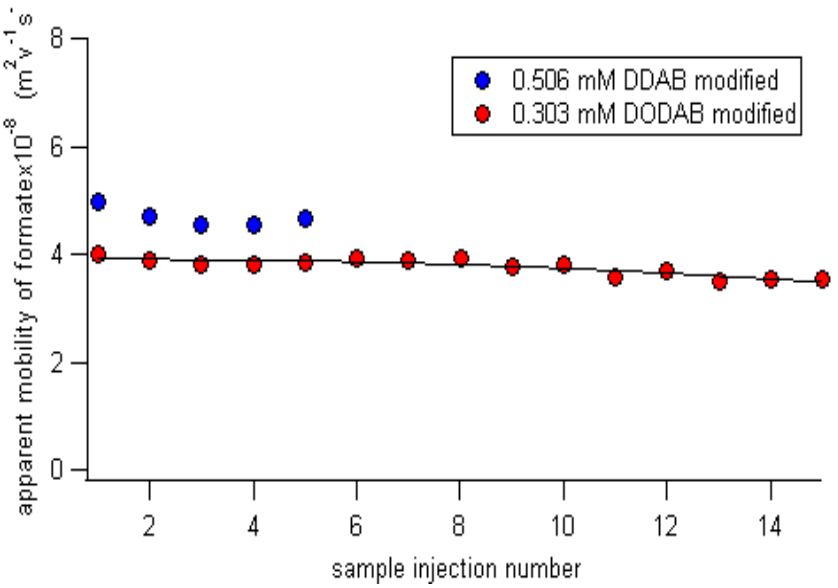

Figure 3-9. Stability of DODAB or DDAB modified capillary. Conditions: applied voltage, 20 kV; sample injection: 20 kV for 15 s; BGE: 5.60 mM NDS, 7.55 mM Piperazine; capillary, I.D.73 µm, total length 54.20 cm, effective length 34.90 cm; EOF modifier: 0.303 mM DODAB or 0.506 mM DDAB.

3.3.2 Optimization of separation conditions

3.3.2.1 Electrode Setup

A Platinum electrode was used in CE for its low resistance. *Macka et al.* [211] have evaluated the effect of electrode position on CE analysis. They observed that the pH varies around the electrode during electrophoresis. This could produce poor reproducibility, peak area and baseline signal. They suggested that placing the capillary end away from the electrode could solve the problem. During my study, the inlet of the capillary was placed ~1 mm vertically below the electrode with a horizontal gap away from the electrode. In this way, it can prevent the

electrophoresis-induced pH fluctuation zone entering the capillary directly without buffering. In this manner, reproducibility and baseline stability was observed to be greatly improved.

3.3.2.2 Sample Injection

In CE, there are two main types of sample injection methods: hydrodynamic (HD) injection, and EK injection. In HD injection, sample is driven by a pressure difference (either by an applied external pressure or through syphoning), while in EK injection, the sample is driven into the capillary by an electric field. In general, more ions are injected into the capillary by EK injection, resulting in higher sensitivity than HD injection [229]. Thus, EK was utilized in this work for its simplicity and good sensitivity.

3.3.2.3 Data analysis

If the mobility of analyte is assumed to be constant when EK injection is used, the amount of analyte entering the capillary can be expressed as [230]:

$$Q_{(a)} = \frac{(\mu_{ep(a)} + \mu_{eo(a)})\pi r^2 V_{inj} t_{inj}}{L} C_{(a)} \qquad \textbf{3-3}$$

where $\mu_{ep(a)}$ and $\mu_{eo(a)}$ are electrophoretic and electroosmotic mobility during sample injection, r is the inner radius of capillary, V_{inj} the sample injection voltage, t_{inj} represents the injection time, L is the total length of capillary, $C_{(a)}$ is the molar concentration of each analyte. Equation 3-3 shows that injected quantity is proportional to sample concentration ($C_{(\alpha)}$) and mobility ($\mu_{ep(a)}$ + $\mu_{eo(a)}$). Thus, more highly mobile ions can be injected, which resulted in mobility bias in EK injection [231]. In this work, indirect UV detection was used and the analyte peak area ($A_{(a)}$) is given by [232]:

$$A_{(a)} = \alpha \frac{\varepsilon_{(a)} \cdot d}{(\mu_{ep(a)} + \mu_{eo(a)})\pi r^2} Q_{(a)} \qquad \textbf{3-4}$$

Here, α is integration constant, which is affected by the charge of analyte ions; $\varepsilon_{(a)}$ is molar absorption coefficient difference between probe and analyte, and d is the optical path length. Combining Equation 3-3 and 3-4, and assuming that the apparent mobility is independent of position along capillary, the analyte peak area can be represented as:

$$A_{(a)} = \alpha \cdot \varepsilon_{(a)} \cdot C_{(a)} \cdot d \cdot t_{inj} \qquad \textbf{3-5}$$

Equation 3-5 suggests that an analyte`s peak area is independent of mobility. Equation 3-5 also links the reproducibility of peak area to the reproducibility of sample injection time and voltage. In this work, sample injection time was controlled manually, which reduces the reproducibility. To solve this problem, the analyte peak area was corrected by an internal standard (IS). If the mobility of analyte and IS are similar, they have the same α. From Equation 3-5, the corrected peak area becomes:

$$A^*_{(a)} = A_{(a)} \cdot \frac{C_{(IS)}}{A_{(IS)}} = \frac{\alpha_{(A)}}{\alpha_{(IS)}} \cdot \frac{\varepsilon_{(a,a)}}{\varepsilon_{(a,IS)}} \cdot C_{(c)} \qquad \textbf{3-6}$$

Hence, $\alpha_{(a)}$ and $\alpha_{(IS)}$ are integration constant for analyte and IS respectively; $\varepsilon_{(a, a)}$ is molar absorption coefficient difference between probe and analyte, $\varepsilon_{(a, IS)}$ is molar absorption coefficient difference between probe and IS. The corrected peak area is independent with injection time and voltage.

3.3.2.4 Optimization of separation conditions

The chosen BGE contained NDS as probe, and was buffered with piperazine. To evaluate the effect of pH on CE separation, BGE of different pH value were prepared. In these

experiments, the concentration of NDS was kept constant around 5 mM. The pH was set by piperazine to pH values in the range from 4.45 to 6.10. When pH of BGE was from 4.45 to 5.11, chloride, nitrite, nitrate and sulfate could be fully resolved. However, no positive peak of IS was observed in the electropherograms. Furthermore, large baseline fluctuations were observed after 15 min separation. Therefore, the capillary wall was recoated after every sample injection.

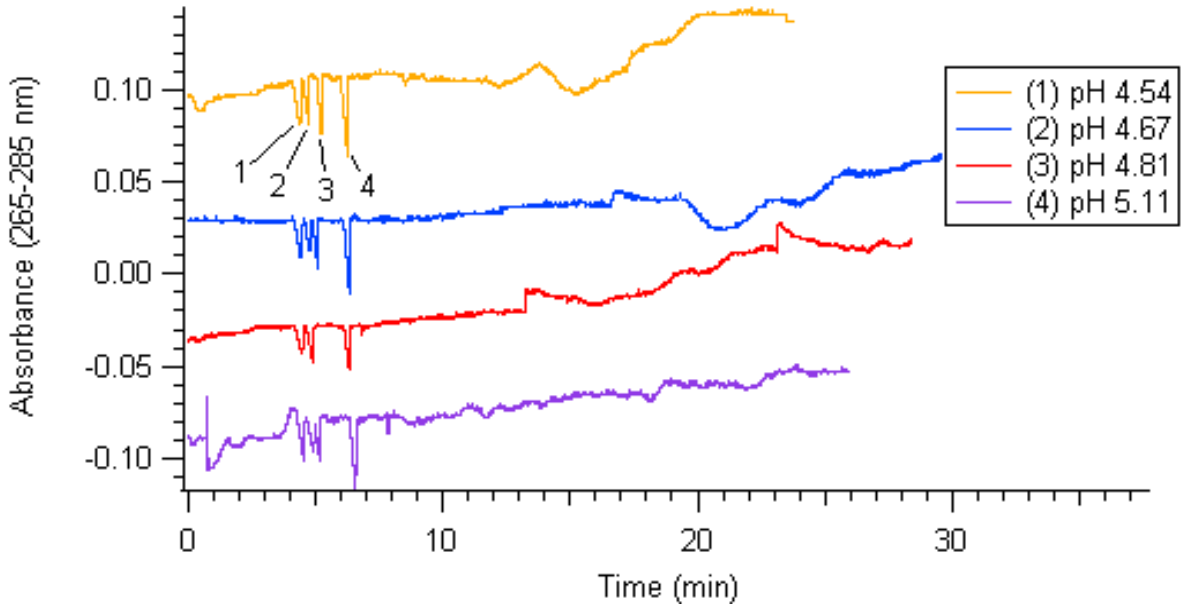

Figure 3-10. Analysis of inorganic ions in BGE of different pH values. Conditions: applied voltage, 25 kV; UV detection, 265 – 285 nm; sample injection: (1) 447 µM Cl^-, (2) 107 µM NO_2^-; (3) 70 µM NO_3^- ; (4) 177 µM SO_4^{2-} ; (5) 584 µM trans-cinnamic acid at 25 kV for 20 s; BGE: 5.6 mM NDS, buffered with Piperazine; capillary, I.D.73 µm, total length 54.20 cm, effective length 34.90 cm; EOF modifier: 0.506 mM DDAB.

Figure 3-11 shows the separation in ions in BGE with pH ranging from 5.32 to 6.24. The mobility of analyte ions gradually decreased with the increase of pH value. At lower pH range, sample peaks were significantly broadened after 2 to 3 times sample injection. At the higher pH

range (5.91 to 6.24), the peak area of sulfate gradually decreased. In the end, pH 5.86 was chosen because a more stable baseline and relatively short separation time was achieved.

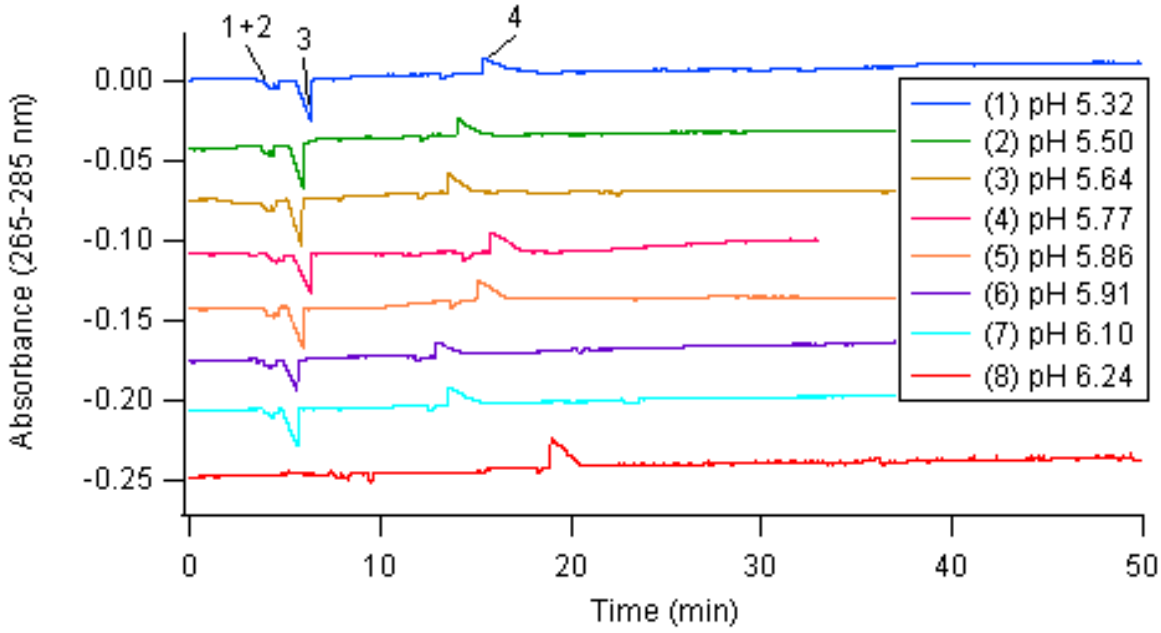

Figure 3-11. Analysis of inorganic ions in BGE of different pH values. Conditions: applied voltage, 25 kV; UV detection, 265 – 285 nm; sample injection: (1) 379 µM Cl^-, (2) 241 µM NO_3^-, (3) 963 µM SO_4^{2-} and (4) 1461 µM trans-cinnamate at 25 kV for 20 s; BGE: 5.6 mM NDS, buffered with Piperazine; capillary, I.D.73 µm, total length 54.20 cm, effective length 34.90 cm; EOF modifier: 0.506 mM DDAB.

The separation efficiency generally increased with increasing of probe concentration [233]. Thus, BGE containing different probe concentrations (3.60 to 19.54 mM) were prepared at a pH of 5.86. Between the concentrations of 3.6 to 5.6 mM, the signal to noise ratio increased from 48 to 85. At higher NDS concentration, the separation current increased to above 30 µA,

resulting in noticeable noise signal and peak distortion from Joule heating [163][164]. Thus, an NDS concentration of 5.6 mM was ultimately chosen.

3.3.3 Optimization of detection limit

The LOD of analyte can be calculated from [234]:

$$C_{LOD} = \frac{C_m}{(DR \cdot TR)} \quad \textbf{3-7}$$

Here, C_{LOD} is the LOD of analyte, C_m is the concentration of probe, DR is the dynamic reserve, which describes the ratio of the background signal to background noise, and TR is the transfer ratio, which is the moles of probe displaced by one mole analyte ions. Based on equation 3-6, C_{LOD} can be optimized by decreasing C_m or increasing DR and TR.

DR describes the ratio between background signal and background noise [235]:

$$DR = \frac{A}{N_{BL}} = \frac{\varepsilon \cdot d \cdot C_m}{N_{BL}} \quad \textbf{3-8}$$

Here, A is the background signal, N_{BL} is the background noise, ε is the probe molar absorptivity coefficient and d is the effective path length. Combining equation 3-7 and 3-8, the LOD can be expressed as:

$$C_{LOD} = \frac{N_{BL}}{\varepsilon \cdot d \cdot TR} \quad \textbf{3-9}$$

Based on Equation 3-9, minimizing LOD involves four main aspects. They are summarized in Table 3-2. To achieve good LOD, high UV absorbing NDS was chosen. Its concentration was optimized to be 5.6 mM to obtain maximum peak area without the effect of Joule heating. Capillary with larger internal diameter (I.D. 73 μm) was chosen over the one with I.D. 30 μm. Increasing the absorption path length can further decrease the LOD.

Table 3-2 Factors affecting limit of detection

Factor	Methods to improve LOD	References
baseline noise (N_{BL})	strong signal output of light source (minimize detector noise); apply capillary cooling system (ensure thermostatting along the capillary); avoid the interactions between capillary walls and ions(minimize chemical noise); optimize probe concentration (minimize visualization noise)	[201, 235-238]
Absorptivity (ε)	probe with high absorptivity	[201]
effective pathlength (d)	maximize capillary internal diameter without band broadening from heating; use multi-reflection cell	[197, 239]
transfer ratio (TR)	match the mobility of probe and analyte ions (minimize peak broadening); probe with lower charge (expend charge ratio between analyte and probe); BGE without ions to compete with analyte ions for probe replacement	[202, 240, 241]

3.3.4 Calibration Curves

3.3.4.1 DDAB Modified Capillary

Under the optimized condition, in which BGE contained 5.6 mM NDS and was titrated to pH 5.86, analyte ions were separated in capillary modified by 0.506 mM DDAB. Nitrate coeluted with chloride under these conditions. Hence, calibration curves were only constructed for sulfate, formate and propionate using corrected peak areas (Equation 3-6). The calibration curve of sulfate is shown in Figure 3-12. It showed a good linear range with correlation coefficient r^2 of 0.998 for the concentration ranging from 7 to 980 μM.

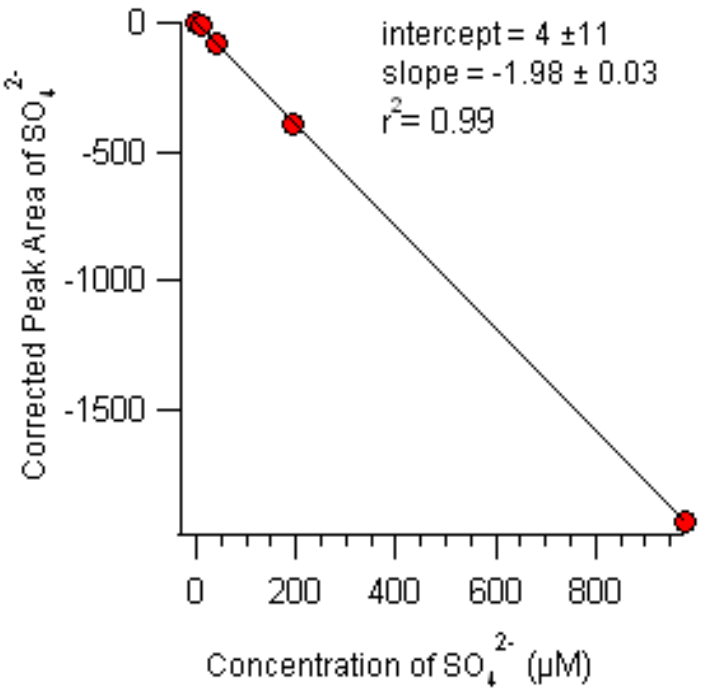

Figure 3-12 The calibration curve for sulfate. Conditions: applied voltage, 20 kV; sample injection: 7-980 µM $CaSO_4$ at 20 kV for 30 s; BGE: 5.6 mM NDS, buffered with piperazine to pH 5.86; capillary, I.D.73 µm, total length 54.20 cm, effective length 34.90 cm; EOF modifier: 0.506 mM DDAB.

Formate and propionate were also analyzed in the same way. A typical electropherogram for their separation is shown in Figure 3-4 B. It showed excellent resolution of all the analyte peaks. The calibration curves are shown in Figure 3-13. They both had excellent linearity (r^2 = 0.99). The linear range of formate and propionate are 8.6 to 1921 µM (HCOOK) and 5.6 to 560.7 µM (C_2H_5COONa), respectively.

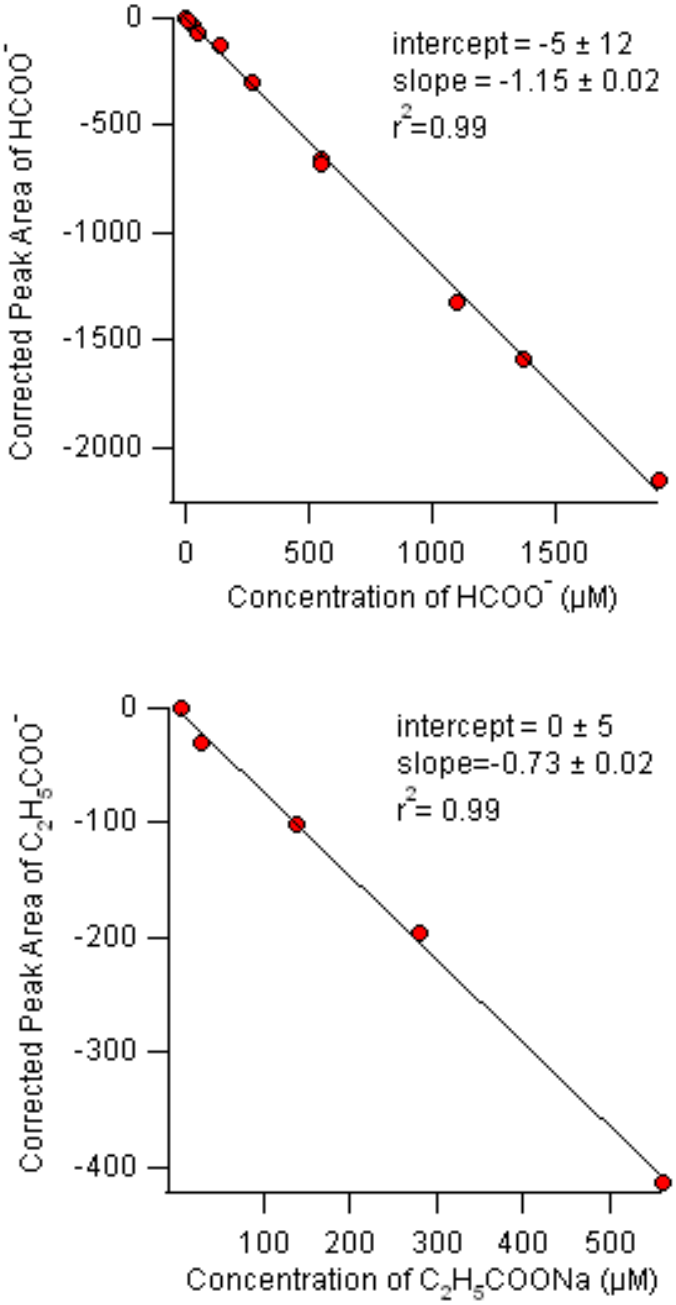

Figure 3-13 The calibration curves for formate and propionate. Conditions: applied voltage, 10 kV; sample injection: 8.6-1921 µM KCOOH and 5.6-560.7 µM C_2H_5COONa at 10 kV for 10 s; BGE: 5.6 mM NDS, buffered with Piperazine to pH 5.86; capillary, I.D.73 µm, total length 54.20 cm, effective length 34.90 cm; EOF modifier: 0.506 mM DDAB.

3.3.4.2 DODAB Modified Capillary

DODAB at the optimum concentration of 0.303 mM was used as EOF modifier. A typical electropherogram is shown in Figure 3-14. The variation of the migration times of formate ion and of internal standards (IS) were evaluated for various sample concentrations. The migration time variation of formate ion was 4.4%, and that of trans-cinnamate was 7.1%. However, after the peak area was corrected, the variation of corrected peak area was only 4.3%.

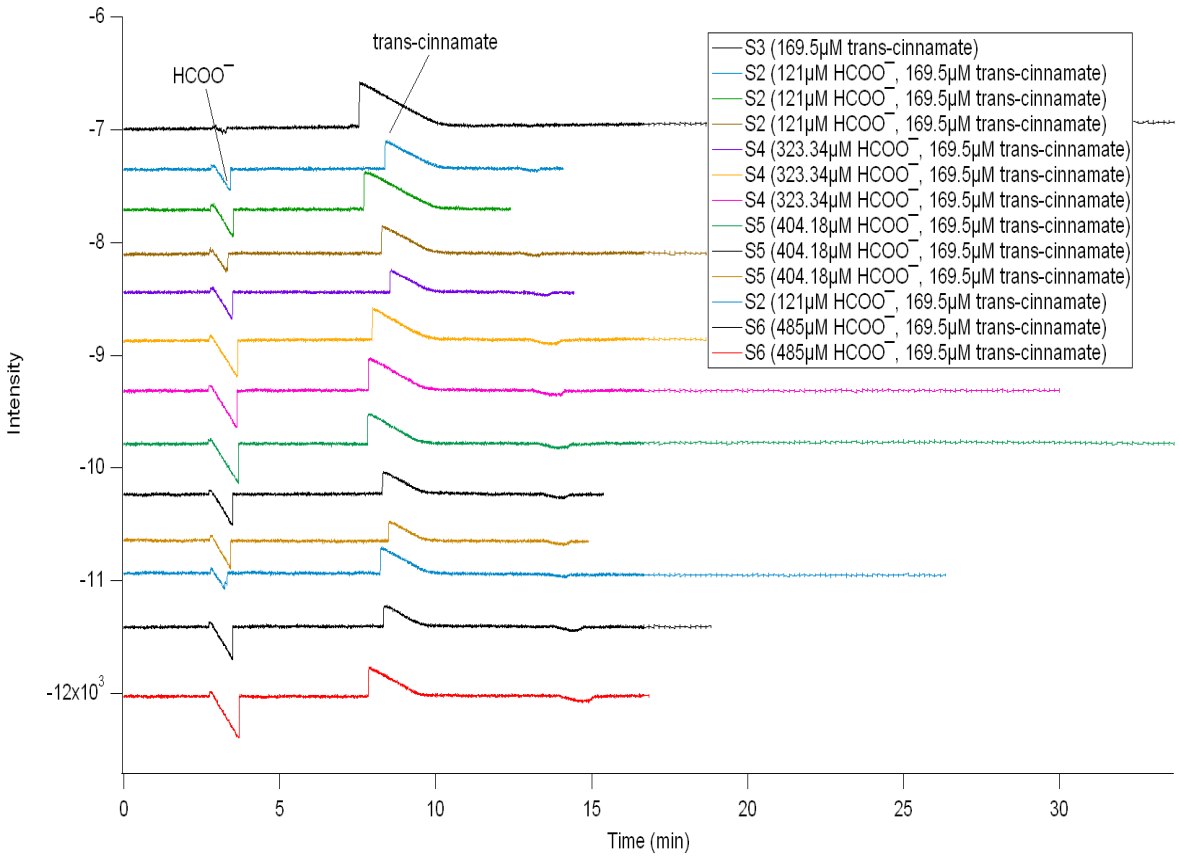

Figure 3-14 Ion analysis in DODAB modified capillary. Conditions: applied voltage, 25 kV; UV detection, 265 – 285 nm; sample injection: 25 kV for 20 s; BGE: 5.6 mM NDS, buffered with

Piperazine to pH 5.86; capillary, I.D. 73 µm, total length 54.20 cm, effective length 34.90 cm; EOF modifier: 0.303 mM DODAB.

The calibration curve for formate is shown in Figure 3-15. It showed excellent linearity (r^2 = 0.99) in the concentration range from 121 to 485 µM. DODAB modified system showed much better reproducibility than DDAB modified system. However, its sensitivity (slope = - 0.25 ± 0.01) was lower than that from DDAB system (slope = - 1.15 ± 0.02). The analytical performance of CE method is summarized in Table 3-3.

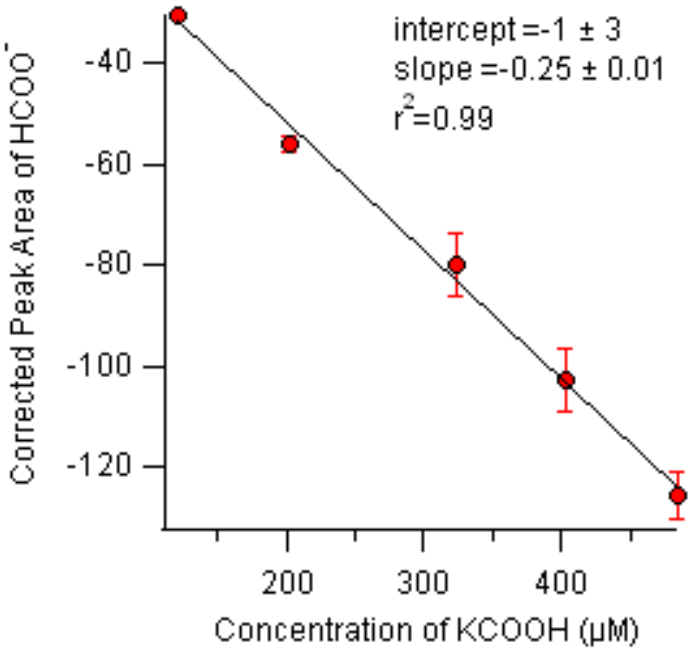

Figure 3-15. The calibration curve for formate using DODAB. Conditions: applied voltage, 25 kV; sample injection: 121-485 µM KCOOH at 25 kV for 20 s; BGE: 5.6 mM NDS, buffered with Piperazine to pH 5.86; capillary, I.D.73 µm, total length 54.20 cm, effective length 34.90 cm; EOF modifier: 0.303 mM DODAB.

Table 3-3 Calibration curve parameters of the CE method developed for the determination of inorganic and organic acid anions

compound	EOF modifier	sensitivity	correlation coefficient (r^2)	linear range (µM)
sulfate	DDAB	- 1.98 ± 0.03	0.99	7 - 980
formate	DDAB	- 1.15 ± 0.02	0.99	8.6 - 1921
formate	DODAB	- 0.25 ± 0.01	0.99	121 - 485
propionate	DDAB	- 0.73 ± 0.02	0.99	5.6 - 560.7

3.3.5 Repeatability of CE analysis

The repeatability of the method was expressed as the relative standard deviation (RSD) of migration time and corrected analyte peak area. The same sample of ~10 µM was analyzed 2-3 times a day on different days using different capillaries. Both migration time and corrected peak area showed good precision (RSD ≤ 8.6%). The inconsistency of capillary modified surfaces conditions could significantly contribute to this variation.

Table 3-4 Repeatability of the CE method developed for the determination of inorganic and organic acid anions

compound	EOF modifier	RSD, % (migration time)	RSD, % (corrected peak area)
sulfate	DDAB	8.6	5.0
formate	DDAB	3.4	7.1
formate	DODAB	3.3	2.8
propionate	DDAB	3.4	2.7

Analyte sample was injected by kinetic injection; n = 6.

3.3.6 Detection limit

The LOD in CE analysis was derived from three times the standard deviation (σ) of repetitive measurements of corrected peak area. Once 3σ was calculated, the LOD was estimated from the calibration curve. All the measurements were carried out in the same conditions, where the BGE was at the pH of 5.86, which contains 5.6 mM NDS and 3.4 mM piperazine. The LOD of sulfate, formate and propionate were in the range of 9 to 21 μM (Table 3-5).

Table 3-5 Detection limits in CE

Compound	EOF modifier	σ of corrected peak area	n	3σ	LOD (μM)
sulfate	DDAB	10.3	6	30.9	16
formate	DDAB	3.8	5	11.3	9
formate	DODAB	1.6	6	4.8	19
propionate	DDAB	5.2	6	15.6	21

3.4 Discussion

3.4.1 Performance of the CE detection

Table 3-3 shows CE has excellent linear response for all analyte ions ($r^2 \geq 0.99$) over a relatively wide dynamic range (from ~10 to ~1000 μM). In the DDAB modified capillary, the highest sensitivity was observed for sulfate, with the slope of calibration curve of -1.98 ± 0.03. Sulfate is doubly charged, whereas other analyte ions are singly charged. Thus, same concentration sulfate can displace more probe ions and result in higher ratio of $\alpha_{(a)}$ to $\alpha_{(IS)}$ in equation (3.6). The detection sensitivity of sulfate was followed by that of formate (slope = -1.15 ± 0.02) and propionate (slope = -0.73 ± 0.02). The lower sensitivity of propionate might be caused by differences in their mobilities, which results in a smaller relative amount of

proprionate being injected. Further, when the probe has higher mobility than analyte (as was the case here), probe ions can diffuse into the sample zone and dilute the sample ions, resulting in tailed analyte peak (as observed for propionate) and lower response (relative to formate).

In the DODAB modified capillary, CE method showed low sensitivity to formate (slope = -0.25±0.01), which was lower than that in DDAB modified capillary for reasons that are unclear. The DODAB modified capillary showed good baseline stability (0.083% shift after 5 injections) and repeatability (RSD of corrected peak area = 2.8%). It also produced very stable coating on the capillary`s inner walls (3.3% mobility shift after 15 injections). However, the analytes had lower mobility (e.g., $\mu_{(formate)} = 3.6\times10^{-8}$ $m^2 \cdot s^{-1} \cdot v^{-1}$). Formate and trans-cinnamate migration time were ~3.5 min and 10 min. In the DDAB modified capillary, in contrast, the migration time of formate and trans-cinnamate were ~3.4 min and 15.1 min, respectively. The IS peak was tailing in both coated capillary, which might have affected the corrected peak area and detection sensitivity. It could have been improved by choosing more mobile IS to match the mobility of probe, for example citrate [242], chlorate, and 5-chlorovalerate [243].

3.4.2 Comparison with other CE methods

The LOD of acids tested from previous indirect UV detection typically ranges from 1 to 10 µM [132, 146]. The results presented in this chapter provided slightly poorer LOD (9 to 21 µM). Longer sample injection time could potentially be adopted to improve the LOD. Coupling CE with pre-concentration method can also provide better sensitivity. Solid phase extraction (SPE), istotachophoresis (ITP) and field-amplified sample stacking (FASS) are the commonly used method to concentrate sample online in CE separation [244].

CE has poor sample loading capacity due to the noise at low concentrations and band broadening at high concentrations. Typically, the linear dynamic range is under 2 orders of magnitude of concentration [146, 201, 245]. Here, the linear dynamic range of all analyte in DDAB modified capillary covered 2 orders of magnitude, which is exceptionally good for indirect UV detection.

The main drawback of reversed-EOF CE is the instability of coating, which can cause interference of detection [151, 152]. DODAB coating showed excellent stability with migration time reproducibility within 3.3% RSD for 15 run over 450 min without coating regeneration. In contrast, the EOF decreased dramatically in TTAB modified capillary once TTAB was removed from BGE [173]. In DDAB coated capillary, the EOF decreased 3% over 75 min after the surfactant was removed from the BGE [136]. The stability of my system enables reproducible separation results and saves time to regenerate coating.

3.5 Conclusions

In this chapter, a reversed-EOF CE method with indirect UV detection was developed for the determination of inorganic and organic ions. BGE, containing 5.6 mM NDS buffered with piperazine to the pH of 5.86, was optimized to provide a selective, sensitive analysis. The capillary surface was modified by DDAB or DODAB, which provided effective reversal of the EOF. Higher sensitivity was achieved using the DDAB modified surface, and better stability was obtained in DODAB modified surface. This CE method offers great calibration linearity over a wide concentration range of analyte. In future work, the LOD may be further improved by using better detection techniques.

Chapter Four: **DETERMINATION OF THE MIST CHAMBER COLLECTION EFFICIENCY**

4.1 Introduction

Over the years, many techniques have been developed for the quantification of LMW acids in ambient air (Chapter 1). Considering the wide variety of applicable compounds, wet extraction methods with off-line detection techniques are commonly used. They typically consist of a wet sampling method (e.g., denuders [84, 246, 247], filter extracts [81] or solutions [248, 249]) combined with a wet chemical analysis techniques such as IC, GC and CE.

In my research, a custom mist chamber (MIST) was constructed for LMW acid sampling. MIST refers to a nebulising-reflux chamber built on the basis of the design by *Cofer et al.* [248]. A MIST is typically operated at high gas flow rates of up to 70 standard liters per minute (slpm); if the extraction time is 10 min, a fairly large air volume of approximately 700 L is sampled and compressed into a small amount (typically 10 mL) trapping solution [249]. Most commonly, the collected solution is then analyzed by IC. MIST/IC has been applied to the extraction and concentration of several gas compounds for decades. It has been developed for studies of various gases, including HCl and Cl_2 [250, 251], Hg (II) [252], carboxylic acids [253], dimethylsulfoxide(DMSO) [96], carbonyls [254], SO_2 [255], HNO_3 and NH_3 [256].

Several other techniques are currently used for LMW acid sampling, including filters and denuders. A denuder is typically operated at a flow rate of 0.5 - 1 slpm and cannot provide high-resolution time data as a large air volume needs to be sampled to collect detectable concentrations [257]. In addition, sampling with denuder or filter techniques requires continuous coating and laborious subsequent sample extraction. These techniques have proven to be time-consuming and to contain artefacts [1]. Moreover, the denuder surface or the filter can be

saturated during sampling. In MIST, in contrast, the trapping solution is able to extract large amounts of target compounds without significant interferences [60, 258]. Thus, MIST sampling is more reproducible than the other techniques. In general, high collection efficiencies (COE) have been reported. For most water-soluble compounds in the atmosphere (i.e. formic acid, pyruvic acid, nitric acid) COE of above 70% are routinely achieved [249, 250, 259]. As for the high gas flow rate, MIST allows for the highly sensitive detection over a short time period.

My research consisted of MIST sampling of atmospheric LMW acids. This chapter focuses on the evaluation and optimization of MIST COE of three LMW acids: HCOOH, C_2H_5COOH and HNO_3.

4.2 Materials and methods

4.2.1 Mist chamber sampling technique

A schematic diagram of the MIST is shown in Figure 4-1. It consists of a glass cylinder chamber of 35.8 mm inner diameter (I.D.) and 38.0 mm outer diameter (O.D.). The total volume of the glass chamber is 237 mL (I.D. = 3.58 cm, height = 23.60 cm). On the body of the chamber, there are two ports. The top one, connected to auto valve 1, is used to add trapping solution by automated 2-way valve. Through the lower one, which is connected to auto valve 2, solution can be drained out and collected into the sample vial. A Teflon cylinder and a hydrophobic filter (Teflon, 47 mm diameter, 1.0 or 2.0 μm pore size, Pall Life Sciences) are put at the top of chamber (downstream of the air flow) to retain mist droplets. To facilitate high gas flow rate in MIST, a 110 slpm capacity scroll pump (Varian SH-110) was connected to the end of gas outlet. The gas flow rate was controlled by a 50 slpm mass flow controller (MFC; model 1559, MKS Instruments) typically operated at flow rates of 30 slpm or less.

At the bottom of the glass chamber, there is a nebulising nozzle which has two orifices. Gas sample is drawn into the glass chamber from the central orifice. The side orifice has one end immersed in the solution and another end in the air located right on the top of central orifice. Thus, trapping solution is continuously pulled through the side orifice by the low pressure inside the chamber. Once it comes out of the side orifice, the fast moving gas in the center aspirates the coming solution and produces an air/droplet mist in the glass chamber. The mist moves up to the chamber with gas stream until it impinges on the Teflon filter. Then the mist forms liquid droplets and eventually deposits back into the reservoir. During this process, sample air is mixed with trapping solution. Soluble gas compounds will be trapped into solution, while the rest of the gas is removed via the gas outlet by the pump. The produced mist increases the interface of the gaseous analyte and trapping solution resulting in higher collection efficiency.

Table 4-1 Geometrical and sampling characteristics of mist chamber sampler

Glass chamber I.D. (cm)	3.58
Glass chamber O.D. (cm)	3.80
Glass chamber height (cm)	23.60
Glass chamber volume (mL)	237
Glass beads volume (mL)	~43
Gas flow rate (slpm)	25.5 - 30.3
Sampling time (min)	10/15
Collected trapping solution volume (mL)	~15

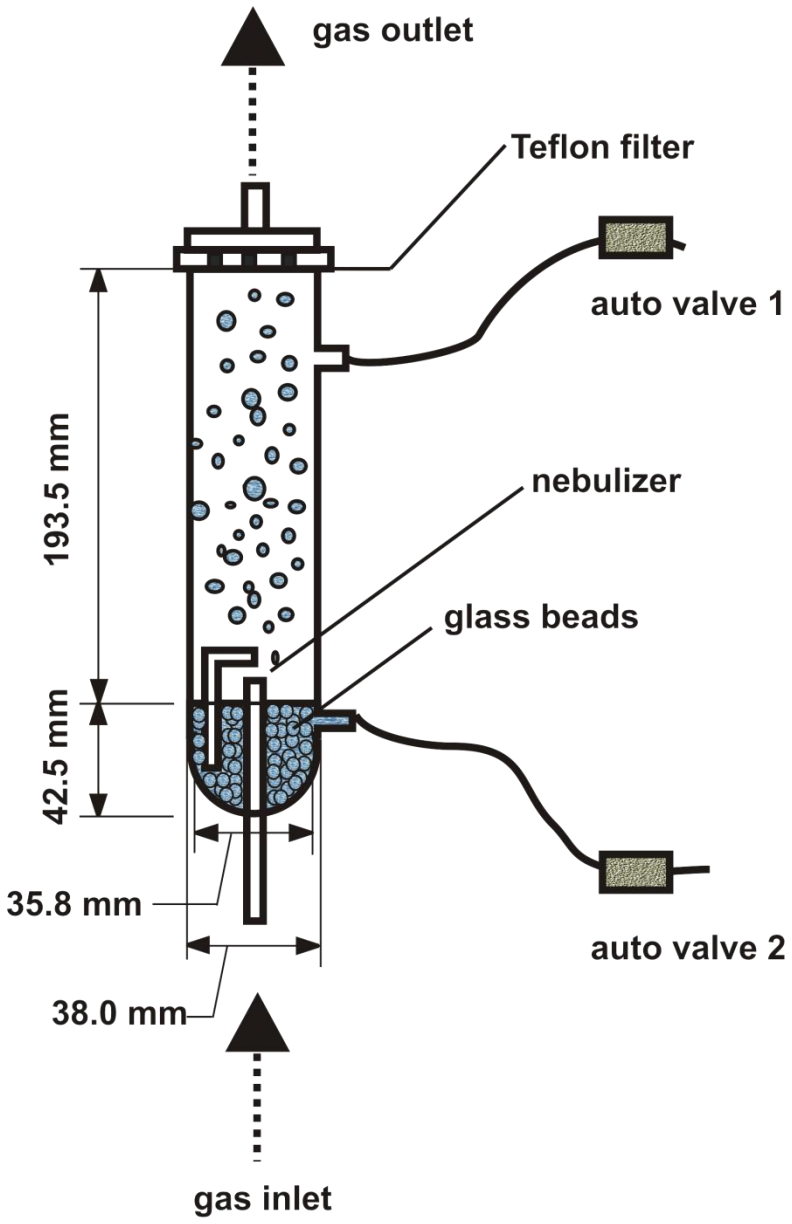

Figure 4-1 Schematic of MIST used for acids sampling. Gas phase acids were sampled at a constant high volume flow. They entered the chamber from the bottom gas inlet, and came out from the gas outlet on the top.

To increase the concentration of the gas analyte in the extraction fluid, a minimum amount of trapping solution should be used. Small glass beads (diameter = 0.35 cm) were added into the chamber to reduce the total volume of the trapping solution from ~48 mL to ~15 mL. The glass beads also act as a flow spoiler to promote the formation of mist [251, 260].

In this work, the MIST was operated at 25.5 - 30.3 slpm. Sample collection intervals were 10 or 15 min. All sampling procedures were carried out at room temperature (22°C). The trapping solution was drained from the bottom port of the chamber by auto valve 2 and analyzed by either IC (see Chapters 5.3.1) or CE. Although a Teflon cylinder and a hydrophobic filter are used, the trapping solution evaporated somewhat at a rate that depended on the humidity of the gas being sampled and on the temperature [260]. Hence, the volume of the collected trapping solution needed to be recorded. In MIST sampling, a Teflon filter is normally added to the sampled air stream [69, 253, 261]. As judged from occasional measurements of room air by a commercial condensation particle counter (model 3775, TSI, USA) there were very few (< 10 particles per cubic centimeter) aerosols present in the lab room air. Since it is not expected that neither the N_2 cylinder nor the permeation standard would emit aerosol, the mist chamber was operated without an inlet filter (which would normally be used to distinguish acids present in the gas phase from those in the aerosol phase).

4.2.2 Determination of collection efficiency

MIST is a sampling device in which gaseous compounds are dissolved into liquid medium through physical or chemical absorption. As MIST can have different COE for different compounds, accurate knowledge of COE is essential for the determination of various compounds.

Two main methods are employed to determine COE in MIST. The first one is to use a known concentration of gas standard. The COE is then calculated by comparing analyte trapped in the solution to its original total amount [253, 259, 262]. However, certified low-level (sub-ppb) gas standards are not readily available that could be directly used to determine COE. Gas standards are usually produced by diluting the output from permeation tubes [262] or from a gas cylinder [255, 256]. While the uncertainty of these standards (after dilution) were reported to be quite low (e.g., around 5% [256, 262]), the accuracy of the standards is often not carefully evaluated.

The other method used to determine COE is to connect two MIST in series. Assuming their operation parameters are identical [96, 250, 254, 263], COE can be derived by detecting analyte concentrations in both chambers [249, 250, 264]. However, this assumption is generally not fulfilled, because the hydrophobic filter of the first MIST will cause there to be a pressure drop, which results in different mist droplet size and COE in the second MIST [93].

In this work, the quantities of a particular target compound entering and exiting the MIST were monitored by chemical ionization mass spectrometry (CIMS). In this way, compound retained in MIST can be continuously monitored. The experimental setup is shown in Figure 4-2. During the measurement, gas standard was generated from a permeation tube inside the dyna-calibrator. Controlling the temperature of dyna-calibrator (from 40°C to 100°C), gas standards of

different concentrations can be produced. To meet the high flow rate, the output of the dyna-calibrator was mixed with N_2 (10 slpm) and room air (18-22.8 slpm). Then, the diluted gas standard was carried into MIST sampler through the FEP Teflon tubing (1/4" O.D., Saint-Gobain Performance Plastics).

During COE measurement, there were two configurations: the first one was inline mode (shown in Figure 4-2 A), which allowed gas flow passing through the MIST. CIMS response (Q_{in}, in the unit of Hz) represented the amount of analyte which is not trapped in MIST. In the second mode – bypassed mode (shown in Figure 4-2 B), gas flow was connected to CIMS directly. CIMS determined the total amount of target compounds (Q_{by}, in the unit of Hz). Thus, the experimental COE of MIST can be determined from:

$$COE = \frac{Q_{by} - Q_{in}}{Q_{by}} \qquad \textbf{4-1}$$

which rarranges to:

$$Q_{in} = Q_{by}(1 - COE) \qquad \textbf{4-2}$$

If Q_{by} is plotted on the ordinate, and Q_{in} is plotted on the abscissa, the parameters of a straight line can be fit to the Q_{by} and Q_{in} data to determine the slope, from which COE can be determined.

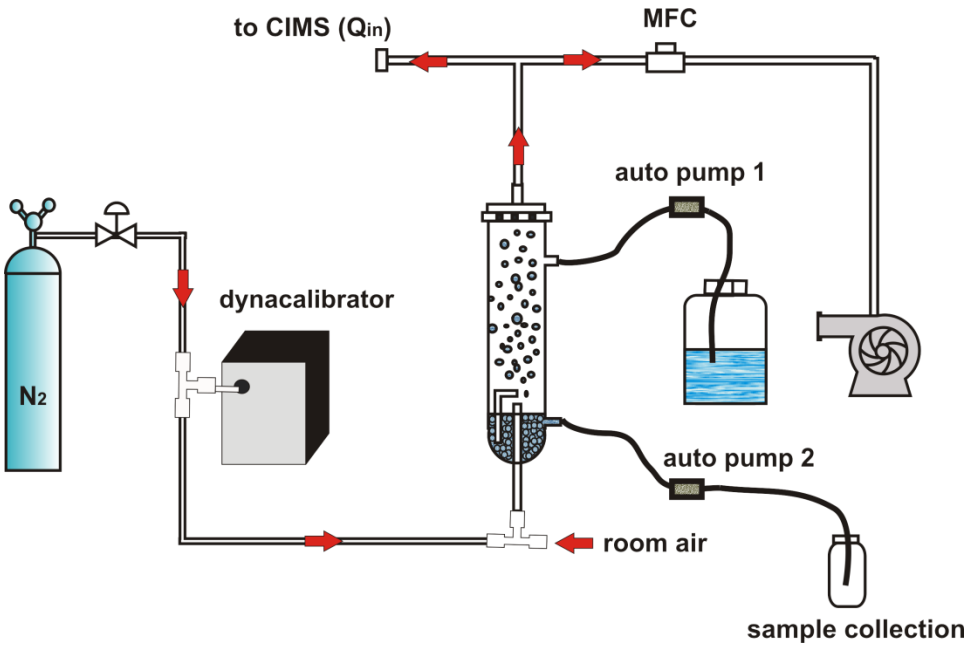

(A)

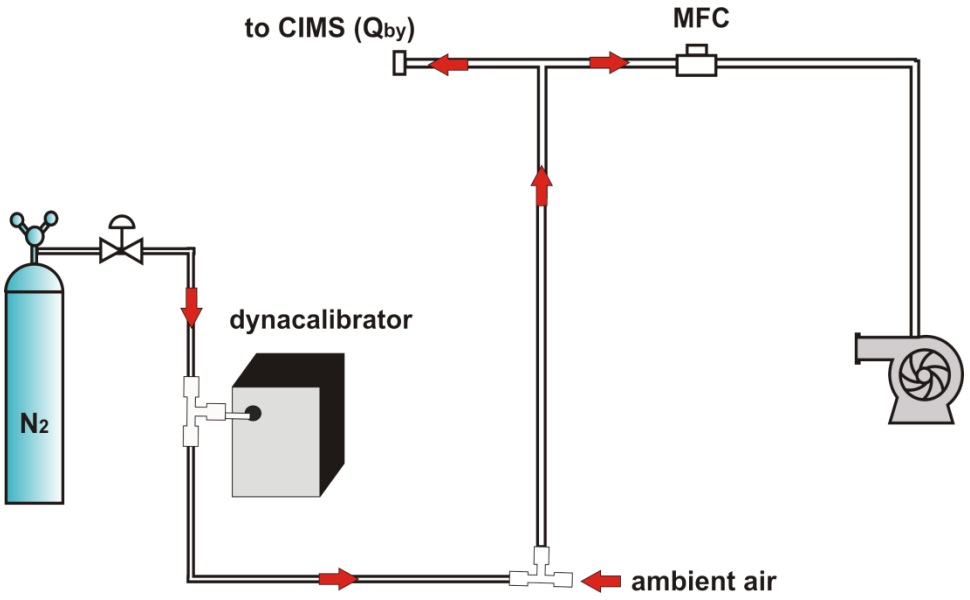

(B)

Figure 4-2 Experimental setup for the determination of COE. In figure A, MIST is inline. In figure B, MIST is bypassed. The red arrow shows gas flow.

4.3 Results

4.3.1 Effect of Teflon filter

A 47 mm diameter hydrophobic Teflon filter (Pall Life Sciences) was placed downstream of MIST to prevent the trapping solution from entering the pump. Filters of different pore diameters were tested for their effect on gas sample collection. Initially, Teflon filters of 2.0 μm pore size were used to collect HCOOH into water. At a flow rate of 25.5 slpm, some water droplets were observed to pass through the filter and to enter the downstream tubing. Then, Teflon filters with pore size of 1.0 μm were utilized. A fine mist was generated at the same gas flow rate. Comparing the CIMS response for the two different filters, it was found that using the CIMS response at m/z 45 using the 1.0 μm pore size filter was half of that by using 2.0 μm pore size one. It indicated that a higher amount of HCOOH was collected into the trapping solution by using filter of smaller pore size.

Filters with pore sizes smaller than 1.0 μm were not tested. After testing several pore-size filters, 1 μm pore size Teflon filter was used in MIST as a liquid barrier.

4.3.2 Collection efficiency of HCOOH (with H_2O trapping solution)

H_2O is commonly used a trapping solution in MIST instruments and was hence investigated first. Gas standard of HCOOH was generated from the permeation tube at 40-70°C (shown in green in Figure 4-3). The standard was determined at m/z 45 in CIMS, shown in blue in Figure 4-3. The total HCOOH was detected in bypassed mode (labeled as sprayer bypass). As shown in the Figure 4-3, during bypassed mode, when the set temperature was changed, it took around 10 min for the dyna-calibrator output to stabilize. But CIMS could respond to the concentration variation right away.

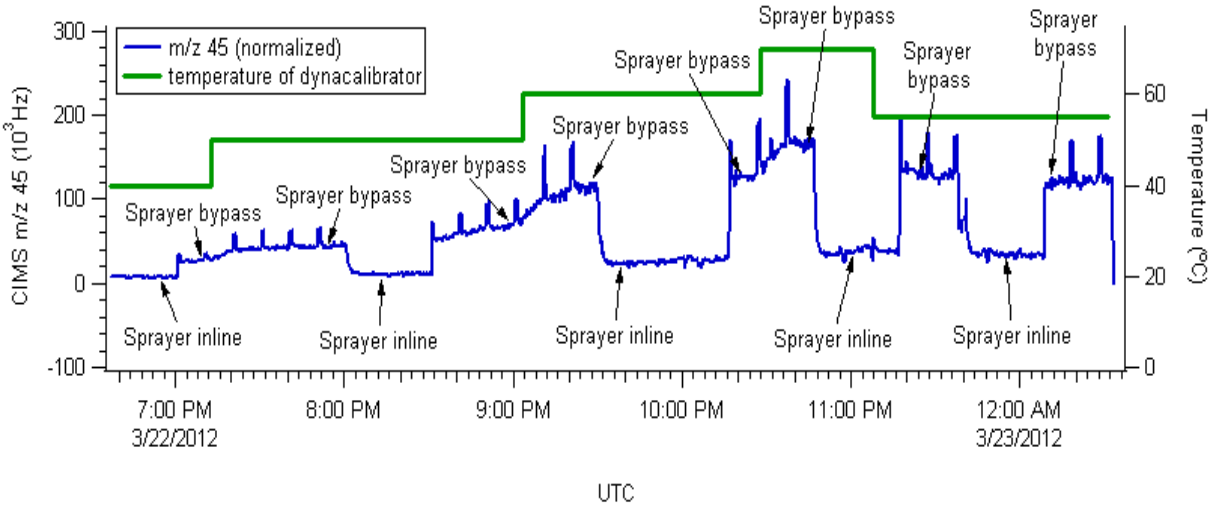

Figure 4-3 Time series of CIMS response while sampling HCOOH. The MIST used H_2O as trapping solution. The green trace represents temperature used to generate HCOOH gas in dyna-calibrator. CIMS response was normalized by reagent ion. The blue trace was CIMS normalized data at m/z 45. UTC = coordinated universal time.

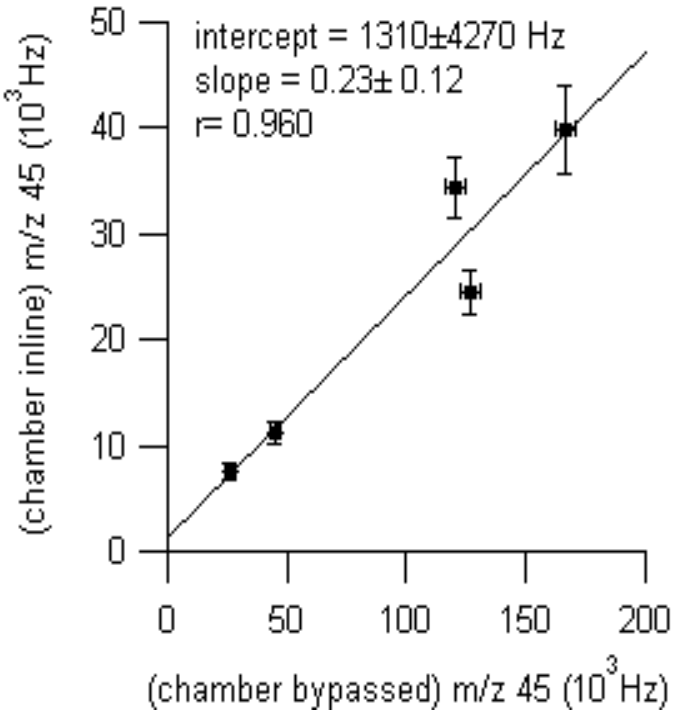

Figure 4-4 Plot of Q_{by} against Q_{in} for HCOOH. The MIST used H_2O as trapping solution.

When MIST was inline (labeled as sprayer inline), HCOOH was collected into trapping solution (H_2O), and the intensity of CIMS response became much lower. No big response difference existed between different temperatures. In MIST, sample was collected in 10 min sampling periods. By the end of each sampling period, the mass flow controller was set to 0 slpm, the trapping solution was drained out of MIST. During these times the CIMS spiked as a result of the pressure increase.

A plot of Q_{by} against Q_{in} is shown in Figure 4-4. Each of the data points is the average CIMS response for the standard of the same concentration. The error bars represent the standard deviation (1σ) in the CIMS measurement. The graph shows that Q_{by} and Q_{in} are highly correlated ($r=0.960$). The slope of the least square regression curve is 0.23 ± 0.12, which corresponds to 1 minus COE. Thus the empirical COE of HCOOH collected by H_2O was equal to $77\% \pm 12\%$.

4.3.3 Collection efficiency of HCOOH (with basic trapping solution)

In another set of experiments, a mixture of 1.16 mM Na_2CO_3 and 1.01 mM $NaHCO_3$ was used to collect HCOOH in MIST at a flow rate of 27.5 slpm. The trapping solution was chosen because of its similarity to the eluent used in IC. HCOOH was generated at dynacalibrator set temperatures of 40 - 60°C. The resulting plot of Q_{by} against Q_{in} is shown in Figure 4-5. From the slope, the COE was determined to be $91\% \pm 10\%$.

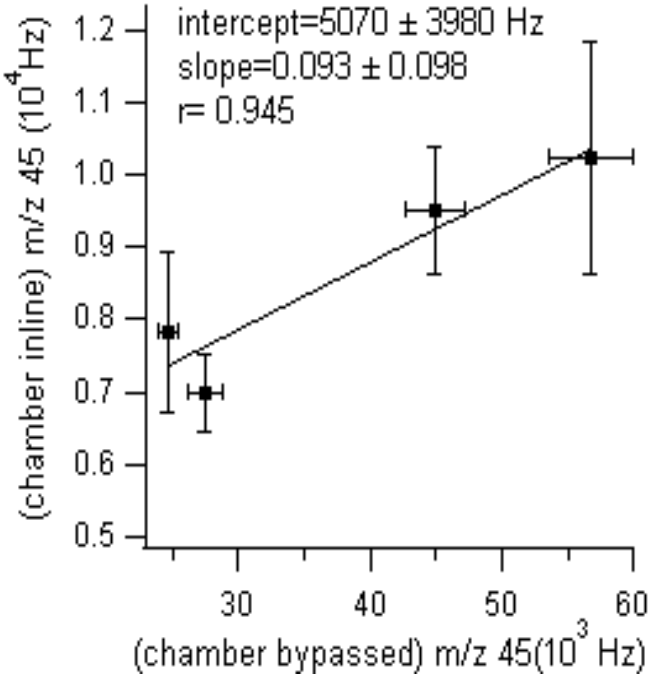

Figure 4-5 Plot of Q_{by} against Q_{in} for HCOOH. The MIST used $NaHCO_3$ and Na_2CO_3 mixture as trapping solution.

4.3.4 Collection efficiency of C_2H_5COOH (with basic trapping solution)

C_2H_5COOH was extracted using 0.18 mM Na_2CO_3 and 0.17 mM $NaHCO_3$ in MIST at a gas flow rate of 30.3 slpm. Gas standards were generated at four different dynacalibrator set temperatures (55 °C, 60 °C, 75 °C and 90 °C). A time series of the CIMS response to the standards is shown in Figure 4-6. Plotting the data as before (Figure 4-7) it was found that 95% ± 8% of C_2H_5COOH was collected into MIST trapping solution (r=0.659).

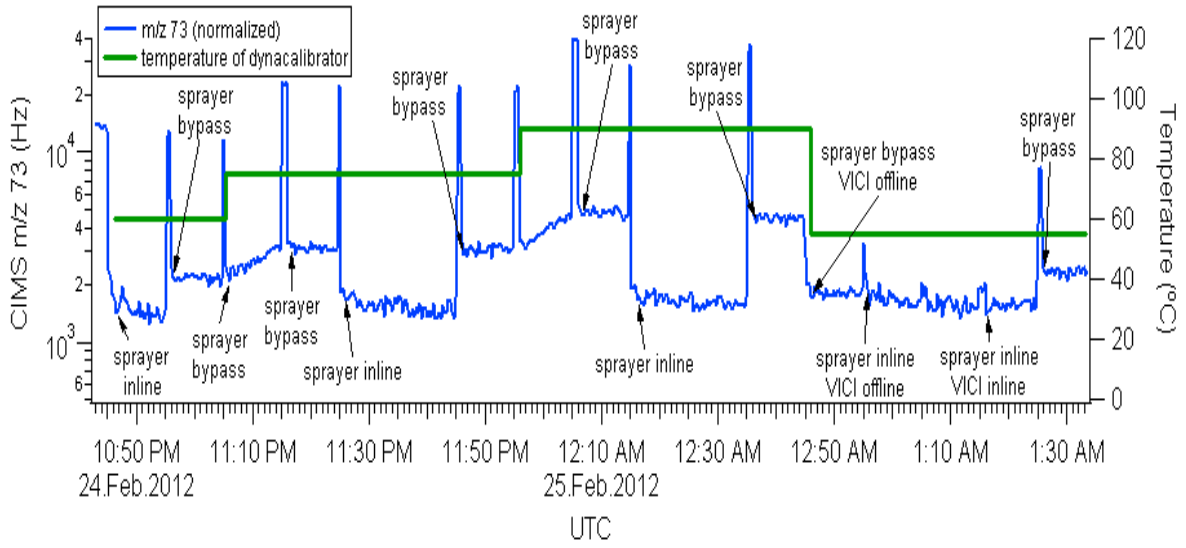

Figure 4-6 Time series of CIMS response while sampling C_2H_5COOH. The MIST used $NaHCO_3$ and Na_2CO_3 as trapping solution. The green trace represents dynacalibrator set temperature used to generate C_2H_5COOH gas. The CIMS response at m/z 73 was normalized to 1,000,000 counts of acetate reagent ion (blue trace).

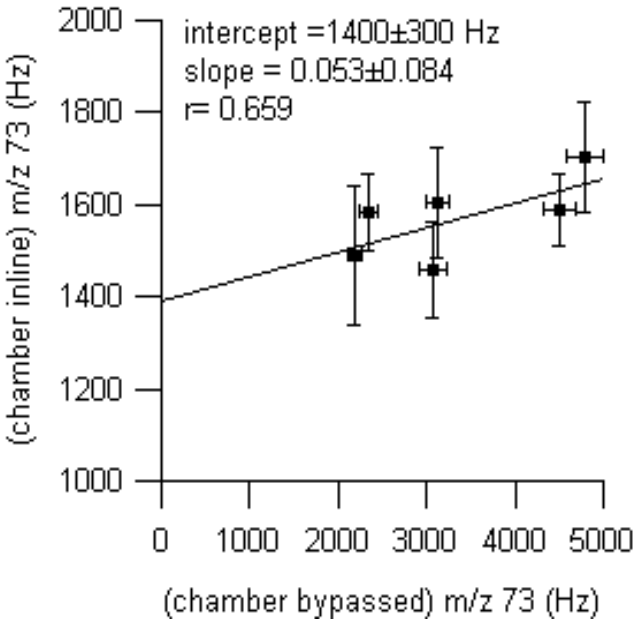

Figure 4-7 Plot of Q_{by} against Q_{in} for C_2H_5COOH. The MIST used $NaHCO_3$ and Na_2CO_3 as trapping solution.

4.3.5 Collection efficiency of HNO_3 (in basic solution)

HNO_3 was extracted by 1.18 mM Na_2CO_3 and 0.98 mM $NaHCO_3$ mixture in MIST at a gas flow rate of 30 slpm for 10 min. Different concentrations of HNO_3 were generated by varying the dynacalibrator set temperature between 40°C and 70° C. The relevant CIMS data are plotted in Figure 4-8. The resulting COE was 95%± 5% (r = 0.868).

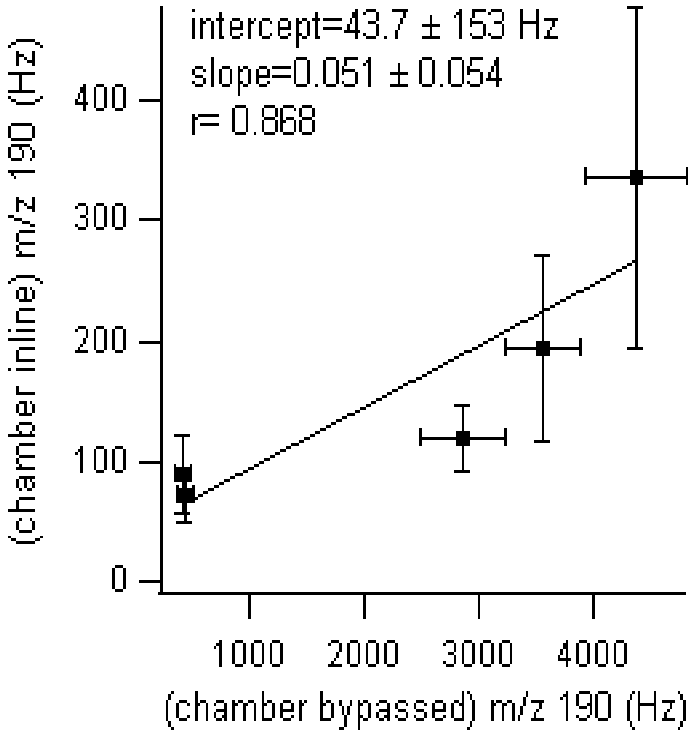

Figure 4-8 Plot of Q_{by} against Q_{in} for HNO_3. The MIST used $NaHCO_3$ and Na_2CO_3 as trapping solution.

4.4 Discussion

4.4.1 Uncertainty analysis and estimates

Table 4-2 summarizes MIST COE for the LMW acids determined in this work. The relative uncertainty of COE determination was estimated to be in the range of 5.7-16% using the

error propagation formula [265]. Potential error sources included in the above error estimates include: variability of the CIMS measurement (both in the signal and the background), drifts in the amount of gas generated by the dynacalibrator, variations in the gas flow rates (and hence dilution factors), impurities present in the room air used to dilute the sample flow, variable trapping solution evaporation rates, and memory effects within the sampling tubing, CIMS, or MIST.

To assess the stability of the CIMS, the relative standard deviation (RSD) and standard deviations of the mean (SDOM) of the CIMS response was calculated for each sampling period (Table 4-3). As shown in Figure 4-4, Figure 4-5, Figure 4-7 and Figure 4-8, the error bars of the ordinate (when the MIST was inline) were larger than those of the abscissa (MIST chamber offline). Thus, the CIMS response had higher RSD when the MIST was inline and the concentrations were smaller. Overall, the uncertainty introduced by the CIMS measurement was small (compared to CE).

Another potential source of error is instability of the gas standard concentrations. The amount of gas generated by the dynacalibrator is affected by set temperature and gas flow. Both of them were controlled and continuously monitored during the measurement. Variation of up to 0.3 slpm gas flow rate was observed during the experiment. Accordingly, around 1% uncertainty could have arisen from fluctuations of the gas flow.

Table 4-2 Determination of COE in MIST

#	compound	Trapping solution	slope	COE (%)	r^2	Relative uncertainty in COE (%)
1	HCOOH	H_2O	0.23 ± 0.12	77 ± 12	0.922	16
2	HCOOH	$NaHCO_3$/ Na_2CO_3	0.093 ± 0.098	91 ± 10	0.893	11
3	C_2H_5COOH	$NaHCO_3$/ Na_2CO_3	0.053 ± 0.084	95 ± 8	0.434	8.9
4	HNO_3	$NaHCO_3$/ Na_2CO_3	0.051 ± 0.054	95 ± 5	0.753	5.7

Table 4-3 Relative standard deviation (RSD) and standard deviation of mean (SDOM) in CIMS determination

#	compound	trapping solution	RSD-inline (%)	SDOM-inline (Hz)	RSD-bypass (%)	SDOM-bypass (Hz)
1	HCOOH	H_2O	9.4	2215	3.6	3188
2	HCOOH	$NaHCO_3$/Na_2CO_3	11.6	1027	4.7	1901
3	C_2H_5COOH	$NaHCO_3$/Na_2CO_3	7	109	4.3	144
4	HNO_3	$NaHCO_3$/Na_2CO_3	34.4	60	13.3	258

During the COE determination experiments, room air was mixed with the gas standards at a flow rate of 18-22.8 slpm. If there had been acids present in it, they would have added to the zero offset (background) signal. As there are strong sinks (e.g., adsorption on the laboratory`s inner walls) and few, if any sources of acids inside the lab, the concentrations of gas-phase acids in room air were relatively small (compared to the mixing ratio of gas standards, > 6 ppm) and relatively constant on the time scale of the experiments. This assumption was also proved by the small intercepts. As a result, the effect of room air on COE determination was negligible.

Measurement errors may also come from the slow adsorption/desorption kinetics of acids within the tubing. Acids are relatively sticky, and their adsorption on instrumentation and tubing can prolong instrument response times. It was shown in Figure 4-6 that, at the highest temperature (90°C), when the dynacalibrator was removed from the MIST (labeled as VICI offline), CIMS response at m/z 73 gradually decreased from 1814 Hz to 1574 Hz. The time constant for the signal to return to the baseline was ~15 min. For HCOOH and C_2H_5COOH, the desorption/absorption kinetics had only a relatively small effect on the results (< 2%), but not for HNO_3. When HNO_3 standard was removed from the line, it took more than 20 min for the signal decaying from 3878 Hz to baseline 3629 Hz (shown in Chapter 5, Figure 5-15). This observation is consistent with the literature. For example, *Neuman et al*. [11] and *Roberts et al.* [159] also showed the strong adsorption of HNO_3 on the walls of tubing. Considering the relatively slow response of the CIMS to changing HNO_3 concentrations, memory effects within the CIMS were a potentially major source of error in its determination.

During the time intervals used in this work (10 - 15 min), the trapping solution volume decreased by between 2.3 and 3.5 mL. This evaporation rate is quite fast compared to other MIST designs. For example, *Stratton et al*. observed that their trapping solution slowly evaporated at a rate of 4 to 6 mL h^{-1} in their MIST [252]. As the solution evaporates, less gas-liquid surface could be formed in the chamber, which resulted in lower COE. Consequently, solution evaporation may explain a small portion of the uncertainty in COE determination.

Of all the parameters discussed above, memory effects were the major source of error contributing to the uncertainty of HNO_3 COE. In contrast, errors associated with gas generation or impurities in room air had insignificant contribution to the uncertainty of our COE values.

4.4.2 Comparison to other measurements of COE

It is informative to compare the results of this work with COE data reported by other groups (Table 4-4). In general, experiments carried out with H_2O trapping solution reported in the literature have COE of 80 to 108% for HCOOH and 70% - 100% for HNO_3. In the MIST used here, the COE for HCOOH was only 77 ± 12% when water was used, lower than most others` research results. It is challenging to directly compare these results, as there are many small differences between instruments and operating parameters. However, it can be concluded that it is inappropriate to assume that MIST is able to collect 100% of all acids into H_2O, as it is sometimes done [251, 252, 256]. It is advisable to use basic solutions to trap acids. Our experiments show that the COE of HCOOH significantly improved to 91 ± 10%.

Table 4-4 Measurements of COE reported in the literature

Group	Trapping solution	COE of collected compounds	COE determination method
Preunkert et al. [1]	H_2O	80 ± 10% (monocarboxylic acid); 70 ± 10% (HNO_3)	2 MIST in series
Lefer et al. [256]	H_2O	100% (HNO_3)	No detection
Talbot et al. [253]	H_2O	100 ± 15% (HNO_3)	gas standards of known concentration
Parmar et al. [263]	H_2O	93% (HNO_3)	2 MIST in series
Keen et al. [258]	H_2O	unknown	unknown
Talbot et al. [69]	H_2O	97.9 ± 1.4% (HCOOH)	gas standards of known concentration
Morikami et al. [259]	H_2O	108 ± 4% (HCOOH)	gas standards of known concentration
Schultztokos et al. [262]	H_2O	100% (HCOOH)	gas standards of known concentration

4.4.3 Relationship between COE and Henry`s law

Spaulding et al. used Henry`s law constants to predict the COE in their MIST [249]. In this approach, the COE is predicted from the equilibrium distribution of acids between the gas- and liquid-phase [249, 266]:

$$COE = \frac{H_x RTr_{liq/gas}}{1 + H_x RTr_{liq/gas}} \qquad \textbf{4-3}$$

In equation 4-3, H_x is the Henry`s law constant of the gas of interest (Table 1-2), R is the ideal gas law constant (0.0826 $L \cdot atm^{-1}\ K^{-1}\ mol^{-1}$), T is the temperature (in K), and $r_{liq/gas}$ is the phase ratio of the liquid water volume contained in the spray to the gas volume in the glass chamber.

Equation 4-3 is applied in this thesis to semi-quantitatively explain the observed trends in COE. It is not meant as an accurate method to evaluate the mist chamber extraction process because it is unlikely that equilibrium is reached in the chamber. Equilibrium is unlikely because the residence time of gases in the chamber is ~0.5 s and short. There are also considerable uncertainties with the phase ratio, which can be only roughly estimated. *Spaulding et al*. estimated that the volume of their mist was ~1 mL, and calculated $r_{liq/gas}$ by dividing the assumed mist volume by the total internal volume of their mist chamber [249]. However, $r_{liq/gas}$ is, in reality, not constant throughout the extraction process. Further, the volume of trapping solution changes (by about 1/5) during sprayer operation, and most of the water volume is actually condensed on the filter at the top of the chamber and on the inner glass walls and is not present as a spray. In this work, two extreme spray volumes, a high estimate of 1 mL and a low estimate of 0.01 mL, were assumed in order to bracket the likely true value. Using a chamber volume of 179 mL and the above assumptions, $r_{liq/gas}$ was calculated to be in the range of 5.6×10^{-3} to 5.6×10^{-5}.

Table 4-4 shows that deionized H_2O is often used for gas sampling in MIST. However, when acids are collected, the solution pH will decrease, which affects their phase partitioning, especially for acids with high pK_a [258]. In basic solution, equation 4-3 needs to be modified to include effective Henry`s law constants (H_x^*) instead of H_x. H_x^* is given by [267]:

$$H_x^* = \frac{[HCOOH_{(aq)}] + [HCOONa_{(aq)}]}{[HCOOH_{(g)}]} = H_x(1 + \frac{K_a}{[H^+]}) \qquad \textbf{4-4}$$

Using equation 4-4, the effective Henry`s law constant in $NaHCO_3$ and Na_2CO_3 was calculated for HCOOH (6.7×10^9 mol·L^{-1} atm^{-1}), C_2H_5COOH (7.4×10^8 mol·L^{-1} atm^{-1}) and HNO_3 (3.2×10^{16} mol·L^{-1} atm^{-1}). These values are larger than those for deionized H_2O (Table 1-2). Basic trapping solutions ($NaHCO_3$ and Na_2CO_3) were used to collect acids in this work. During the sampling of HCOOH, basic trapping solution has showed much higher COE than H_2O (91 ± 10% versus 77 ± 12%, Table 4-5). For comparison, the theoretical COE was calculated using equations 4-3 and 4-4 and is summarized in Table 4-5 for the two assumed $r_{liq/gas}$ values (5.6×10^{-3} and 5.6×10^{-5}).

Table 4-5 Theoretical collection efficiency (COE) in mist chamber

#	compound	trapping solution	theoretical COE (%) with 1 mL mist	theoretical COE (%) with 0.01 mL mist	empirical COE (%)
1	HCOOH	H_2O	99.8	83.5	77 ±12
2	HCOOH	$NaHCO_3/Na_2CO_3$	100.0	100.0	91±10
3	C_2H_5COOH	$NaHCO_3/Na_2CO_3$	100.0	100.0	95±8
4	HNO_3	$NaHCO_3/Na_2CO_3$	100.0	100.0	95±5

The lower-limit estimates of the theoretical COE (i.e., calculated with an assumed mist of 0.01 mL) and the empirical COEs are plotted in Figure 4-9. In all cases, the empirical values are below the predicted ones. This suggests that equilibrium is not achieved within the chamber. However, for all three analyte acids, the empirical error bars encompass the theoretical values. Thus, the trend of theoretical COE values shows good qualitative agreement with the trend in empirical COE, but not necessarily quantitative.

In addition to having an effect on gas-liquid phase partitioning, adding base into the trapping solution also alters the solution density and viscosity. *Zhang et al.* have shown that those solution properties can dramatically affect the spray drop size and liquid flow [268], which can cause a significant change in COE. It was observed in my experiments that basic solution produced smaller and more homogeneous mist droplets in the MIST glass chamber. Hence, better COE would be expected. However, the empirical values are below the predicted values, which even more strongly suggests that the assumption of equilibrium within the chamber is invalid.

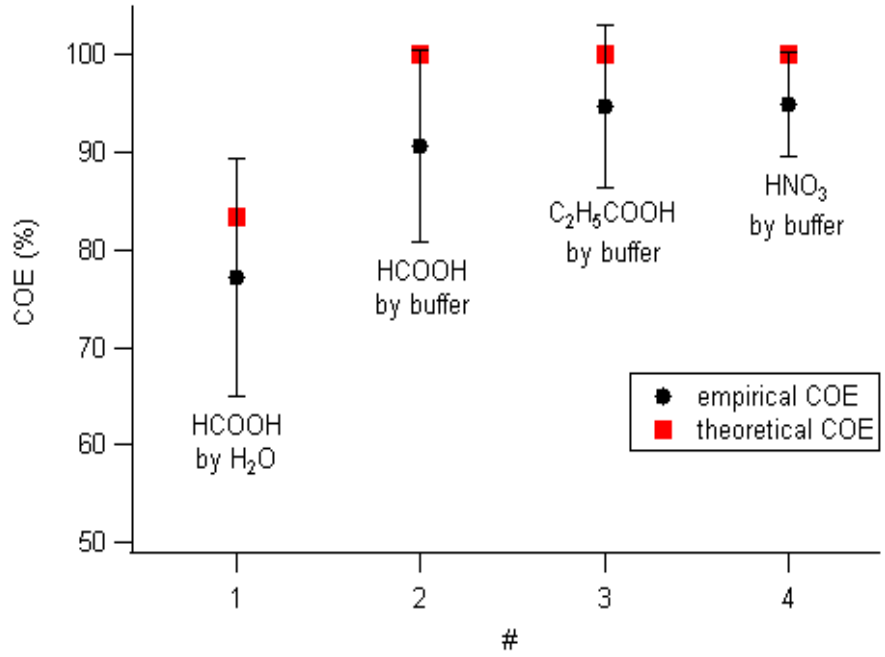

Figure 4-9 Comparison of empirical and theoretical COE. Empirical COE determined from experiment is shown in black. The error bars represented the uncertainties in determination. Theoretical COE is shown as red squares.

4.5 Conclusion

The MIST COE for HCOOH in H_2O was 77 ±12%. Higher COE values were achieved by using buffered solutions:. The MIST COE for HNO_3, HCOOH and C_2H_5COOH were 95 ± 5%, 91 ± 10% and 95 ± 8% in $NaHCO_3/Na_2CO_3$ solution. The trends in the empirical COE could be qualitatively rationalized using Henry`s law.

Chapter Five: **CALIBRATION OF A CHEMICAL IONIZATION MASS SPECTROMETER FOR ANALYSIS OF ATMOSPHERIC ACIDS USING MIST-IC**

5.1 Introduction

Acids are prevalent in the atmosphere. They have important effects on atmospheric acidity [269], heterogeneous reactions [46] and human health [270]. Hence, accurate and fast determination of acids in the air has attracted a lot of scientists` attention. However, the reliable measurement of acids remains a challenge. For example, since acids partition between phases (gas, liquid or solid), many measurement methods can be subject to artefacts [271] In addition, there are issues when air is sampled using an inlet as most acids are sticky [272]. For example, nitric acid can adsorb on many materials which can affect the detection results and degrade instrument response times to changing atmospheric concentrations [11].

Various detection techniques have been developed for acids, including impinger/ion chromatography [273] and filter/ion chromatography [274-276]. These techniques can be accurate (within 10%) [272] and sensitive. They are able to reach low parts per billion (ppbv) level detection limit (LOD), but have usually poor time resolution [271]. Recently, NI-PT-CIMS using acetate reagent ion has been developed to quantify atmospheric acids. It has proved to be a selective and unique technique for the on-line monitoring of acids [277, 278]. Air is sampled and analyzed directly with second or even sub-second time resolution [159].

In this chapter, the calibration of a CIMS operated with either acetate or iodide reagent ion for detection of HNO_3, HCOOH and C_2H_5COOH using the mist chamber - ion chromatography (MIST-IC) method is described. Such calibrations are required because while the relative abundances of ion peaks in a CIMS mass spectrum are proportional to ion concentration

(equation 2-4), they by themselves do not provide the quantitative information of sample components [279]. Hence, response factors need to be determined for monitored each species. IC was chosen for this calibration because it provided higher reproducibility and concentration sensitivity than CE: In Chapters 4 and 3, the RSD of IC was determined to be 1% (compared to 5% of CE), and the LOD for IC was 2 μM (compared to 10 - 20 μM for CE). The focus of the calibration was to derive the factors which relate CIMS response signal to the true concentrations of LMW acids. This also provided an opportunity to directly compare the performance (detection limits, response times, etc.) of the MIST-IC and the CIMS.

5.2 Experimental

5.2.1 Setup

The CIMS was calibrated by sampling dilute mixtures of gas standards, which were generated from a permeation device in parallel to the MIST-IC (see chapter 4). The concentrations of standards were measured by MIST sampling followed by IC determination. In this way, the quantitative information of standards was used for the calibration of CIMS.

To generate gas standards, a permeation device was chosen for it can provide stable and adjustable concentrations of standards. Besides, it also offers the advantages of low cost, small size, portability and safety over other techniques, such as calibrated gas cylinder standards. The emission rates of the latter are rather uncertain and prone to drift because acids adsorb on cylinder surfaces and degrade easily [280]. In contrast, a permeation device shows a much better long term stability and is easier to use [281].

Figure 5-1 shows the setup of this experiment. The output from the dynacalibrator was diluted by a flow of N_2, whose flow rate was controlled by a valve. Moving though Teflon

tubing, part of the dilute gas stream was sampled into CIMS directly at a flow rate of 2 slpm. The remainder was diluted with room air (whose flow rate was around 10 slpm) and sampled by the MIST chamber. The total gas flow rate at the MIST outlet was controlled by a mass flow controller (MFC) to around 30 slpm. Both the MIST and CIMS exhaust were vented into the fume hood to prevent accumulation of acidic gases in the room air. In MIST, gas standard was trapped in solution. The sampling period of the MIST was 10 or 15 min at the end of which the trapping solution was collected and transferred into a glass sample vial, which was capped immediately. The solutions were stored at room temperature without further treatment and analyzed by IC within a week.

In CIMS, HCOOH and C_2H_5COOH were ionized by acetate reagent ion through dissociative electron attachment reaction [157-159]. They were monitored at m/z 45 and m/z 73, respectively. This ionization scheme was not used for HNO_3 as it usually results in high CIMS response (>10^5 Hz) relative to those of the reagent ion (~10^6 Hz); at these count levels, the CIMS response is above the pseudo-first order conditions required for the CIMS to have a linear response. Thus, HNO_3 was ionized using iodide reagent ion which generated fewer ion counts. HNO_3 was monitored as the iodide cluster ion at m/z 190 (see Chapter 2.2.2). Details of the ionization mechanism have been described elsewhere [282]. This method has the advantage of low background counts but it is less sensitive than using acetate reagent ion.

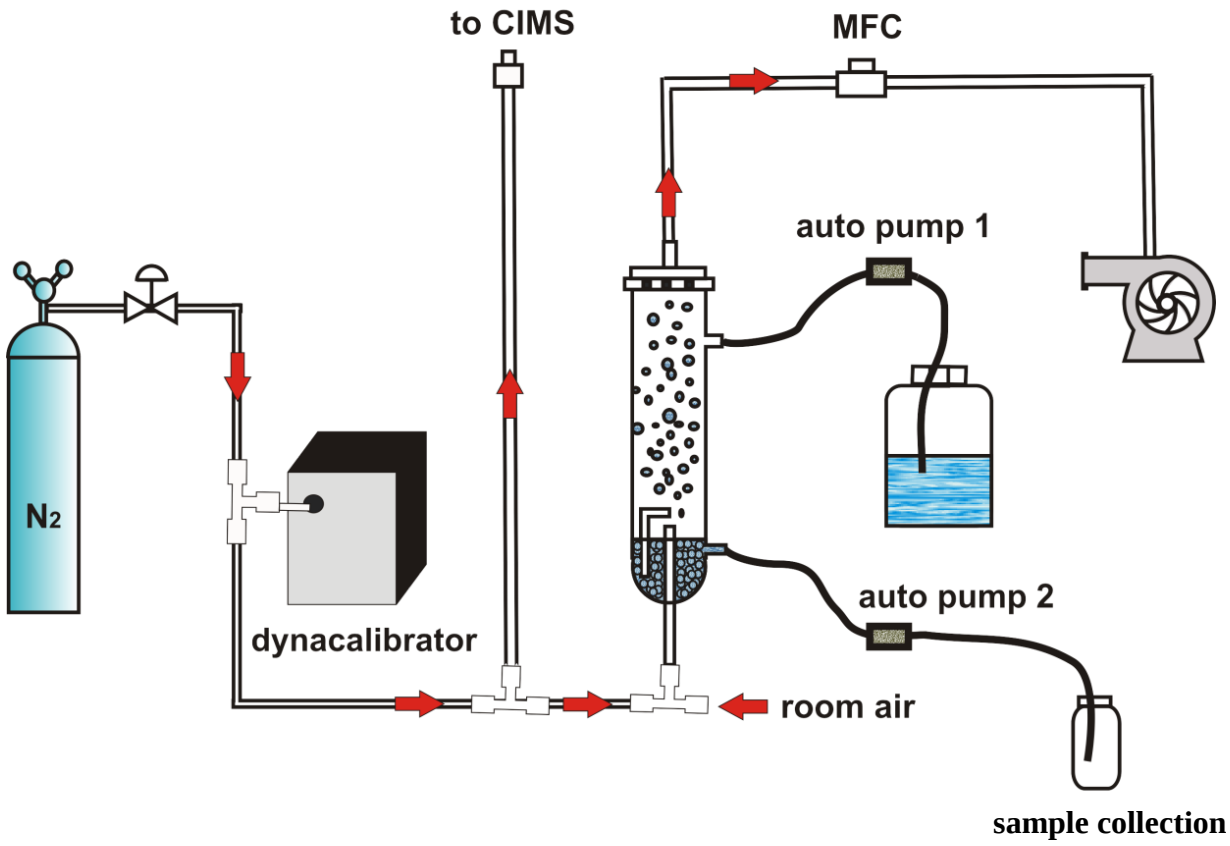

Figure 5-1. CIMS Calibration Setup. The red arrows show the direction of gas flow. Generated from dyna-calibrator, acid standard was pumped out and mixed with N_2. N_2 gas diluted standard concentration and increased its flow rate. The diluted gas standard was introduced into CIMS at the downstream 3-way valve. Part of gas standard kept on moving to another 3-way valve and mixed with room air before entering MIST. At the beginning of sampling period, trapping solution was pumped into MIST through auto pump 1. At the end of the sampling period, solution was drained out from auto pump 2. The sample solutions were analyzed offline by IC.

5.2.2 Evaluation of CIMS

5.2.2.1 Calibration of CIMS mass axis

In CIMS, instability or drift of its mass axis can have a large effect on its response. Thus, the CIMS mass axis was calibrated at the beginning of each experiment. It was calibrated using mass scans in the regions m/z 55 - 65, m/z 120 - 135 and m/z 185 - 195 when only N_2 was introduced. These regions were chosen because the mass spectrum always contained typical peaks at m/z 59, 61, 127 and 190. Peaks at m/z 59 and 127 came from the reagent ions CH_3COO^- and I^-. Even if they were not used in a particular experiment, their peaks were still present due to memory effects from the Teflon tubing and fittings through which the reagent ions were delivered. Counts at m/z 61 were due to $^{13}CH_3{}^{13}COOH$ which was used in previous experiments. The m/z 190 peak resulted from the attachment of HNO_3 with I^-. It was present even when the CIMS is sampling ultrapure ("zero" grade) air. Hence, those four typical peaks were chosen to calibrate the mass axis.

5.2.2.2 Determination of CIMS background and CIMS Data Reduction

Figure 5-2 shows a time series of CIMS data in a typical experiment, in which HNO_3 was detected by CIMS as well as collected by $NaHCO_3/Na_2CO_3$ in MIST. The green dashed line on the top shows temperatures used to generate gas standards in the dyna-calibrator. A larger amount of HNO_3 was generated at higher temperature. There were three kinds of measurements performed to calibrate CIMS: room air (labeled as A), background (labeled as B) and calibration measurements (labeled as C).

In calibration measurement (C), the dyna-calibrator was kept on, and gas standards mixed with N_2 were sampled. During background measurements (B), the output of the dyna-calibrator

was closed. N_2 flushed though the same route of tubing and entered CIMS. CIMS counts were significantly lower at this time. The remaining counts were likely due to desorption of HNO_3 from the inner walls of tubing and instruments [283]. During room air measurements (A), both the N_2 and the dyna-calibrator were disconnected. Data from this measurement informed us about the background levels of acids in room air, which were the indistinguishable from measurements made in N_2 (B).

In Figure 5-2, the red trace shows the "raw" CIMS response at m/z 190. It is common practice in CIMS measurements to normalize the response to 10^6 counts of reagent ion (shown as a light green trace).

In the experiment shown in Figure 5-2, the background (black dashed line) was (average ± 1 standard deviation) 4850 ± 638 Hz and decreased slightly over time. A straight line fit was determined for the background measurement. The regression coefficient (r^2) was 0.99 and the slope -0.1 Hz/s. The drift in the background is likely due to HNO_3 desorbing from within the ^{210}Po source, which is cleaned with HNO_3 at the factory; as the reagent gas is flowing through the ion source, the rate of HNO_3 desorption slowly decreases. For the calibration, the background response was subtracted from the normalized CIMS data. Since the background was changing slowly and linearly, the final CIMS response was obtained by subtracting the least-square fitting curve from m/z 190 (normalized), labeled as m/z 190 (background subtracted) in Figure 5-2. It is shown as a blue trace.

During room air measurement (A), the average counts of m/z 190 normalized data were 3859 ± 246 Hz. If the background is subtracted, the CIMS response was very close to zero (238 ± 205 Hz), indicating that HNO_3 was present only at a very low level in room air. Hence, acids present in room air did not affect the accuracy of acid detection by MIST-IC.

For the determination of C_2H_5COOH (Figure 5-3), the background signal was 669 ± 160 Hz. The background signal increased marginally over time, with r^2 of 0.86 and slope equal to 0.012 ± 0.003 Hz/s. The origin of this slight drift is unclear, but since it was well-characterized, it did not pose a problem to the quantitative analysis.

When HCOOH was determined, the background signal was 3850 ± 19 Hz (Figure 5-4). However, they gradually decreased over time (slope = -0.09 ± 0.08 Hz/s). Since the slope was close to zero, it indicated the absence of any significant background drift.

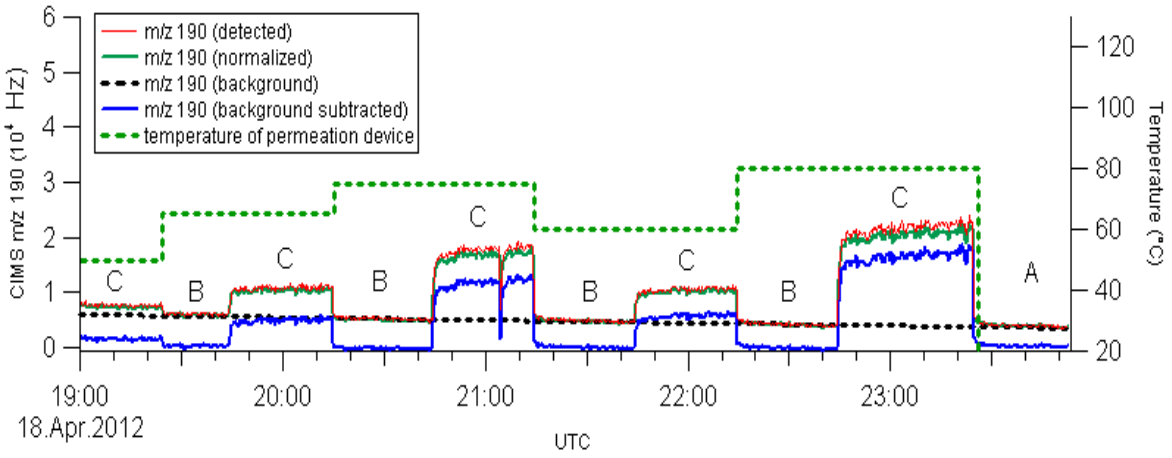

Figure 5-2 Time series of HNO_3 calibration experiment. It included three modes—room air (A), background (B) and calibration (C) measurements.

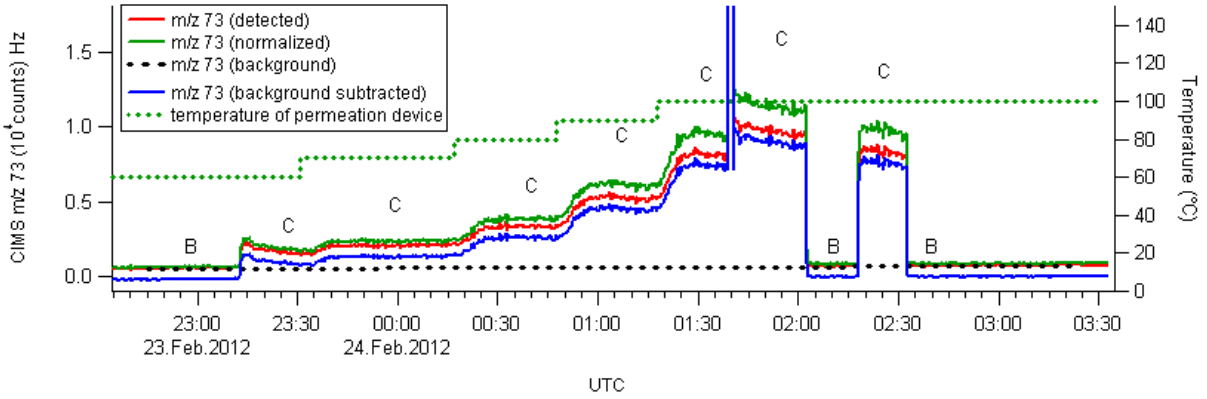

Figure 5-3 Time series of C_2H_5COOH calibration experiment. Temperature is shown as a dashed green trace. Measured counts at m/z 73 are labeled as "m/z 73 (detected)" (red solid line). Data normalized by reagent ion are labeled as "m/z 73 (normalized)" (green solid line). The background signal is labeled as "m/z 73 (background)" (dashed black line). After subtraction from background signal, data are labeled as "m/z 73 (background subtracted)" (blue solid line).

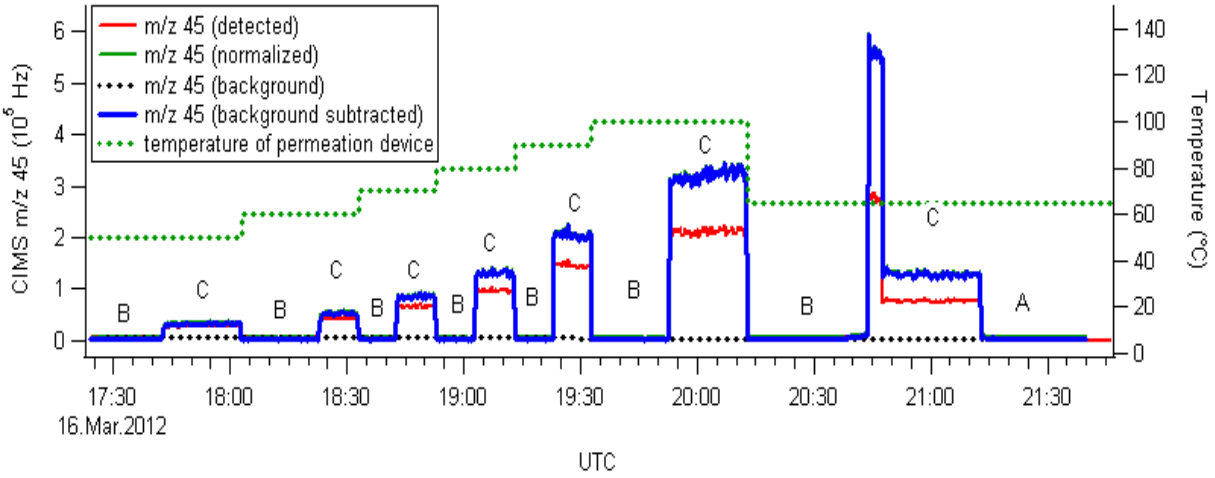

Figure 5-4 Time Series of HCOOH calibration experiment. Data points of "m/z 45 (normalized)" overlapped with data points of "m/z 45 (background subtracted)".

5.2.3 Calculation of gas-phase mixing ratios from IC data

In MIST-IC, acids were determined in liquid phase, while in CIMS, they were in the gas phase. To convert sample concentration in liquid ($C_{(l)}$) to gas phase mixing ratio ($C_{(g)}$), the following equation was used:

$$C_{(g)} = \frac{V_{mist} \cdot C_{(l)}}{t \cdot (F_{mist} - F_{air}) \cdot \eta_{eta} \cdot COE} \quad \textbf{5-1}$$

Here, $C_{(l)}$ is the sample concentration in trapping solution (in units of M), V_{mist} is the volume of trapping sample solution in MIST (in L), t is the sampling time (in min), F_{mist} was total gas flow rate (in slpm), F_{air} is the flow rate of room air entering MIST (in slpm), COE is the collection efficiency of MIST, $\eta_{e.g}$ and is the sample air density (in mol/L).

Air density ($\eta_{e.g}$) is affected by temperature and pressure. It is calculated using the ideal gas law:

$$\eta_{eta} = \frac{P}{0.08205 \frac{L \cdot atm}{K \cdot mol} \cdot T} \quad \textbf{5-2}$$

At the conditions used in the experiments (P=0.895 atm, T=295.15 K), the air density was 2.23×10^{19} molecules cm^{-3}. From Equation 5-1 and 5-2, the gas phase mixing ratio was calculated and used to determine CIMS response factors.

5.3 Results

5.3.1 IC Detection

The calibration of $HCOO^-$, $C_2H_5COO^-$ and NO_3^- in IC was discussed in Chapter 2. In Figure 5-5, when water was injected, two negative system peaks appear in the chromatogram

(shown in red). One is likely an artefact arising from the injection (i.e., an air bubble). They may also be caused by contaminants on the IC column or inlet, as this instrument is usually used to analyze wine samples. The top black trace in Figure 5-5 (A) shows a propionate standard of 126 µM. The propionate peak was identified as the positive peak eluted at 1.8 min. System peaks do not interfere with it. Peaks of $HCOO^-$ (retention time=1.25 min) and NO_3^- (retention time=2.14 min) were also resolved from system peaks. Their retention times were quite reproducible (1% RSD).

To verify the absence of any effects resulting from using a basic trapping solution components on the IC analysis, the MIST trapping solution (2.2 mM $NaHCO_3$/2.4 mM Na_2CO_3) was injected into IC (in light blue trace, 3rd from top; Figure 5-5 (A)). It exhibited the same peaks as the H_2O sample. Thus, the trapping solution did not bring in any extra peaks. MIST sample of propionic acid was analyzed in IC (shown in dark blue). The positive peak eluted at 1.8 min was identified as the $C_2H_5COO^-$ peak. An expansion of this peak is shown in Figure 5-5 (B). It was slightly asymmetric. Both peak area and peak height have been used to make calibration curve. Peak area (units of µS·min) was used because of its better linearity.

(A)

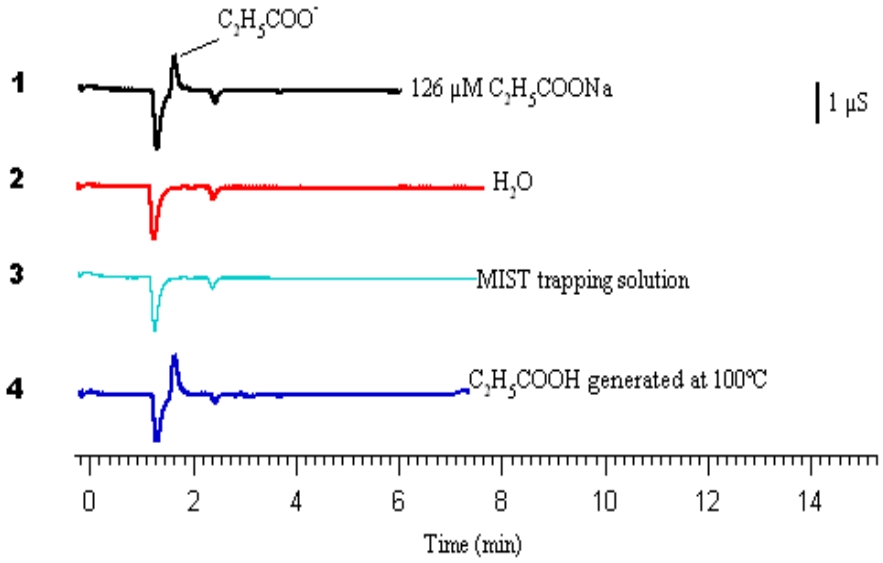

(B)

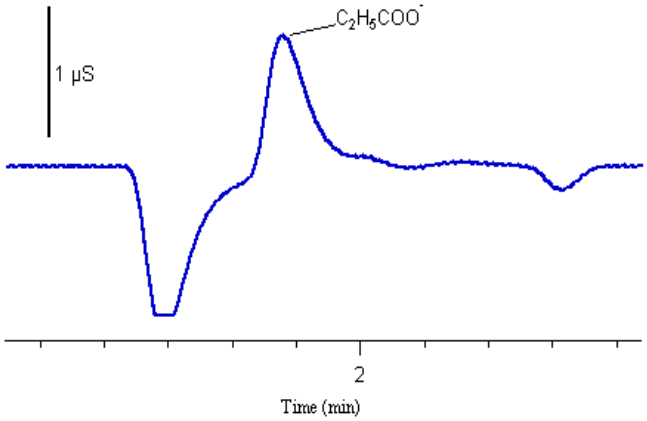

Figure 5-5 (A) Sample IC chromatograms of (1) IC standard, 126 µM C_2H_5COONa; (2) H_2O; (3) MIST trapping solution, 2.2 mM $NaHCO_3$/2.4 mM Na_2CO_3; (4) C_2H_5COOH sample collected in MIST. (B) Expansion of the 4th chromatogram.

5.3.2 Uncertainty of MIST-IC analysis

A summary of the factors affecting MIST-IC analysis is presented in Table 5-1. Due to variation of gas flow rate (~0.3 slpm), uncertainty in trapping solution volume and gas flow rate may introduce around 5% error in the analysis. As discussed previously, uncertainty in COE of MIST is up to 10.8% for HCOOH sampling. Error of 4.3% is in IC detection based on the uncertainties in the slope and y-intercept of IC calibration.

Based on the analysis of background signal, a memory effect was observed in MIST. It is shown in Figure 5-6, when it was switched from calibration measurement to background measurement. The CIMS response decreased to background level instantly, while MIST-IC data gradually returned to baseline (~15 min for C_2H_5COOH, discussed in Chapter 4). This might be caused by the residual of analyte on the inner wall of chamber or filter. The effect of wall losses is unknown. But the sampling was carried out above 10 °C to minimize the loss of acids to the tubing walls [11]. Wall losses effect can be further improved by using tubing covered with PFA [11, 284]. Consequently, the total uncertainty of HCOOH analysis in MIST-IC was around 13%. For the analysis of C_2H_5COOH and HNO_3, uncertainties in MIST-IC were 21% and 17%, respectively.

Table 5-1 Uncertainty in MIST-IC analysis of HCOOH**.**

Factors	Uncertainty (%)
Gas flow rates	5
COE of MIST	10.8
IC calibration	4.3
Total error	~13

5.3.3 CIMS Calibration

5.3.3.1 CIMS Calibration of C_2H_5COOH

Experimental parameters of CIMS calibration were summarized in Table 5-2. The gas generation temperature was chosen randomly ensuring adequate response in CIMS. C_2H_5COOH was sampled into basic solution in MIST. Figure 5-6 shows a time series of its typical calibration experiment. The normalized and background-subtracted counts at m/z 73 are shown as a blue line. CIMS response (shown in blue) changed according to the change of the set temperature in the dyna-calibrator (shown in green). The MIST-IC data are shown as black and red solid circles. At 1:39, the N_2 cylinder was changed, resulting in a temporary overexposure of the instruments to C_2H_5COOH. The CIMS recovered quickly, whereas the mist chamber data were compromised, exhibiting a considerable memory effect. The data (in red) were not used in the analysis. The error bar of the abscissa represents the sampling time of 15 min, while error bar of the ordinate is uncertainty in MIST-IC measurement.

The CIMS response averaged over MIST-IC sampling period is plotted against gas phase mixing ratio in Figure 5-7. IC data points shown in red were caused by memory effect of MIST, which were not used for CIMS calibration. From the slope of Figure 5-7, the CIMS response factor for $C_2H_5COO^-$ was determined as 41 ± 5 Hz/ppb (r = 0.97). In Figure 5-7, error bars of abscissa represented the total uncertainties in MIST-IC determination. Error bars of the ordinate represented uncertainties originating from CIMS detection, which was the standard deviation of normalized CIMS signal at m/z 73 during 15 min sampling time.

Table 5-2 Parameters of acids sampling in MIST-IC for CIMS calibration

compounds	trapping solution in MIST	T (ºC) for gas generation	F_{mist} (slpm)	Sampling time (min)
HCOOH	1.0 mM $NaHCO_3$/1.2 mM Na_2CO_3	40-60	27.5	10
HCOOH	H_2O	40-100	27.5	10
C_2H_5COOH	0.17 mM $NaHCO_3$/0.18 mM Na_2CO_3	60-100	30.3	15
HNO_3	0.98 mM $NaHCO_3$/1.18 mM Na_2CO_3	40-70	30.0	10

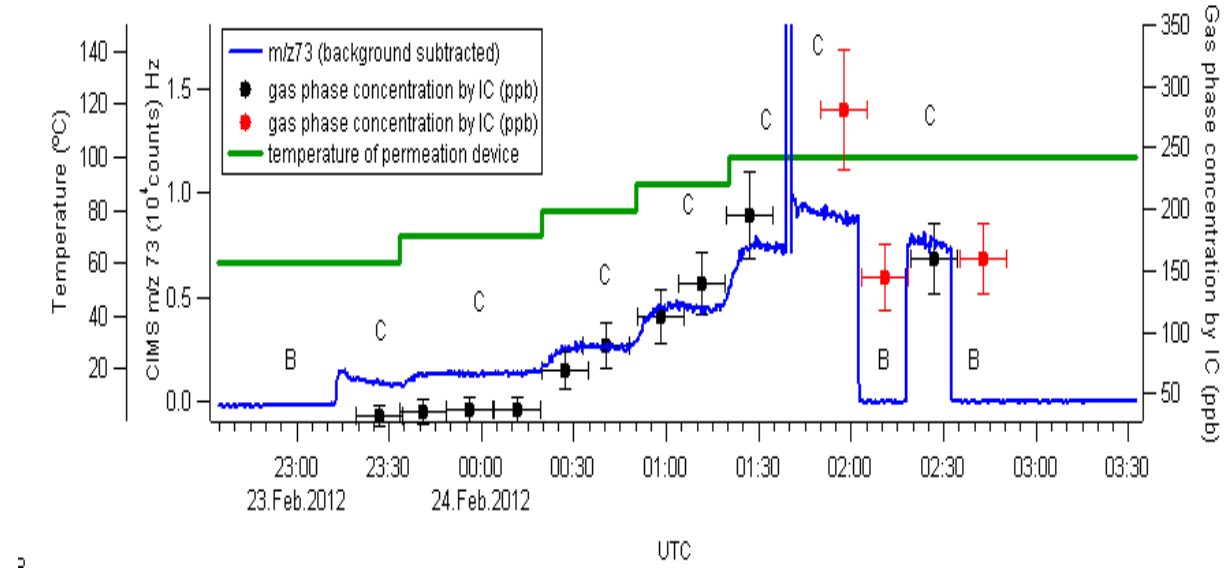

Figure 5-6 Determination of propionate ($C_2H_5COO^-$) in CIMS and MIST-IC. CIMS response is shown in blue line and MIST-IC result is shown in black or red solid circles. 0.17 mM $NaHCO_3$/0.18 mM Na_2CO_3 was the trapping solution in MIST.

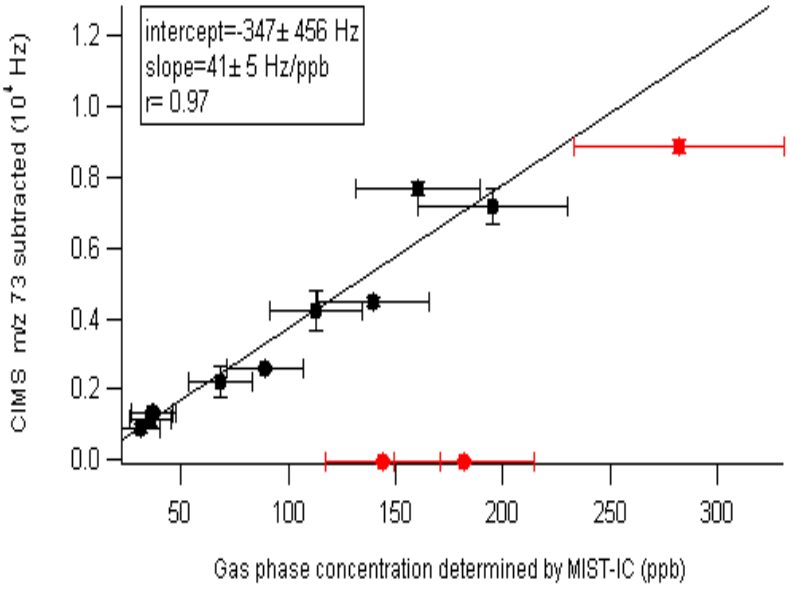

Figure 5-7 Calibration of propionate detection in CIMS by using MIST-IC. $NaHCO_3/Na_2CO_3$ was used as trapping solution in MIST. Abscissa is gas phase mixing ratio determined by IC, while ordinate is CIMS response at m/z 73. Error bars represent the respective precisions of the IC and CIMS measurements. The red solid circles, which resulted from the memory effect in MIST-IC, were not used for the calibration.

5.3.3.2 CIMS Calibration of HCOOH

A typical calibration experiment is shown in Figure 5-8. 1.0 mM $NaHCO_3$/1.2 mM Na_2CO_3 was trapping solution in MIST. The CIMS counts at m/z 45 followed closely the temperature changes of permeation device, whereas the MIST-IC tended to have higher concentration when permeation device was switched from calibration mode to blank mode (data was shown in red solid circle in Figure 5-8). This indicated that there are memory effects in the MIST that are not present in the CIMS. There were two points (shown in red solid circle in Figure 5-8) having low response in MIST-IC detection, while the CIMS response during the

sampling period was very high. The cause of this low response in MIST-IC was unknown. As it was observed that the data in red circle was not correlated to CIMS response, they were not used for CIMS calibration.

During the measurement of HCOOH, the gas standard mixing ratio was in the range of 2 to 14 ppb, which was close to the MIST-IC LOD (6.3 ppb). Thus, it was difficult to determine concentration at this level in MIST-IC with high accuracy. Consequentially, Figure 5-9 shows large error bars on the abscissa. When CIMS data was plotted against IC response, the correlation coefficient (r) was lower than in the other experiments (0.82). Based on the least square regression analysis, response factor of CIMS to formate was 7 ± 2 Hz/ppt.

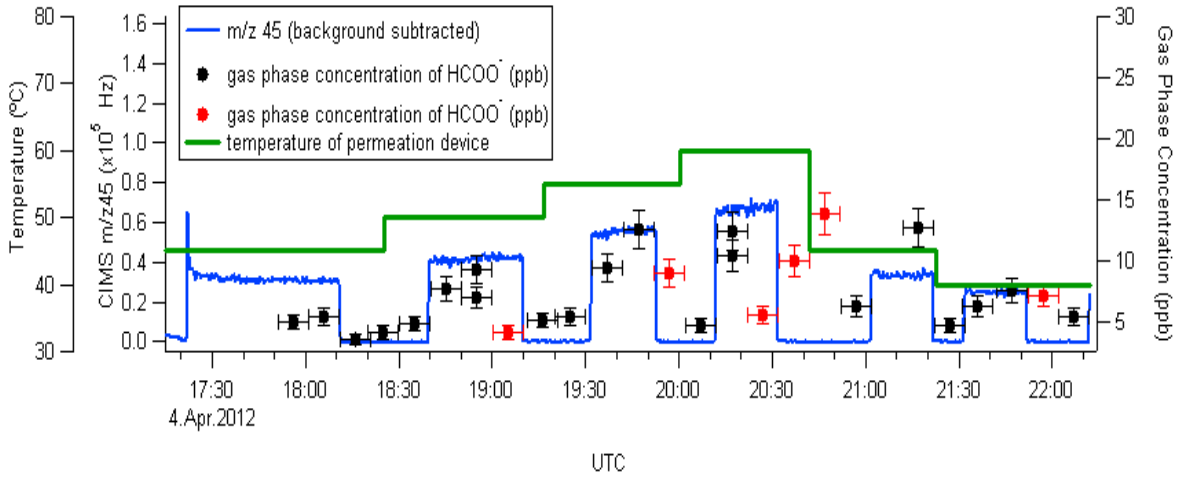

Figure 5-8 Determination of formate ion in CIMS and MIST-IC. HCOOH was collected into 1.0 mM $NaHCO_3$/1.2 mM Na_2CO_3 in MIST. CIMS response is shown in blue line and MIST-IC result is shown in black or red solid circles.

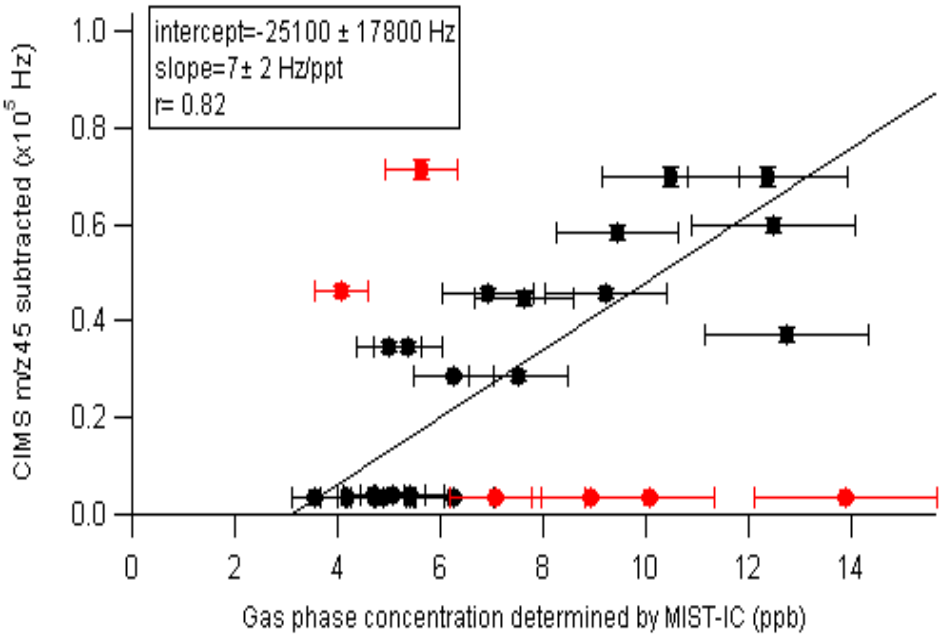

Figure 5-9 Calibration of formate detection in CIMS by using MIST-IC. 1.0 mM $NaHCO_3$/1.2 mM Na_2CO_3 was the trapping solution in MIST. Data in red circle were not used to fit the calibration line. The red solid circles were not used for the calibration.

H_2O was also used to collect HCOOH in MIST in the calibration experiments (Figure 5-10). The CIMS response correlated with the set point change of the dyna-calibrator. However, most sample collected by CIMS-IC showed similar concentrations (20 to 30 ppb, in black solid circle), even though the dyna-calibrator delivered different sample concentrations. Two samples (shown as red solid circles) showed much higher concentration (50 to 60 ppb). When MIST-IC data was plotted against CIMS response in Figure 5-11, the data were not correlated.

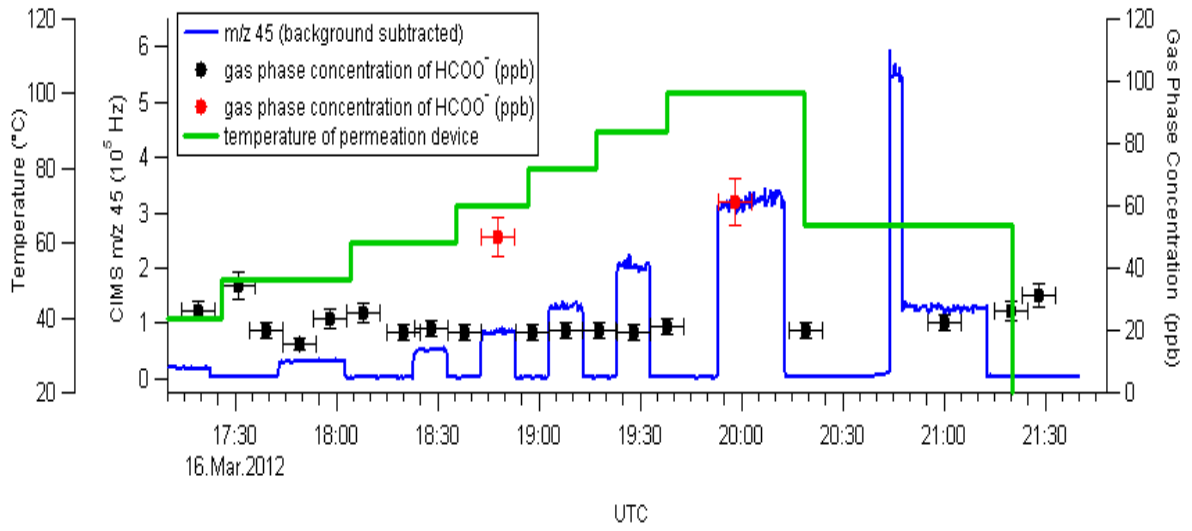

Figure 5-10 Time series of formic acid calibration. H_2O was used as trapping solution in MIST. The red solid circle showed high concentrations in MIST-IC results.

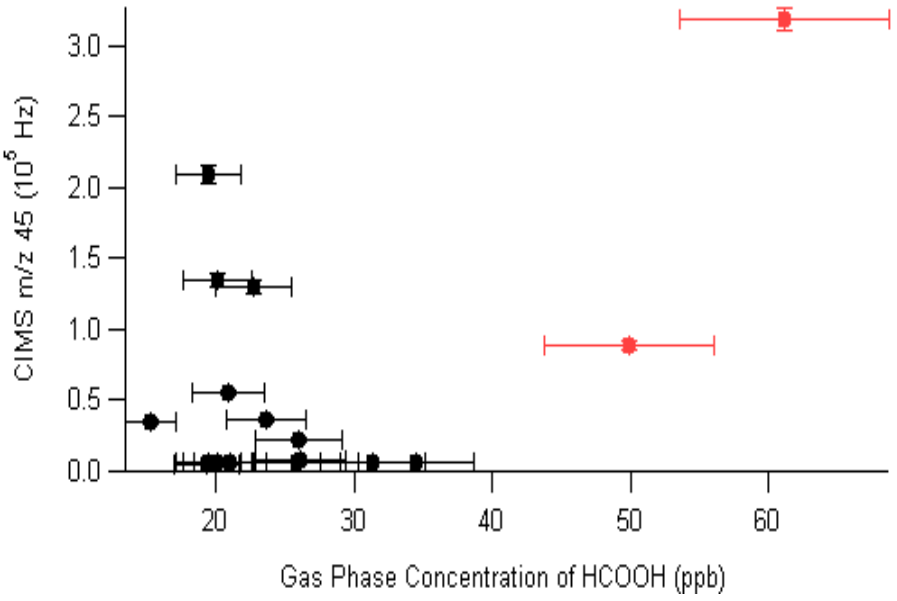

Figure 5-11 Attempted calibration of HCOOH. H_2O was used as trapping solution in MIST. Data points in red showed high concentrations of formate in MIST-IC detection.

5.3.3.3 CIMS Calibration of HNO_3

Na_2CO_3/$NaHCO_3$ was used to collect HNO_3 in MIST (details of sampling conditions were shown in Table 5-2). The COE was 95 ± 5% (Chapter 4). Figure 5-12 shows that both MIST-IC and CIMS correlated well with dynacalibrator temperature changes. In Figure 5-13, two sets of data were plotted against each other. The slope of least-square regression line was 259 ± 69 Hz/ppb with correlation coefficient (r) of 0.82. At low mixing ratio (< 15 ppb), MIST-IC response did not correlate with CIMS well. As the standard`s concentration increased, a better positive correlation was shown. CIMS showed higher response to nitrate than to propionate. However, the r of nitrate fitting was much lower.

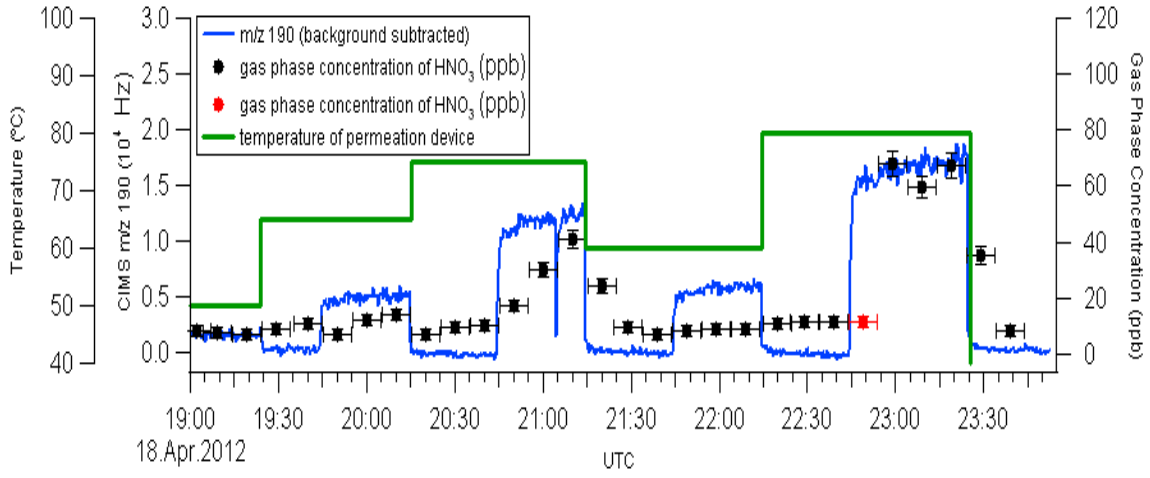

Figure 5-12 Determination of nitrate ion in CIMS and MIST-IC. 0.98mM $NaHCO_3$/1.18mM Na_2CO_3 was used as trapping solution in MIST. The red solid circle showed low response in MIST-IC, which was not correlated with CIMS response.

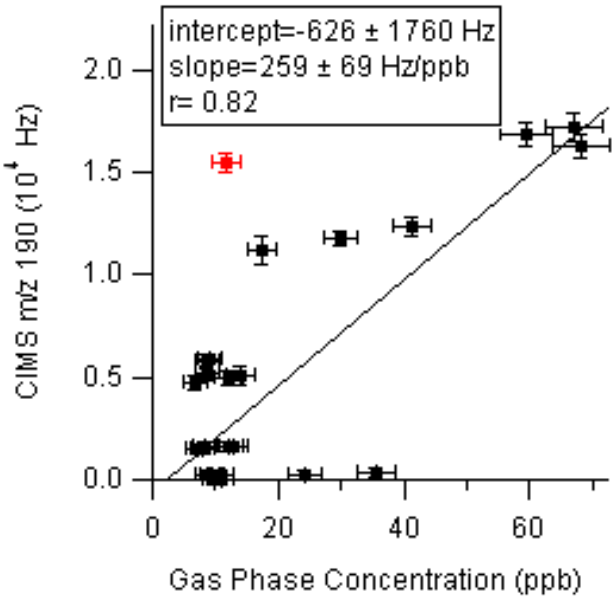

Figure 5-13 Calibration of nitrate ion in CIMS by using MIST-IC. 0.98 mM $NaHCO_3$/1.18 mM Na_2CO_3 was used as trapping solution in MIST. The red solid circle was not used for calibration.

5.3.4 Detection Limit of CIMS

The CIMS detection limits were estimated from three times the standard deviation of the background, divided by the slopes of the calibration plots, which were 7 ± 2 Hz/ppt (HCOOH), 41 ± 5 Hz/ppb (C_2H_5COOH), and 259 ± 69 Hz/ppb (HNO_3). Table 5-3 summarizes the results.

Table 5-3 Detection Limit of CIMS

compound	**σ (Hz)**	**n**	**3σ (Hz)**	**LOD (ppb)**
HCOOH	392	8	1270	0.18 ± 0.06
C_2H_5COOH	35	8	114	2.8 ± 0.1
HNO_3	189	8	613	2.2 ± 0.6

5.4 Discussion

5.4.1 CIMS calibration factors

This work demonstrated that the MIST-IC can be used to determine CIMS response factors of LMW acids. It is dynamic and inexpensive. Compared to other calibration methods, such as the mobile organic carbon calibration system developed by *Veres et al.*, which calibrated volatile organic compounds through combustion and quantified the CO_2 product [160], MIST-IC is a more universal calibration method. It can, in principle, be used for any acid, including non-carbon containing ones. In the cases of C_2H_5COOH and HCOOH, the major source of CIMS calibration error was the relatively large uncertainty in MIST COE. They were as high as 8.9% (C_2H_5COOH) and 11% (HCOOH). In the case of HNO_3, the major error source was the uncertainty of IC calibration (7.1%).

There were stark differences in the observed CIMS response factors: CIMS has the lowest sensitivity to C_2H_5COOH among three LMW acids, which was 0.041 ± 0.005 Hz/ppt (using acetate as reagent ion). It has considerably higher sensitivity to HCOOH - 7 ± 2 Hz/ppt (using acetate reagent ion). The CIMS response factor to HNO_3 was 0.26 ± 0.07 Hz/ppt (using I^- as reagent ion).

These response factors compare well to the work by others, considering that no effort was made to optimize them. For the detection of HNO_3, for example, *Abida and Osthoff* used the same CIMS instrument as calibrated against a total odd nitrogen (NO_y) analyzer. They reported a response factor of 1.2 Hz/ppt [282]. The 4-fold greater sensitivity in their work can be rationalized by the use of a newer ^{210}Po ion source (i.e., more radioactive) and a greater pressure (21 vs 19 Torr) in the ion-molecule reaction region. *Roberts et al.* used acetate reagent ion to measure HNO_3 and reported the sensitivity of 6 counts/ppt and LOD of 30 ppt [159]. In the

experiments here, a less sensitive ionization method was used to ionize HNO_3. Thus, my CIMS showed much lower sensitivity.

For quantification of HCOOH using acetate reagent ion, *Veres et al*. [157] reported a sensitivity of 21 ± 4 Hz/ppt, three times higher than the sensitivity in this work. These calibration factors correspond to LODs in the range of 80 to 90 ppt for a 1 second integration period for their instrument, while ours were in the range of 120 to 240 ppt. While instrumental background signal is an important factor affecting the LOD, the signal to noise ratio could in principle be improved further, for example by optimizing gas flow rate, temperature and pressure in the flow tube [283]. Another factor to be investigated is if, and if so, how, the sensitivity of an acid CIMS is affected by humidity. While *Veres et al*. reported no humidity-dependence [157], *Zondlo et al.* reported that ambient humidity affects the sensitivity [285]. In the experiments described here, the relative humidity was maintained at a constant level using a bubbler as described by *Mielke et al*. [178] On a side note, in my research, acetate ion was produced from glacial acetic acid (CH_3COOH), where *Veres et al*. used acetic anhydride ($(CH_3CO)_2O$) to generate the reagent ion [157]. The results provided here show that glacial acetic acid can be a substitute in acids analysis in CIMS to detect organic acids. However, it might lead to the lower sensitivity of CIMS response.

Veres et al. have studied the measurement of propionic acid by CIMS using acetate reagent ion [158]. Their CIMS response factor to propionic acid was much lower than that of formic acid (around 1/20). This finding is qualitatively consistent with the results of this work (ratio of 1/150). The lower sensitivity can be rationalized by the relatively lower gas phase acidity of propionic acid [158]. It is unclear why the sensitivity of this work is almost an order of magnitude lower than what was published by *Veres et al.*

5.4.2 Comparison of MIST-IC, MIST-CE and CIMS

Both MIST-IC and CIMS were used to determine LMW acids in my research. Based on the COE in MIST, detection limit of MIST-IC was calculated and shown in Table 5-4. If capillary electrophoresis (CE) method (details were discussed in Chapter 3) was used to analyze the trapping solutions from MIST, its detection limit can also be derived. The LOD of propionate in CE was 21.4 μM. As 95±8% C_2H_5COH could be trapped into buffer solution by MIST, the LOD of CE was converted into gas phase mixing ratio of 39 ppb. The COE of HCOOH was 91 ± 10%. Thus, the LOD in MIST-CE was expected to be 58 ppb in DDAB-modified capillary and 120 ppb in DODAB-modified capillary.

Table 5-4 shows that among the three techniques, CIMS had the lowest LOD of all three acids. Besides, CIMS is a fast and sensitive quantification method. It is shown in Figure 5-8, 5-10, 5-12 that once the concentration of gas standard varied, CIMS response to the change was instantaneous. To MIST-IC, the response time is limited by sampling period (10 or 15 min). It is hard to achieve real time analysis. The memory effects within the mist chamber may also affect the accuracy of MIST sampling, as not all of the trapping solution is totally exchanged and the chamber is not fully "rinsed" or washed between samples. In this study, MIST-IC had slightly higher LOD than CIMS. This could be limited by the poor performance of a budget IC used as an undergraduate teaching tool. The LOD can be lowered in principle, for example by increasing the sampling time (and collecting a larger volume of air) or by purchasing a more sensitive IC detector which are commercially available. In spite of the disadvantages of poor time-resolution and memory effects, the MIST-IC method has one key advantage of being able to determine concentrations from first principles, as it is calibrated using standard analytical techniques (i.e., using balances, volumetric flasks, flow meters, etc.).

In MIST-CE, the LOD is higher than that of MIST-IC by the order of magnitude (Table 5-4). Lower LOD in CE can be anticipated by using different detection methods, such as laser induced fluorescence [286], mass spectrometry [287]. Sample preconcentration methods are also applied to achieve better LOD, such as in-capillary solid phase extraction (SPE) [288], or isotachophoretic stacking [289, 290]. MIST-CE has substantially higher LOD than MIST-IC and CIMS, and is too high to analyze atmosphere sample in real time.

Table 5-4 Comparison of detection limit (LOD) of LMW acids in MIST-IC, MIST-CE and CIMS

Techniques	**MIST-IC**	**MIST-CE**	**CIMS**	**CIMS**
Integration time (s)	**900**	**900**	**1**	**900**
LOD of C_2H_5COOH (ppb)	~3.1	39	~2.8	~0.093
LOD of HCOOH (ppb)	~6.3	58/120	~0.2	~0.0067
LOD of HNO_3 (ppb)	~2.9	N/A	~2.2	~0.073

5.5 Conclusion

A MIST-IC was used to calibrate response factors of CIMS to HCOOH, C_2H_5COOH and HNO_3. The comparison between MIST-IC and CIMS has shown good correlation ($r > 0.8$) in our experiments. Since both measurement techniques operate on very different principles, the high level of agreement confirms both CIMS and MIST-IC as quantitative analysis methods for the three model LMW acids. The high sensitivity, low LOD and great precision associated with fast time response make CIMS a promising technique for the determination of LMW acids in field studies and reveal some of the limitations of the mist chamber methods. Future measurements using the CIMS technique will be able to provide insights in production and losses of acids, which will be very important to constrain regional and global models.

Chapter Six: **CONCLUSIONS AND FUTURE DIRECTIONS**

6.1 Summary

The main goal of this thesis has been the development of an instrument that combines a high capacity sampling method, a mist chamber, with a highly efficient and usually sensitive analysis method, capillary electrophoresis, for quantification of low molecular weight acids that occur in ambient air.

The first milestone was to develop a co-electroosmotic CE method with indirect UV detection for the common LMW acids-HNO_3, HCOOH and C_2H_5COOH (Chapter 3). For this purpose, the separation pH needed to be optimized and an appropriate indirect UV probe and a suitable electroosmotic flow modifier needed to be selected. At pH values lower than 5.1, good separation efficiency was obtained for chloride, nitrite, nitrate and sulfate. At pH values higher than 6.1, loss of peaks occurred, in particular for highly mobile ions. Ultimately, napthalenedisulfonate at a concentration of 5.6 mM titrated to a pH of 5.86 with piperazine was chosen as indirect probe. To reduce separation time and surface absorption, an EOF modifier was selected from a choice of three surfactants: single-chained TTAB and two-chained DDAB and DODAB. 0.30 mM DODAB provided the optimum ion mobility and separation for sulfate, formate and propionate anion. Separations in the same BGE using either DDAB or DODAB showed similar detection limits, which were in the range from 15 to 20 µM. However, the DDAB modified capillary showed five times higher sensitivity than the DODAB modified capillary. The combination of indirect UV detection, reversed-EOF operation and electrokinetic injection allow the fast, reliable and cheap analysis of acids anions.

The second milestone was to determine the sampling performance of the custom mist chamber (Chapter 4). A chemical ionization mass spectrometer was used to determine the collection efficiency of MIST. As far as I know, this was the first time CIMS was used to determine the COE of a MIST. The COEs of LMW acids were significantly affected by choice of trapping solution, instrument and operation parameters. The COE was generally less than unity, in disagreement with many values used in the literature [251, 252, 256]. Higher COEs (>90%) were achieved for all three model acids using buffered trapping solution. Henry`s law could be used to rationalize the COE trends among the acids tested, in agreement with *Spaulding et al*. [249].

Next, mist chamber samples were analyzed. Using CE to analyze the collected solutions, the LODs were 58 ppb for formate and 39 ppb for propionate. These levels are well above typical atmospheric concentrations. Hence, for a 10 to 15 min sampling interval, MIST-CE in its current configuration is not suitable for atmospheric measurements. Lower detection limits of 6.3 ppb, 3.1 ppb and 2.9 ppb for formate, propionate and nitrate were obtained using IC (Chapter 5).

Finally, the MIST-IC method was used to determine the response factors of an acetate ion CIMS for HNO_3, HCOOH and C_2H_5COOH. The CIMS had the highest response factor to HCOOH (7 Hz/ppt). It has effective LODs of 0.2 ppb, 2.8 ppb and 2.2 ppb for formate, propionate and nitrate (Chapter 5). Compared to either MIST-IC or MIST-CE, CIMS provided the lowest LODs, low enough to analyze atmospheric samples. Further, the CIMS is able to provide sensitive, real time monitoring data. In contrast, significant memory effects were observed in the mist chamber. Thus, CIMS is currently the clearly preferable analysis method for acids in the atmosphere.

6.2 Future Work

An obvious goal for future work is to attempt to improve the LOD of CE, for example, using sample preconcentration methods. Candidates for such methods include in-capillary solid phase extraction [288], isotachophoretic stacking [289, 290], or a combination of those two (i.e., large volume sample stacking with field enhanced sample injection[291]). An alternative is to use a more sensitive detection methods, such as CE coupled to laser induced fluorescence [286] (e.g., using a fluorescent indirect probe) or mass spectrometry [287].

Another issue is the relatively slow throughput of the current CE method, which needs to be improved for MIST-CE applied to be practical. *Rose et al*. [292] have designed an auto-sampler for CE, in which a solution tray was rotated by a stepper motor controlled by a computer. It allowed the automation of sample injection in CE as well as achieved a greater reproducibility. This kind of autosampler could be used to connect CE with MIST. Once the trapping solution is collected into a sample vial on a tray, the tray could be rotated to the position of capillary and electrode. The sample could be easily injected through electrokinetic injection. This automated sample injection could greatly improve the reproducibility of sample injection time, which can avoid the tedious addition of internal standards into CE sample.

Microfabrication could be also applied to improve the throughput of CE. The short channel has better Joule heat dissipation and higher separation field strength [293]. Those characteristics allow microchip CE to perform extremely fast yet reproducible separations. If microchip CE were to be combined with MIST, atmosphere sampling and analysis could potentially be achieved in a very short time resolution, which may result in real time analysis.

REFERENCES

[1] S. Preunkert, M. Legrand, B. Jourdain, and I. Dombrowski-Etchevers, "Acidic gases (HCOOH, CH_3COOH, HNO_3, HCl, and SO_2) and related aerosol species at a high mountain Alpine site (4360 m elevation) in Europe," *Journal of Geophysical Research-Atmospheres,* vol. 112, Sep 6 2007.

[2] A. Chebbi and P. Carlier, "Carboxylic acids in the troposphere, occurrence, sources, and sinks: A review," *Atmospheric Environment,* vol. 30, pp. 4233-4249, Dec 1996.

[3] J. N. Galloway, "Acid Deposition: Perspectives in Time and Space," *Water Air and Soil Pollution,* vol. 85, pp. 15-24, Dec 1995.

[4] R. R. O. Hazewinkel, A. P. Wolfe, S. Pla, C. Curtis, and K. Hadley, "Have Atmospheric Emissions from the Athabasca Oil Sands Impacted Lakes in Northeastern Alberta, Canada?," *Canadian Journal of Fisheries and Aquatic Sciences,* vol. 65, pp. 1554-1567, Aug 2008.

[5] "2004 Acid Deposition Assessment for Alberta," WBK & Associates Inc. 2006.

[6] J. Clark, S. Kumbhani, J. C. Hansen, and J. S. Francisco, "HNO_3-NH_x, H_2SO_4-NH_x, $CH(O)OH$-NH_x, and $CH_3C(O)OH$-NH_x Complexes and Their Role in the Formation of Condensation Nuclei," *Journal of Chemical Physics,* vol. 135, p. 11, Dec 2011.

[7] D. Danalatos and S. Glavas, "Gas Phase Nitric Acid, Ammonia and Related Particulate Matter at A Mediterranean Coastal Site, Patras, Greece," *Atmospheric Environment,* vol. 33, pp. 3417-3425, Sep 1999.

[8] S. K. Ghosh, P. V. Bhave, J. M. Davis, and H. Lee, "Spatio-Temporal Analysis of Total Nitrate Concentrations Using Dynamic Statistical Models," *Journal of the American Statistical Association,* vol. 105, pp. 538-551, Jun 2010.

[9] E. D. Baboukas, M. Kanakidou, and N. Mihalopoulos, "Carboxylic acids in gas and particulate phase above the Atlantic Ocean," *Journal of Geophysical Research-Atmospheres,* vol. 105, pp. 14459-14471, Jun 2000.

[10] R. W. Talbot, A. S. Vijgen, and R. C. Harriss, "Measuring Tropospheric HNO_3-Problems and Prospects for Nylon Filer and Mist Chamber Techniques," *Journal of Geophysical Research-Atmospheres,* vol. 95, pp. 7553-7561, May 1990.

[11] J. A. Neuman, L. G. Huey, T. B. Ryerson, and D. W. Fahey, "Study of inlet materials for sampling atmospheric nitric acid," *Environmental Science & Technology,* vol. 33, pp. 1133-1136, Apr 1999.

[12] P. Khare, N. Kumar, K. M. Kumari, and S. S. Srivastava, "Atmospheric formic and acetic acids: An overview," *Reviews of Geophysics,* vol. 37, pp. 227-248, May 1999.

[13] P. Saxena and L. M. Hildemann, "Water-soluble Organics in Atmospheric Particles: A Critical Review of the Literature and Application of Thermodynamics to Identify Candidate Compounds," *Journal of Atmospheric Chemistry,* vol. 24, pp. 57-109, May 1996.

[14] R. B. Norton, M. A. Carroll, D. D. Montzka, G. Hubler, B. J. Huebert, G. Lee, W. W. Warren, B. A. Ridley, and J. G. Walega, "Measurements of Nitric Acid and Aerosol Nitrate at the Maunal Loa Observatory during the Mauna Loa Observatroy Photochemistry Experiemnt 1988," *Journal of Geophysical Research-Atmospheres,* vol. 97, pp. 10415-10425, Jun 1992.

[15] M. Hanke, B. Umann, J. Uecker, F. Arnold, and H. Bunz, "Atmospheric Measurements of Gas-phase HNO_3 and SO_2 using Chemical Ionization Mass Spectrometry During the

MINATROC Field Campaign 2000 on Monte Cimone," *Atmospheric Chemistry and Physics*, vol. 3, pp. 417-436, Apr 2003.

[16] K. Gorzelska, R. W. Talbot, K. Klemm, B. Lefer, O. Klemm, G. L. Gregory, B. Anderson, and L. A. Barrie, "Chemical Composition of the Atmospheric Aerosol in the Troposphere over the Hudson Bay Lowlands and Quebec Laberador Regions of Canada," *Journal of Geophysical Research-Atmospheres*, vol. 99, pp. 1763-1779, Jan 1994.

[17] F. L. Eisele and D. J. Tanner, "Measuremtn of the Gas Phase Concentration of H2SO4 and Methane Sulfonic Acid and Estimates of H2SO4 Production and Loss in the Atmosphere," *Journal of Geophysical Research-Atmospheres*, vol. 98, pp. 9001-9010, May 1993.

[18] I. Khan and P. Brimblecombe, "Henry`s Law Constants of Low Molecular Weight (<130) Organic Acids," *J. Aerosol Sci.*, vol. 23, pp. S897-S900, 1992.

[19] I. Khan, P. Brimblecombe, and S. L. Clegg, "Solubilities of Pyruvic-acid and the Lower (C-1-C-6) Carboxylic-acids-experimental-determination of Equilibrium Vapor-pressures above Pure Aqueous and Salt-solutions," *Journal of Atmospheric Chemistry*, vol. 22, pp. 285-302, Nov 1995.

[20] J. Lelieveld and P. J. Crutzen, "The Role of Clouds in Tropospheric Photochemistry," *Journal of Atmospheric Chemistry*, vol. 12, pp. 229-267, Apr 1991.

[21] S. N. Pandis and J. H. Seinfeld, "Should Bulk Cloudwater or Fogwater Samples Obey Henry`s Law," *Journal of Geophysical Research-Atmospheres*, vol. 96, pp. 10791-10798, Jun 1991.

[22] J. Barbier-Jr, F. Delanoe, F. Jabouille, D. Duprez, G. Blanchard, and P. Isnard, "Total Oxidation of Acetic Acid in Aqueous Solutions over Noble Metal Catalysts," *Journal of Catalysis,* vol. 177, pp. 378-385, Jul 1998.

[23] H. Tanaka and T. Tachibana, "Determination of Acid/Base Dissociation Constants Based on a Rapid Detection of the Half Equivalence Point by Feedback-Based Flow Ratiometry," *Analytical Sciences,* vol. 20, pp. 979-981, Jun 2004.

[24] C. L. Yaws, *Handbook of Vapor Pressure* vol. 4. Houston: Gulf Publishing Company, 1994.

[25] J. I. Gmitro and T. Vermeulen, "Vapor Liquid Equilibria for Aqueous Sulfuric Acid," *Aiche Journal,* vol. 10, pp. 740-746, 1964.

[26] H. J. Choi, J. Y. Kang, I. Y. Jeon, S. M. Eo, L. S. Tan, and J. B. Baek, "Immobilization of Platinum Nanoparticles on 3,4-diaminobenzoyl- Functionalized Multi-Walled Carbon Nanotube and Its Electrocatalytic Activity," *Journal of Nanoparticle Research,* vol. 14, p. 11, Feb 2012.

[27] J. F. Gleason, A. Sinha, and C. J. Howard, "Kinetics of the Gas Phase Reaction $HOSO_2+O_2^-]HO_2+SO_3$," *Journal of Physical Chemistry,* vol. 91, pp. 719-724, Jan 1987.

[28] J. G. Calvert, A. Lazrus, G. L. Kok, B. G. Heikes, J. G. Walega, J. Lind, and C. A. Cantrell, "Chemical Mechanisms of Acid Generation in the Troposphere," *Nature,* vol. 317, pp. 27-35, 1985.

[29] A. Jefferson, D. J. Tanner, F. L. Eisele, and H. Berresheim, "Sources and Sinks of H2SO4 in the Remote Antarctic Marine Boundary Layer," *Journal of Geophysical Research-Atmospheres,* vol. 103, pp. 1639-1645, Jan 1998.

[30] R. L. Mauldin, T. Berndt, M. Sipila, P. Paasonen, T. Petaja, S. Kim, T. Kurten, F. Stratmann, V. M. Kerminen, and M. Kulmala, "A New Atmospherically Relevant Oxidant of Sulphur Dioxide," *Nature,* vol. 488, pp. 193-197, Aug 2012.

[31] J. R. Pierce, M. J. Evans, C. E. Scott, S. D. D. Andrea, D. K. Farmer, E. Swietlicki, and D. V. Spracklen, "Weak Global Sensitivity of Cloud Condensation Nuclei and the Aerosol Indirect Effect to Criegee+SO_2 Chemistry," *Atmos. Chem. Phys,* vol. 13, pp. 3163-3176, 2013.

[32] G. J. Doyle, "Self-Nucleaton in Sulfuric Acid-Water System," *Journal of Chemical Physics,* vol. 35, pp. 795-799, 1961.

[33] M. Sipila, T. Berndt, T. Petaja, D. Brus, J. Vanhanen, F. Stratmann, J. Patokoski, R. L. Mauldin, A. P. Hyvarinen, H. Lihavainen, and M. Kulmala, "The Role of Sulfuric Acid in Atmospheric Nucleation," *Science,* vol. 327, pp. 1243-1246, Mar 2010.

[34] C. Kuang, P. H. McMurry, A. V. McCormick, and F. L. Eisele, "Dependence of Nucleation Rates on Sulfuric Acid Vapor Concentration in Diverse Atmospheric Locations," *Journal of Geophysical Research-Atmospheres,* vol. 113, p. 9, May 2008.

[35] J. R. Pierce and P. J. Adams, "Efficiency of Cloud Condensation Nuclei Formation from Ultrafine Particles," *Atmospheric Chemistry and Physics,* vol. 7, pp. 1367-1379, Feb 2007.

[36] T. Stavrakou, J. F. Muller, J. Peeters, A. Razavi, L. Clarisse, C. Clerbaux, P. F. Coheur, D. Hurtmans, M. De Maziere, C. Vigouroux, N. M. Deutscher, D. W. T. Griffith, N. Jones, and C. Paton-Walsh, "Satellite Evidence for A Large Source of Formic Acid from Boreal and Tropical Forests," *Nature Geoscience,* vol. 5, pp. 26-30, Jan 2012.

[37] J. Calvert, A. Mellouki, and J. J. orlando, in *Mechnisims of Atmospheric Oxidation of the Oxygenates* New York: Oxford University Press. Inc., 2011.

[38] V. Fiedler, M. Dal Maso, M. Boy, H. Aufmhoff, J. Hoffmann, T. Schuck, W. Birmili, M. Hanke, J. Uecker, F. Arnold, and M. Kulmala, "The Contribution of Sulphuric acid to Atmospheric Particle Formation and Growth: a Comparison between Boundary Layers in Northern and Central Europe," *Atmospheric Chemistry and Physics,* vol. 5, pp. 1773-1785, Jul 2005.

[39] P. J. Rasch, S. Tilmes, R. P. Turco, A. Robock, L. Oman, C. C. Chen, G. L. Stenchikov, and R. R. Garcia, "An Overview of Geoengineering of Climate Using Stratospheric Sulphate Aerosols," *Philosophical Transactions of the Royal Society a-Mathematical Physical and Engineering Sciences,* vol. 366, pp. 4007-4037, Nov 2008.

[40] McConnel.Jc and M. B. McElroy, "Odd Nitrogen in Atmosphere," *Journal of the Atmospheric Sciences,* vol. 30, pp. 1465-1480, 1973.

[41] J. Kleffmann, T. Gavriloaiei, Y. Elshorbany, M. Rodenas, and P. Wiesen, "Detection of Nitric Acid (HNO3) in the Atmosphere Using the LOPAP Technique," *Journal of Atmospheric Chemistry,* vol. 58, pp. 131-149, Oct 2007.

[42] S. S. Brown, J. E. Dibb, H. Stark, M. Aldener, M. Vozella, S. Whitlow, E. J. Williams, B. M. Lerner, R. Jakoubek, A. M. Middlebrook, J. A. DeGouw, C. Warneke, P. D. Goldan, W. C. Kuster, W. M. Angevine, D. T. Sueper, P. K. Quinn, T. S. Bates, J. F. Meagher, F. C. Fehsenfeld, and A. R. Ravishankara, "Nighttime Removal of NOx in the Summer Marine Boundary Layer," *Geophysical Research Letters,* vol. 31, p. 5, Apr 2004.

[43] G. A. Dawson and J. C. Farmer, "Soluble Atmospheric Trace Gases in the Southwestern United-States. 2. Organic-Species HCHO, HCOOH, CH_3COOH," *Journal of Geophysical Research-Atmospheres,* vol. 93, pp. 5201-5206, May 1988.

[44] T. J. Garrett, L. Avey, P. I. Palmer, A. Stohl, J. A. Neuman, C. A. Brock, T. B. Ryerson, and J. S. Holloway, "Quantifying Wet scavenging Processes in Aircraft Observations of Nitric Acid and Cloud Condensation Nuclei," *Journal of Geophysical Research-Atmospheres,* vol. 111, p. 12, Nov 2006.

[45] J. N. Galloway and E. B. Cowling, "Reactive Nitrogen and the World: 200 Years of Change," *Ambio,* vol. 31, pp. 64-71, Mar 2002.

[46] M. S. Jang, N. M. Czoschke, S. Lee, and R. M. Kamens, "Heterogeneous atmospheric aerosol production by acid-catalyzed particle-phase reactions," *Science,* vol. 298, pp. 814-817, Oct 2002.

[47] M. Hallquist, J. C. Wenger, U. Baltensperger, Y. Rudich, D. Simpson, M. Claeys, J. Dommen, N. M. Donahue, C. George, A. H. Goldstein, J. F. Hamilton, H. Herrmann, T. Hoffmann, Y. Iinuma, M. Jang, M. E. Jenkin, J. L. Jimenez, A. Kiendler-Scharr, W. Maenhaut, G. McFiggans, T. F. Mentel, A. Monod, A. S. H. Prevot, J. H. Seinfeld, J. D. Surratt, R. Szmigielski, and J. Wildt, "The Formation, Properties and Impact of Secondary Organic Aerosol: Current and Emerging Issues," *Atmospheric Chemistry and Physics,* vol. 9, pp. 5155-5236, 2009.

[48] M. Claeys, B. Graham, G. Vas, W. Wang, R. Vermeylen, V. Pashynska, J. Cafmeyer, P. Guyon, M. O. Andreae, P. Artaxo, and W. Maenhaut, "Formation of Secondary Organic Aerosols through Photooxidation of Isoprene," *Science,* vol. 303, pp. 1173-1176, Feb 2004.

[49] S. B. Hong, W. H. Kim, H. J. Ko, S. B. Lee, D. E. Lee, and C. H. Kang, "Characteristics of Formate and Acetate Concentrations in Precipitation at Jeju Island, Korea," *Atmospheric Research,* vol. 101, pp. 427-437, Jul 2011.

[50] A. T. Archibald, M. R. McGillen, C. A. Taatjes, C. J. Percival, and D. E. Shallcross, "Atmospheric Transformation of Enols: A Potential Secondary Source of Carboxylic Acids in the Urban Troposphere," *Geophysical Research Letters,* vol. 34, p. 4, Nov 2007.

[51] J. M. Liu, X. L. Zhang, E. T. Parker, P. R. Veres, J. M. Roberts, J. A. de Gouw, P. L. Hayes, J. L. Jimenez, J. G. Murphy, R. A. Ellis, L. G. Huey, and R. J. Weber, "On the gas-particle partitioning of soluble organic aerosol in two urban atmospheres with contrasting emissions: 2. Gas and particle phase formic acid," *Journal of Geophysical Research-Atmospheres,* vol. 117, p. 15, Oct 2012.

[52] U. Kuhn, S. Rottenberger, T. Biesenthal, C. Ammann, A. Wolf, G. Schebeske, S. T. Oliva, T. M. Tavares, and J. Kesselmeier, "Exchange of Short-Chain Monocarboxylic Acids by Vegetation at A Remote Tropical Forest site in Amazonia," *Journal of Geophysical Research-Atmospheres,* vol. 107, p. 18, Sep-Oct 2002.

[53] W. L. Chameides, "The Photochemistry of A Remote Marine Stratiform Cloud," *Journal of Geophysical Research-Atmospheres,* vol. 89, pp. 4739-4755, 1984.

[54] P. Khare and B. P. Baruah, *Geochemical Cycles of Atmospheric Organic Acids and Aldehydes*. Athens: World Scientific and Engineering Acad and Soc, 2010.

[55] L. Montero, P. C. Vasconcellos, S. R. Souza, M. A. F. Pires, O. R. Sanchez-Ccoyllo, M. F. Andrade, and L. R. F. Carvalho, "Measurements of Atmospheric Carboxylic Acids and Carbonyl Compounds in Sao Paulo City, Brazil," *Environmental Science & Technology,* vol. 35, pp. 3071-3081, Aug 2001.

[56] W. C. Keene and J. N. Galloway, "The Biogeochemical Cycling of Formic and Acetic Acids through the troposphere: an Overview of Current Understanding," *Tellus Series B Chemical and Physical Meteorology,* vol. 40, pp. 322-334, 1988.

[57] D. U. Andrews, B. R. Heazlewood, A. T. Maccarone, T. Conroy, R. J. Payne, M. J. T. Jordan, and S. H. Kable, "Photo-Tautomerization of Acetaldehyde to Vinyl Alcohol: A Potential Route to Tropospheric Acids," *Science,* vol. 337, pp. 1203-1206, Sep 2012.

[58] K. Kawamura, L. L. Ng, and I. R. Kaplan, "Determination of Organic-acids(C1-C10) in the Atmosphere, Motor Exhausts, and Engine Oils," *Environmental Science & Technology,* vol. 19, pp. 1082-1086, 1985.

[59] J. E. Lawrence and P. Koutrakis, "Measurement of Atmospheric Formic and Acetic Acids: Methods Evaluation and Results from Field Studies," *Environmental Science & Technology,* vol. 28, pp. 957-964, May 1994.

[60] R. W. Talbot, M. O. Andreae, H. Berresheim, D. J. Jacob, and K. M. Beecher, "Sources and Sinks of Formic, Acetic and Pyruvic Acids over Central Amazonia 2. Wet Season," *Journal of Geophysical Research-Atmospheres,* vol. 95, pp. 16799-16811, Sep 1990.

[61] D. Grosjean, "Organic Acids in Southern California Air Ambient Concentrations, Mobile Source Emissions, In Situ Formation and Removal Processes," *Environmental Science & Technology,* vol. 23, pp. 1506-1514, Dec 1989.

[62] C. P. Rinsland, G. Dufour, C. D. Boone, P. F. Bernath, L. Chiou, P. F. Coheur, S. Turquety, and C. Clerbaux, "Satellite Boreal Measurements over Alaska and Canada during June-July 2004: Simultaneous Measurements of Upper Tropospheric CO, C_2H_6, HCN, CH_3Cl, CH_4, C_2H_2, CH_3OH, HCOOH, OCS, and SF_6 Mixing Ratios," *Global Biogeochemical Cycles,* vol. 21, p. 13, Aug 2007.

[63] P. H. Wine, R. J. Astalos, and R. L. Mauldin, "Kinetic and Mechanistic Study of the OH+HCOOH Reaction," *Journal of Physical Chemistry,* vol. 89, pp. 2620-2624, 1985.

[64] D. J. Jacob, "Chemistry of OH in Remote Clouds and Its Role in the Production of Formic-acid and Peroxymonosulfate," *Journal of Geophysical Research-Atmospheres,* vol. 91, pp. 9807-9826, Aug 1986.

[65] X. L. Zhou, N. Zhang, M. TerAvest, D. Tang, J. Hou, S. Bertman, M. Alaghmand, P. B. Shepson, M. A. Carroll, S. Griffith, S. Dusanter, and P. S. Stevens, "Nitric Acid Photolysis on Forest Canopy Surface as A Source for Tropospheric Nitrous Acid," *Nature Geoscience,* vol. 4, pp. 440-443, Jul 2011.

[66] D. B. Millet, "Atmospheric Chemistry Natural Atmospheric Acidity," *Nature Geoscience,* vol. 5, pp. 8-9, Jan 2012.

[67] D. J. Jacob, "Heterogeneous Chemistry and Tropospheric Ozone," *Atmospheric Environment,* vol. 34, pp. 2131-2159, 2000.

[68] K. Jardine, A. Y. Serrano, A. Arneth, L. Abrell, A. Jardine, P. Artaxo, E. Alves, J. Kesselmeier, T. Taylor, S. Saleska, and T. Huxman, "Ecosystem-Scale Compensation Points of Formic and Acetic Acid in the Central Amazon," *Biogeosciences,* vol. 8, pp. 3709-3720, 2011.

[69] R. W. Talbot, K. M. Beecher, R. C. Harriss, and W. R. Cofer, "Atmospheic Geochemistry of Formic and Acetic Acids at a Mid-Latitude Temperate Site," *Journal of Geophysical Research-Atmospheres,* vol. 93, pp. 1638-1652, Feb 1988.

[70] K. Kawamura and O. Yasui, "Diurnal Changes in the Distribution of Dicarboxylic Acids, Ketocarboxylic Acids and Dicarbonyls in the Urban Tokyo Atmosphere," *Atmospheric Environment,* vol. 39, pp. 1945-1960, Mar 2005.

[71] J. F. Galasyn, K. L. Tschudy, and B. J. Huebert, "Seasonal and Diurnal Variability of Nitric Acid Vapor and Ionic Aerosol Species in the Remote Free Troposphere at Mauna Loa, Hawaii," *Journal of Geophysical Research-Atmospheres,* vol. 92, pp. 3105-3113, Mar 1987.

[72] J. Dewulf and H. VanLangenhove, "Analytical Techniques for the Determination and Measurement Data of 7 Chlorinated C-1- and C-2-Hydrocarbons and 6 Monocyclic Aromatic Hydrocarbons in Remote Air Masses: An Overview," *Atmospheric Environment,* vol. 31, pp. 3291-3307, Oct 1997.

[73] J. Dewulf and H. Van Langenhove, "Anthropogenic Volatile Organic Compounds in Ambient Air and Natural Waters: A Review on Recent Developments of Analytical Methodology, Performance and Interpretation of Field Measurements," *Journal of Chromatography A,* vol. 843, pp. 163-177, May 1999.

[74] A. Kumar and I. Viden, "Volatile Organic Compounds: Sampling Methods and Their Worldwide Profile in Ambient Air," *Environmental Monitoring and Assessment,* vol. 131, pp. 301-321, Aug 2007.

[75] M. Rosa Ras, F. Borrull, and R. Maria Marce, "Sampling and Preconcentration Techniques for Determination of Volatile Organic Compounds in Air Samples," *Trac-Trends in Analytical Chemistry,* vol. 28, pp. 347-361, Mar 2009.

[76] M. Harper, "Sorbent Trapping of Volatile Organic Compounds from Air," *Journal of Chromatography A,* vol. 885, pp. 129-151, Jul 2000.

[77] A. Howe, D. Musgrove, D. Breuer, K. Gusbeth, A. Moritz, M. Demange, V. Oury, D. Rousset, and M. Dorotte, "Evaluation of Sampling Methods for Measuring Exposure to Volatile Inorganic Acids in Workplace Air. Part 1: Sampling Hydrochloric Acid (HCl)

and Nitric Acid (HNO_3) from a Test Gas Atmosphere," *Journal of Occupational and Environmental Hygiene,* vol. 8, pp. 492-502, 2011.

[78] P. A. Clausen and P. Wolkoff, "Degradation Products of Tenax TA Formed During Sampling and Thermal Desorption Analysis: Indicators of Reactive Species Indoors," *Atmospheric Environment,* vol. 31, pp. 715-725, Mar 1997.

[79] D. Helmig, "Ozone Removal Techniques in the Sampling of Atmospheric Volatile Organic Trace Gases," *Atmospheric Environment,* vol. 31, pp. 3635-3651, Nov 1997.

[80] T. Okita, S. Morimoto, M. Izawa, and S. Konno, "Measurement of Gaseous and Particulate Nitrates in Atmosphere," *Atmospheric Environment,* vol. 10, pp. 1085-1089, 1976.

[81] C. W. Spicer, J. E. Howes, T. A. Bishop, L. H. Arnold, and R. K. Stevens, "Nitric-Acid Measurement Methods-An Intercomparison," *Atmospheric Environment,* vol. 16, pp. 1487-1500, 1982.

[82] M. Schilling and D. Klockow, "Determination of C1-C3 Carboxylic Acids in Air with Diffusion Controlled Sampling at Elevated Flow Rates," *Fresenius Journal of Analytical Chemistry,* vol. 346, pp. 738-744, Jun-Jul 1993.

[83] D. A. Philips and P. K. Dasgupta, "A Diffusion Scrubber for the Collection of Gaseous Nitric-Acid," *Separation Science and Technology,* vol. 22, pp. 1255-1267, 1987.

[84] A. J. Peters, D. A. Lane, L. A. Gundel, G. L. Northcott, and K. C. Jones, "A Comparison of High Volume and Diffusion Denuder Samplers for Measuring Semivolatile Organic Compounds in the Atmosphere," *Environmental Science & Technology,* vol. 34, pp. 5001-5006, Dec 2000.

[85] K. C. Clemitshaw, "A Review of Instrumentation and Measurement Techniques for Gound-based and Airborne Field Studies of Gas-phase Tropospheric Chemistry," *Critical Reviews in Environmental Science and Technology,* vol. 34, pp. 1-108, 2004.

[86] P. K. Simon and P. K. Dasgupta, "Continuous Automated Measurement of the Soluble Fraction of ATmospheric Particulate Matter," *Analytical Chemistry,* vol. 67, pp. 71-78, Jan 1995.

[87] I. Trebs, F. X. Meixner, J. Slanina, R. Otjes, P. Jongejan, and M. O. Andreae, "Real-Time Measurements of Ammonia, Acidic Trace Gases and Water-Soluble Inorganic Aerosol Species at a Rural Site in the Amazon Basin," *Atmospheric Chemistry and Physics,* vol. 4, pp. 967-987, Jun 2004.

[88] M. Takeuchi, H. Tsunoda, H. Tanaka, and Y. Shiramizu, "Parallel-Plate Wet Denuder Coupled Ion Chromatograph for Near-Real-Time Detection of Trace Acidic Gases in Clean Room Air," *Analytical Sciences,* vol. 27, pp. 805-810, Aug 2011.

[89] M. Sax, M. Kalberer, and R. Zenobi, "Sampling Gaseous Oxidation Products of Aromatic Compounds in Gas/Particle Separation Systems," *Journal of Environmental Monitoring,* vol. 5, pp. 103N-107N, Sep 2003.

[90] S. V. Hering, D. R. Lawson, I. Allegrini, A. Febo, C. Perrino, M. Possanzini, J. E. Sickles, K. G. Anlauf, A. Wiebe, B. R. Appel, W. John, J. Ondo, S. Wall, R. S. Braman, R. Sutton, G. R. Cass, P. A. Solomon, D. J. Eatough, N. L. Eatough, E. C. Ellis, D. Grosjean, B. B. Hicks, J. D. Womack, J. Horrocks, K. T. Knapp, T. G. Ellestad, R. J. Paur, W. J. Mitchell, M. Pleasant, E. Peake, A. Maclean, W. R. Pierson, W. Brachaczek, H. I. Schiff, G. I. Mackay, C. W. Spicer, D. H. Stedman, A. M. Winer, H. W. Biermann,

and E. C. Tuazon, "The Nitric Acid Shootout-Field Comparison of Measurement Methods," *Atmospheric Environment,* vol. 22, pp. 1519-1539, 1988.

[91] M. B. Jacobs and S. Hochheiser, "Continuous Sampling and Ultramicrodetermination of Nitrogen Dioxide in Air," *Analytical Chemistry,* vol. 30, pp. 426-428, 1958.

[92] D. Grosjean and K. Fung, "Collection Efficiencies of Cartridges and Micro-impingers for Sampling of Aldehydes in Air as 2,4-Dinitrophenylhydrazones," *Analytical Chemistry,* vol. 54, pp. 1221-1224, 1982.

[93] S. Francois, V. Perraud, M. Pflieger, A. Monod, and H. Wortham, "Comparative study of glass tube and mist chamber sampling techniques for the analysis of gaseous carbonyl compounds," *Atmospheric Environment,* vol. 39, pp. 6642-6653, Nov 2005.

[94] Y. H. Lee, I. Wangberg, and J. Munthe, "Sampling and analysis of gas-phase methylmercury in ambient air," *Science of the Total Environment,* vol. 304, pp. 107-113, Mar 2003.

[95] H. A. Khwaja, "Atmospheric Concentrations of Carboxylic Acids and Related Compounds at A Semiurban Site," *Atmospheric Environment,* vol. 29, pp. 127-139, Jan 1995.

[96] J. Sciare and N. Mihalopoulos, "A new technique for sampling and analysis of atmospheric dimethylsulfoxide (DMSO)," *Atmospheric Environment,* vol. 34, pp. 151-156, 2000.

[97] D. A. Lane, "Sample Preparation and Sample Pretreatment," in *Handbook of Spectroscopy*. vol. 1, G. Gauglitz and T. Vo-Dinh, Eds. Weinheim: Wiley-VCH Verlag GmbH & Co. KGaA, 2003.

[98] S. R. Souza, P. C. Vasconcellos, and L. R. F. Carvalho, "Low Molecular Weight Carboxylic Acids in An Urban Atmosphere: Winter Measurements in Sao Paulo City, Brazil," *Atmospheric Environment,* vol. 33, pp. 2563-2574, Jul 1999.

[99] P. K. Simon and P. K. Dasgupta, "Continuous Automated Measurement of Gaseous Nitrous and Nitric Acids and Particulate Nitrite and Nitrate," *Environmental Science & Technology,* vol. 29, pp. 1534-1541, Jun 1995.

[100] L. Riddick and W. C. Brumley, "Capillary electrophoresis with laser-induced fluorescence: Environmental applications," in *CE from small ions to Macromolecules*, P. Schmitt-Kopplin, Ed. Totowa, New Jersey: Humana Press, 2006.

[101] K. Fukushi, S. Takeda, K. Chayama, and S. Wakida, "Application of Capillary Electrophoresis to the Analysis of Inorganic Ions in Environmental Samples," *Journal of Chromatography A,* vol. 834, pp. 349-362, Feb 1999.

[102] J. Romano, P. Jandik, W. R. Jones, and P. E. Jackson, "Optimization of Inorganic Capillary Electrophoresis for the Analysis of Anionic Solutes in Real Samples," *Journal of Chromatography*, vol. 546, pp. 411-421, Jun 21 1991.

[103] Z. Krivacsy, A. Molnar, E. Tarjanyi, A. Gelencser, G. Kiss, and J. Hlavay, "Investigation of Inorganic Ions and Organic Acids in Atmospheric Aerosol by Capillary Electrophoresis," *Journal of Chromatography A,* vol. 781, pp. 223-231, Sep 1997.

[104] P. K. Dasgupta and S. Kar, "Measurement of Gases by A Suppressed Conductometric Capillary Electrophoresis Separation System," *Analytical Chemistry*, vol. 67, pp. 3853-3860, Nov 1995.

[105] E. Dabekzlotorzynska and J. F. Dlouhy, "Capillary Zone Electrophoresis with Indirect UV Detection of Organic-Anions Using 2,6-Naphthalenedicarboxylic Acid," *Journal of Chromatography A*, vol. 685, pp. 145-153, Nov 1994.

[106] S. D. Noblitt, L. R. Mazzoleni, S. V. Hering, J. L. Collett, and C. S. Henry, "Separation of common organic and inorganic anions in atmospheric aerosols using a piperazine buffer and capillary electrophoresis," *Journal of Chromatography A*, vol. 1154, pp. 400-406, Jun 2007.

[107] H. J. Neu, "Gas Chromatography in Environmental Analysis-Aims and Challeges," *Fresenius Journal of Analytical Chemistry*, vol. 337, pp. 583-588, 1990.

[108] R. L. Grob, "Environmenral Analyses Utilizing Gas and Liquid Chromatography," *Journal of Liquid Chromatography*, vol. 16, pp. 1783-1802, 1993.

[109] H. Satsumabayashi, H. Kurita, Y. Yokouchi, and H. Ueda, "Mono- and Di-Carboxylic Acids under Long-Range Transport of Air Pollution in Central Japan," *Tellus Series B-Chemical and Physical Meteorology*, vol. 41, pp. 219-229, Jul 1989.

[110] S. Sinkkonen, E. Kolehmainen, J. Paasivirta, S. Hamalainen, and M. Lahtipera, "Analysis of Chlorinated Acetic and Propionic Acids as Their Pentafluorobenzyl Derivatives .1. Preparation of the Derivatives," *Journal of Chromatography A*, vol. 718, pp. 391-396, Dec 1995.

[111] J. S. Tumuluru, S. Shokhansanj, C. T. Wright, and T. Kremer, "GC Analysis of Volatiles and Other Products from Biomass Torrefaction Process," in *Advanced Gas Chromatography-Progress in Agricultural, Boimedical and Industrial Applications*. vol. 11, M. A. Mohd, Ed.: InTech, 2012.

[112] T. Suzuki, K. Yaguchi, S. Suzuki, and T. Suga, "Monitoring of Phthalic Acid Monoesters in River Water by Solid-Phase Extraction and GC-MS Determination," *Environmental Science & Technology,* vol. 35, pp. 3757-3763, Sep 2001.

[113] M. C. Pietrogrande, D. Bacco, and M. Mercuriali, "GC-MS Analysis of Low-Molecular-Weight Dicarboxylic Acids in Atmospheric Aerosol: Comparison between Silylation and Esterification Derivatization Procedures," *Analytical and Bioanalytical Chemistry,* vol. 396, pp. 877-885, Jan 2010.

[114] M. P. Fraser, G. R. Cass, and B. R. T. Simoneit, "Air Quality Model Evaluation Data for Organics. 6. C3-C24 Organic Acids," *Environmental Science & Technology,* vol. 37, pp. 446-453, Feb 2003.

[115] F. Hernandez, J. V. Sancho, M. Ibanez, E. Abad, T. Portoles, and L. Mattioli, "Current Use of High-Resolution Mass Spectrometry in the Environmental Sciences," *Analytical and Bioanalytical Chemistry,* vol. 403, pp. 1251-1264, May 2012.

[116] D. K. W. Wang and C. C. Austin, "Determination of Complex Mixtures of Volatile Organic Compounds in Ambient Air: An Overview," *Analytical and Bioanalytical Chemistry,* vol. 386, pp. 1089-1098, Oct 2006.

[117] Y. Ghoos, B. Geypens, M. Hiele, P. Rutgeerts, and G. Vantrappen, "Analysis for Short-Chain Carboxylic-Acids in Feces by Gas-Chromatography with An Ion-Trap Detector," *Analytica Chimica Acta,* vol. 247, pp. 223-227, Jul 1991.

[118] J. F. Hamilton, A. C. Lewis, C. Bloss, V. Wagner, A. P. Henderson, B. T. Golding, K. Wirtz, M. Martin-Reviejo, and M. J. Pilling, "Measurements of Photo-Oxidation Products from the Reaction of A Series of Alkyl-Benzenes with Hydroxyl Radicals During

EXACT Using Comprehensive Gas Chromatography," *Atmospheric Chemistry and Physics*, vol. 3, pp. 1999-2014, Nov 2003.

[119] C. J. Chien, M. J. Charles, K. G. Sexton, and H. E. Jeffries, "Analysis of airborne carboxylic acids and phenols as their pentafluorobenzyl derivatives: Gas chromatography ion trap mass spectrometry with a novel chemical ionization reagent, PFBOH," *Environmental Science & Technology,* vol. 32, pp. 299-309, Jan 1998.

[120] L. Pan and J. Pawliszyn, "Derivatization/Solid-Phase Microextraction: New Approach to Polar Analytes," *Analytical Chemistry,* vol. 69, pp. 196-205, Jan 1997.

[121] B. Lee, Y. Hwangbo, and D. S. Lee, "Determination of Low Molecular Weight Monocarboxylic Acid Gases in the Atmosphere by Parallel Plate Diffusion Scrubber-Ion Chromatography," *Journal of Chromatographic Science,* vol. 47, pp. 516-522, 2009.

[122] M. C. Bruzzoniti, R. M. De Carlo, and C. Sarzanini, "The Challenging Role of Chromatography in Environmental Problems," *Chromatographia,* vol. 73, pp. S15-S28, Jun 2011.

[123] S. R. Souza, M. F. M. Tavares, and L. R. F. de Carvalho, "Systematic Approach to the Separation of Mono- and Hydroxycarboxylic Acids in Environmental Samples by Ion Chromatography and Capillary Electrophoresis," *Journal of Chromatography A,* vol. 796, pp. 335-346, Feb 1998.

[124] A. A. Ammann and T. B. Ruttimann, "Simultaneous Determination of Small Organic and Inorganic Anions in Environmental Water Samples by Ion-Exchange Chromatography," *Journal of Chromatography A,* vol. 706, pp. 259-269, Jul 1995.

[125] A. Vairavamurthy, J. M. Roberts, and L. Newman, "Methods for Determination of Low-Molecular-Weight Carbonyl Compounds in the Atmosphere," *Atmospheric Environment Part a-General Topics,* vol. 26, pp. 1965-1993, Aug 1992.

[126] I. D. Wilson and C. Poole, "Liquid Chromatography: Mechanisms: Ion Chromatography," in *Handbook of Methods and Instrumentation in Separation Science*. vol. 1, I. D. Wilson, E. R. Adlard, M. Cooke, and C. F. Poole, Eds.: Elsevier Ltd., 2009, p. 514.

[127] R. Fisseha, J. Dommen, M. Sax, D. Paulsen, M. Kalberer, R. Maurer, F. Hofler, E. Weingartner, and U. Baltensperger, "Identification of Organic Acids in Secondary Organic Aerosol and the Corresponding Gas Phase from Chamber Experiments," *Analytical Chemistry,* vol. 76, pp. 6535-6540, Nov 2004.

[128] M. Loflund, A. Kasper-Giebl, W. Tscherwenka, M. Schmid, H. Giebl, R. Hitzenberger, G. Reischl, and H. Puxbaum, "The Performance of A Gas and Aerosol Monitoring System (GAMS) for the Determination of Acidic Water Soluble Organic and Inorganic Gases and Ammonia as well as Related Particles from the Atmosphere," *Atmospheric Environment,* vol. 35, pp. 2861-2869, Jun 2001.

[129] V. D. Nguyen, H. Neumeister, and G. Subklew, "Application of Ion Chromatography for the Investigation of the Anionic and Cationic Composition in High-Purity Water Production," *Fresenius Journal of Analytical Chemistry,* vol. 363, pp. 783-788, Apr 1999.

[130] M. Takeuchi, K. Yoshioka, Y. Toyama, A. Kagami, and H. Tanaka, "On-Line Measurement of Perchlorate in Atmospheric Aerosol Based on Ion Chromatograph

Coupled with Particle Collector and Post-Column Concentrator," *Talanta*, vol. 97, pp. 527-532, Aug 2012.

[131] Z. Krivacsy, A. Gelencser, G. Kiss, E. Meszaros, A. Molnar, A. Hoffer, T. Meszaros, Z. Sarvari, D. Temesi, B. Varga, U. Baltensperger, S. Nyeki, and E. Weingartner, "Study on the Chemical Character of Water Soluble Organic Compounds in Fine Atmospheric Aerosol at the Jungfraujoch," *Journal of Atmospheric Chemistry*, vol. 39, pp. 235-259, 2001.

[132] A. Levart, M. Gucek, B. Pihlar, and M. Veber, "Determination of Organic Acids in Air by Capillary Electrophoresis and Ion-Exclusion Chromatography," *Chromatographia*, vol. 51, pp. S321-S324, 2000.

[133] D. van Pinxteren and H. Herrmann, "Determination of Functionalised Carboxylic Acids in Atmospheric Particles and Cloud Water Using Capillary Electrophoresis/Mass Spectrometry," *Journal of Chromatography A*, vol. 1171, pp. 112-123, Nov 2007.

[134] J. Horvath and V. Dolnik, "Polymer Wall Coatings for Capillary Electrophoresis," *Electrophoresis*, vol. 22, pp. 644-655, Feb 2001.

[135] S. F. Y. Li, *Capillary Electrophoresis: Principles, Practice and Appliations*. Amsterdam: Elsevier 1992.

[136] J. E. Melanson, N. E. Baryla, and C. A. Lucy, "Dynamic capillary coatings for electroosmotic flow control in capillary electrophoresis," *Trac-Trends in Analytical Chemistry*, vol. 20, pp. 365-374, Jun-Jul 2001.

[137] X. H. Huang, J. A. Luckey, M. J. Gordon, and R. N. Zare, "Quantitative Analysis of Low Molecular Weight Carboxylic Acids by Capillary Zone Electrophoresis/Conductivity Detection," *Analytical Chemistry*, vol. 61, pp. 766-770, Apr 1989.

[138] V. Unterholzner, M. Macka, P. R. Haddad, and A. Zemann, "Simultaneous Separation of Inorganic Anions and Cations Using Capillary Electrophoresis with A Movable Contactless Conductivity Detector," *Analyst,* vol. 127, pp. 715-718, Jun 2002.

[139] J. Chen, B. P. Preston, and M. J. Zimmerman, "Analysis of Organic Acids in Industrial Samples - Comparison of Capillary Electrophoresis and Ion Chromatography," *Journal of Chromatography A,* vol. 781, pp. 205-213, Sep 1997.

[140] P. L. Ferguson, A. H. Grange, W. C. Brumley, J. R. Donnelly, and J. W. Farley, "Capillary Electrophoresis/Laser-Induced Fluorescence Detection of Fluorescein as A Groundwater Migration Tracer," *Electrophoresis,* vol. 19, pp. 2252-2256, Sep 1998.

[141] M. M. Yassine, E. Dabek-Zlotorzynska, and P. Schmitt-Kopplin, "CE-MS: A Useful Tool for the Identification of Water-Soluble Polar Organics in Air and Vehicular Emitted Particulate Matter," *Electrophoresis,* vol. 30, pp. 1756-1765, May 2009.

[142] K. A. Pratt and K. A. Prather, "Mass Spectrometry of Atmospheric Aerosols: Recent Developments and Applications. Part I: Off-Line Mass Spectrometry Techniques," *Mass Spectrometry Reviews,* vol. 31, pp. 1-16, Jan-Feb 2012.

[143] M. M. Yassine, E. Dabek-Zlotorzynska, M. Harir, and P. Schmitt-Kopplin, "Identification of Weak and Strong Organic Acids in Atmospheric Aerosols by Capillary Electrophoresis/Mass Spectrometry and Ultra-High-Resolution Fourier Transform Ion Cyclotron Resonance Mass Spectrometry," *Analytical Chemistry,* vol. 84, pp. 6586-6594, Aug 2012.

[144] A. Bogolitsyna, M. Becker, A. L. Dupont, A. Borgards, T. Rosenau, and A. Potthast, "Determination of Carbohydrate- and Lignin-Derived Components in Complex Effluents from Cellulose Processing by Capillary Electrophoresis with Electrospray Ionization-

Mass Spectrometric Detection," *Journal of Chromatography A,* vol. 1218, pp. 8561-8566, Nov 2011.

[145] D. H. Craston and M. Saeed, "Analysis of Carboxylic and Related Acids in the Environment by Capillary Electrophoretic Techniques," *Journal of Chromatography A,* vol. 827, pp. 1-12, Dec 1998.

[146] E. Dabek-Zlotorzynska, M. Piechowski, M. McGrath, and E. P. C. Lai, "Determination of Low-Molecular-Mass Carboxylic Acids in Atmospheric Aerosol and Vehicle Emission Samples by Capillary Electrophoresis," *Journal of Chromatography A,* vol. 910, pp. 331-345, Mar 2001.

[147] B. M. Simonet, A. Rios, and M. Valcarcel, "Enhancing Sensitivity in Capillary Electrophoresis," *Trac-Trends in Analytical Chemistry,* vol. 22, pp. 605-614, Oct 2003.

[148] E. Bouskova, C. Presutti, P. Gebauer, S. Fanali, J. L. Beckers, and P. Bocek, "Experimental assessment of electromigration properties of background electrolytes in capillary zone electrophoresis," *Electrophoresis,* vol. 25, pp. 355-359, Jan 2004.

[149] M. D. Gulcev and C. A. Lucy, "Effect of coating electrolytes on two-tailed surfactant bilayer coatings in capillary electrophoresis," *Analytica Chimica Acta,* vol. 690, pp. 116-121, Mar 2011.

[150] T. F. Svitova, Y. P. Smirnova, S. A. Pisarev, and N. A. Berezina, "Self-assembly in Double-tailed Surfactants in Dilute Aqueous-solutions," *Colloids and Surfaces a-Physicochemical and Engineering Aspects,* vol. 98, pp. 107-115, May 1995.

[151] M. M. Yassine and C. A. Lucy, "Factors affecting the temporal stability of semipermanent bilayer coatings in capillary electrophoresis prepared using double-chained surfactants," *Analytical Chemistry,* vol. 76, pp. 2983-2990, Jun 2004.

[152] M. M. Yassine and C. A. Lucy, "Enhanced stability self-assembled coatings for protein separations by capillary zone electrophoresis through the use of long-chained surfactants," *Analytical Chemistry,* vol. 77, pp. 620-625, Jan 2005.

[153] H. Corstjens, H. A. H. Billiet, J. Frank, and K. Luyben, "Variation of the pH of the Background Electrolyte due to Electrode Reactions in Capillary Electrophoresis: Theoretical Approach and in Situ Measurement," *Electrophoresis,* vol. 17, pp. 137-143, Jan 1996.

[154] Z. K. Shihabi and M. E. Hinsdale, "Some Variables Affecting Reproducibility in Capillary Electrophoresis," *Electrophoresis,* vol. 16, pp. 2159-2163, Nov 1995.

[155] N. J. Petersen and S. H. Hansen, "Improving the Reproducibility in Capillary Electrophoresis by Incorporating Current Drift in Mobility and Peak Area Calculations," *Electrophoresis,* vol. 33, pp. 1021-1031, Mar 2012.

[156] A. Detournay, S. Sauvage, N. Locoge, V. Gaudion, T. Leonardis, I. Fronval, P. Kaluzny, and J. C. Galloo, "Development of A Sampling Method for the Simultaneous Monitoring of Straight-Chain Alkanes, Straight-Chain Saturated Carbonyl Compounds and Monoterpenes in Remote Areas," *Journal of Environmental Monitoring,* vol. 13, pp. 983-990, Apr 2011.

[157] P. Veres, J. M. Roberts, C. Warneke, D. Welsh-Bon, M. Zahniser, S. Herndon, R. Fall, and J. de Gouw, "Development of negative-ion proton-transfer chemical-ionization mass spectrometry (NI-PT-CIMS) for the measurement of gas-phase organic acids in the atmosphere," *International Journal of Mass Spectrometry,* vol. 274, pp. 48-55, Jul 2008.

[158] P. Veres, J. M. Roberts, I. R. Burling, C. Warneke, J. de Gouw, and R. J. Yokelson, "Measurements of Gas-phase Inorganic and Organic Acids from Biomass Fires by

Negative-ion Proton-transfer Chemical-ionization Mass Spectrometry," *Journal of Geophysical Research-Atmospheres,* vol. 115, p. 15, Dec 2010.

[159] J. M. Roberts, P. Veres, C. Warneke, J. A. Neuman, R. A. Washenfelder, S. S. Brown, M. Baasandorj, J. B. Burkholder, I. R. Burling, T. J. Johnson, R. J. Yokelson, and J. de Gouw, "Measurement of HONO, HNCO, and other inorganic acids by negative-ion proton-transfer chemical-ionization mass spectrometry (NI-PT-CIMS): application to biomass burning emissions," *Atmospheric Measurement Techniques,* vol. 3, pp. 981-990, 2010.

[160] P. Veres, J. B. Gilman, J. M. Roberts, W. C. Kuster, C. Warneke, I. R. Burling, and J. de Gouw, "Development and Validation of A Portable Gas Phase Standard Generation and Calibration System for Volatile Organic Compounds," *Atmospheric Measurement Techniques,* vol. 3, pp. 683-691, 2010.

[161] Z. Krivacsy, G. Kiss, B. Varga, I. Galambos, Z. Sarvari, A. Gelencser, A. Molnar, S. Fuzzi, M. C. Facchini, S. Zappoli, A. Andracchio, T. Alsberg, H. C. Hansson, and L. Persson, "Study of Humic-Like Substances in Fog and Interstitial Aerosol by Size-Exclusion Chromatography and Capillary Electrophoresis," *Atmospheric Environment,* vol. 34, pp. 4273-4281, 2000.

[162] X. F. Huang, M. Hu, L. Y. He, and X. Y. Tang, "Chemical Characterization of Water-Soluble Organic Acids in PM2.5 in Beijing, China," *Atmospheric Environment,* vol. 39, pp. 2819-2827, May 2005.

[163] P. R. Haddad, "Comparison of ion chromatography and capillary electrophoresis for the determination of inorganic ions," *Journal of Chromatography A,* vol. 770, pp. 281-290, May 1997.

[164] W. L. Ding, M. J. Thornton, and J. S. Fritz, "Capillary Electrophoresis of Anions at High Salt Concentrations," *Electrophoresis,* vol. 19, pp. 2133-2139, Sep 1998.

[165] T. Tsuda, "Modification of Electroosmotic Flow with Cetyltrimethylammonium Bromide in Capillary Zone Electrophoresis," *Journal of High Resolution Chromatography & Chromatography Communications,* vol. 10, pp. 622-624, Nov 1987.

[166] M. T. Galceran, L. Puignou, and M. Diez, "Comparison of Different Electroosmotic Flow Modifiers in the Analysis of Inorganic Anions by Capillary Electrophoresis," *Journal of Chromatography A,* vol. 732, pp. 167-174, Apr 1996.

[167] M. A. Hayes and A. G. Ewing, "Electroosmotic Flow Control and Monitoring with an Applied Radial Voltage for Capillary Zone Electrophoresis," *Analytical Chemistry,* vol. 64, pp. 512-516, Mar 1992.

[168] N. A. Polson and M. A. Hayes, "Electroosmotic Flow Control of Fluids on A Capillary Electrophoresis Microdevice Using An Applied External Voltage," *Analytical Chemistry*, vol. 72, pp. 1088-1092, Mar 2000.

[169] M. F. M. Tavares, R. Colombara, and S. Massaro, "Modified Electroosmotic Flow by Cationic Surfactant Additives in Capillary Electrophoresis - Evaluation of Electrolyte Systems for Anion Analysis," *Journal of Chromatography A,* vol. 772, pp. 171-178, Jun 1997.

[170] K. I. Roy and C. A. Lucy, "Dielectric Friction in Capillary Electrophoresis: Mobility of Organic Anions in Mixed Methanol-Water Media," *Analytical Chemistry,* vol. 73, pp. 3854-3861, Aug 2001.

[171] C. Schwer and E. Kenndler, "Electrophoresis in Fused-Silica Capillaries-the Influence of Organic Solvents on the Electroosmotic Velocity and the Zeta Potential," *Analytical Chemistry,* vol. 63, pp. 1801-1807, Sep 1991.

[172] N. E. Baryla, J. E. Melanson, M. T. McDermott, and C. A. Lucy, "Characterization of surfactant coatings in capillary electrophoresis by atomic force microscopy," *Analytical Chemistry,* vol. 73, pp. 4558-4565, Oct 1 2001.

[173] J. E. Melanson, N. E. Baryla, and C. A. Lucy, "Double-chained surfactants far semipermanent wall coatings in capillary electrophoresis," *Analytical Chemistry,* vol. 72, pp. 4110-4114, Sep 1 2000.

[174] C. A. Lucy and R. S. Underhill, "Characterization of the cationic surfactant induced reversal of electroosmotic flow in capillary electrophoresis," *Analytical Chemistry,* vol. 68, pp. 300-305, Jan 15 1996.

[175] A. M. MacDonald, M. F. Bahnasy, and C. A. Lucy, "A Modified Supported Bilayer/diblock Polymer - Working towards A Tunable Coating for Capillary Electrophoresis," *Journal of Chromatography A,* vol. 1218, pp. 178-184, Jan 2011.

[176] "DX-120 Ion Chromatograph Operator`s Manual," Dionex Corporation September 1998 1998.

[177] D. C. Harris, "Statistics," in *Quantitative Chemical Analysis,* J. Fiorillo, Ed. New York: Clancy Marshall, 2010, p. 114.

[178] L. H. Mielke, A. Furgeson, and H. D. Osthoff, "Observation of ClNO2 in a Mid-Continental Urban Environment," *Environmental Science & Technology,* vol. 45, pp. 8889-8896, Oct 15 2011.

[179] A. E. Okeeffe and G. C. Ortman, "Primary Standards for Trance Gas Analysis," *Analytical Chemistry,* vol. 38, pp. 760-&, 1966.

[180] G. D. Mitchell, "A Review of Permeation Tubes and Permeators," *Separation and Purification Methods,* vol. 29, pp. 119-128, 2000.

[181] J. A. Neuman, T. B. Ryerson, L. G. Huey, R. Jakoubek, J. B. Nowak, C. Simons, and F. C. Fehsenfeld, "Calibration and Evaluation of Nitric Acid and Ammonia Permeation Tubes by UV Optical Absorption," *Environmental Science & Technology,* vol. 37, pp. 2975-2981, Jul 2003.

[182] R. Baziramakenga, R. R. Simard, and G. D. Leroux, "Determination of Organic Acids in Soil Extracts by Ion Chromatography," *Soil Biology & Biochemistry,* vol. 27, pp. 349-356, Mar 1995.

[183] M. J. Nozal, J. L. Bernal, J. C. Diego, L. A. Gomez, and M. Higes, "HPLC determination of low molecular weight organic acids in honey with series-coupled ion-exclusion columns," *Journal of Liquid Chromatography & Related Technologies,* vol. 26, pp. 1231-1253, 2003.

[184] Y. Xu, W. L. Wang, and S. F. Y. Li, "Simultaneous Determination of Low-Molecular-Weight Organic Acids and Chlorinated Acid Herbicides in Environmental Water by a Portable CE System with Contactless Conductivity Detection," *Electrophoresis,* vol. 28, pp. 1530-1539, May 2007.

[185] M. Fournier, J. Lesage, C. Ostiguy, and H. Van Tra, "Sampling and Analytical Methodology Development for the Determination of Primary and Secondary Low Molecular Weight Amines in Ambient Air," *Journal of Environmental Monitoring,* vol. 10, pp. 379-386, 2008.

[186] E. Dabek-Zlotorzynska and M. McGrath, "Determination of low-molecular-weight carboxylic acids in the ambient air and vehicle emissions: a review," *Fresenius Journal of Analytical Chemistry,* vol. 367, pp. 507-518, Jul 2000.

[187] F. J. Santos and M. T. Galceran, "Modem Developments in Gas Chromatography-Mass Spectrometry-Based Environmental Analysis," *Journal of Chromatography A,* vol. 1000, pp. 125-151, Jun 2003.

[188] C. Sarzanini and M. C. Bruzzoniti, "New Materials: Analytical and Environmental Applications in Ion Chromatography," *Analytica Chimica Acta,* vol. 540, pp. 45-53, May 2005.

[189] J. D. Pfaff, "Method 300.0 Determination of Inorganic Anions by Ion Chromatography," U. S. E. P. Agency, Ed. Cincinnati, Ohio, 1993.

[190] A. A. Okemgbo, H. H. Hill, W. F. Siems, and S. G. Metcalf, "Reverse Polarity Capillary Zone Electrophoretic Analysis of Nitrate and Nitrite in Natural Water Samples," *Analytical Chemistry,* vol. 71, pp. 2725-2731, Jul 1999.

[191] W. R. Jones and P. Jandik, "Controlled Changes of Selectivity in the Separation of Ions by Capillary Electrophoresis," *Journal of Chromatography,* vol. 546, pp. 445-458, Jun 21 1991.

[192] W. R. Jones and P. Jandik, "Various Approaches to Analysis of Difficult Sample Matrices of Anions Using Capillary Electrophoresis," *Journal of Chromatography,* vol. 608, pp. 385-393, Sep 1992.

[193] P. Doble and P. R. Haddad, "Indirect photometric detection of anions in capillary electrophoresis," *Journal of Chromatography A,* vol. 834, pp. 189-212, Feb 1999.

[194] C. Y. Tsai, Y. R. Chen, and G. R. Her, "Analysis of Triazines by Reversed Electroosmotic Flow Capillary Electrophoresis Electrospray Mass Spectrometry," *Journal of Chromatography A,* vol. 813, pp. 379-386, Jul 1998.

[195] S. A. Shamsi and N. D. Danielson, "Naphthalenesulfonates as Electrolytes for Capillary Electrophoresis of Inorganic Anions, Organic0acids, and Surfactants with Indirect Photometric Detection," *Analytical Chemistry,* vol. 66, pp. 3757-3764, Nov 1994.

[196] P. Doble, M. Macka, and P. R. Haddad, "Design of background electrolytes for indirect detection of anions by capillary electrophoresis," *Trac-Trends in Analytical Chemistry,* vol. 19, pp. 10-17, Jan 2000.

[197] F. Foret, S. Fanali, L. Ossicini, and P. Bocek, "Indirect Photometric Detection in Capillary Zone Electrophoresis," *Journal of Chromatography,* vol. 470, pp. 299-308, May 1989.

[198] F. E. P. Mikkers, F. M. Everaerts, and T. Verheggen, "Concentration Distributions in Free Zone Electrophoresis," *Journal of Chromatography,* vol. 169, pp. 1-10, 1979.

[199] S. Ghosal, "Electrokinetic flow and dispersion in capillary electrophoresis," in *Annual Review of Fluid Mechanics*. vol. 38 Palo Alto: Annual Reviews, 2006, pp. 309-338.

[200] C. Johns, M. Macka, and P. R. Haddad, "Indirect Photomeric Detection of Anions in Capillary Electrophoresis Using Dyes as Probes and Electrolytes Buffered with An Isoelectric Ampholyte," *Electrophoresis,* vol. 21, pp. 1312-1319, Apr 2000.

[201] P. Jandik and W. R. Jones, "Optimization of Detection Sensitivity in the Capillary Electrophoresis of Inorganic Anions

" *Journal of Chromatography,* vol. 546, pp. 431-443, Jun 1991.

[202] P. Doble, P. Andersson, and P. R. Haddad, "Determination and Prediction of Transfer Ratios for Anions in Capillary Zone Electrophoresis with Indirect UV Detection," *Journal of Chromatography A,* vol. 770, pp. 291-300, May 1997.

[203] M. Trevaskis and V. C. Trenerry, "An Investigation into the Determination of Oxalic Acid in Vegetables by Capillary Electrophoresis," *Food Chemistry,* vol. 57, pp. 323-330, Oct 1996.

[204] J. B. Kim, K. Otsuka, and S. Terabe, "Anion Selective Exhaustive Injection-Sweep-Micellar Electrokinetic Chromatography," *Journal of Chromatography A,* vol. 932, pp. 129-137, Oct 2001.

[205] G. V. Bol`shakov, V. S. Vatago, and F. B. Agrest, *Ultraviolet Absorption Spectra of Heteroorganic Compounds*: Chemistry, Leningrad Department, Leningrad, 1969.

[206] W. Buchberger, S. M. Cousins, and P. R. Haddad, "Optimization of Indirect UV Detection in Capillary Zone Electrophoresis of Low-Molecular-Mass Anions," *Trac-Trends in Analytical Chemistry,* vol. 13, pp. 313-319, Sep 1994.

[207] V. I. Esteves, S. S. F. Lima, D. L. D. Lima, and A. C. Duarte, "Using Capillary Electrophoresis for the Determination of Organic Acids in Port Wine," *Analytica Chimica Acta,* vol. 513, pp. 163-167, Jun 2004.

[208] S. Tomoyoshi and G. A. Ross, "Simultaneous Determination of Inorganic Anions, Organic Acids and Metal Cations by Capillary Electrophoresis," *Journal of Chromatography A,* vol. 834, pp. 65-71, Feb 1999.

[209] S. H. Yalkowsky and Y. He, *Handbook of Aqueous Solubility Data*. Boca Raton, Florida: CRC Press, 2003.

[210] S. A. Shamsi and N. D. Danielson, "Naphthalenesulfonates as Electrolytes for Capillary Electrophoresis of Inorganic Anions, Organic-acids, and Srfactants with Indirect Photometric Detection," *Analytical Chemistry,* vol. 66, pp. 3757-3764, Nov 1994.

[211] M. Macka, P. Andersson, and P. R. Haddad, "Changes in electrolyte pH due to electrolysis during capillary zone electrophoresis," *Analytical Chemistry,* vol. 70, pp. 743-749, Feb 1998.

[212] S. J. Gluck and J. A. Cleveland, "nvestigation of Experimental Approaches to the Determination of pKa Values by Capillary Electrophoresis," *Journal of Chromatography A,* vol. 680, pp. 49-56, Sep 1994.

[213] B. Gas, M. Stedry, and E. Kenndler, "Peak Broadening in Capillary Zone Electrophoresis," *Electrophoresis,* vol. 18, pp. 2123-2133, Nov 1997.

[214] M. A. Hayes, I. Kheterpal, and A. G. Ewing, "Effects of Buffer pH on Electroosmotic Flow Control by An Applied Radial Voltage for Capillary Zone Electrophoresis," *Analytical Chemistry,* vol. 65, pp. 2407-2407, Sep 1993.

[215] B. B. VanOrman, G. G. Liversidge, and G. L. McIntire, "Effects of Buffer Composition on Electroosmotic Flow in Capillary Electrophoresis," *Journal of Microcolumn Separation,* vol. 2, pp. 176-180, 1990.

[216] N. Fang, E. Ting, and D. D. Y. Chen, "Determination of Shapes and Maximums of Analyte Peaks Based on Solute Mobilitiess in Capillary Electrophoresis," *Analytical Chemistry,* vol. 76, pp. 1708-1714, Mar 2004.

[217] E. Kenndler and W. Friedl, "Adjustment of Resolution and Analysis Time in Capillary Zone Electrophoresis by Varying the pH of the Buffer," *Journal of Chromatography,* vol. 608, pp. 161-170, Sep 1992.

[218] J. M. Busnel, S. Descroix, D. Godfrin, M. C. Hennion, and G. Peltre, "Loading Capacity of Carrier Ampholytes Based Buffers in Capillary Electrophoresis," *Electrophoresis,* vol. 27, pp. 563-571, Feb 2006.

[219] A. V. Stoyanov and P. G. Righetti, "Fundamental Properties of Isoelectric Buffers for Capillary Zone Electrophoresis," *Journal of Chromatography A,* vol. 790, pp. 169-176, Nov 1997.

[220] J. L. Beckers, "Ampholytes as Background Electrolytes in Capillary Zone Electrophoresis: Sense or Nonsense? Histidine as A Model Ampholyte," *Electrophoresis,* vol. 24, pp. 548-556, Feb 2003.

[221] P. Doble, M. Macka, P. Andersson, and P. R. Haddad, "Buffered chromate electrolytes for separation and indirect absorbance detection of inorganic anions in capillary electrophoresis," *Analytical Communications,* vol. 34, pp. 351-353, Nov 1997.

[222] S. K. Wiedmer, M. Jussila, R. M. S. Hakala, K. H. Pystynen, and M. L. Riekkola, "Piperazine-Based Buffers for Liposome Coating of Capillaries for Electrophoresis," *Electrophoresis,* vol. 26, pp. 1920-1927, May 2005.

[223] S. J. O. Varjo, J. T. Hautala, S. K. Wiedmer, and M. L. Riekkola, "Small Diamines as Modifiers for Phosphatidylcholine/phosphatidylserine Coatings in Capillary Electrochromatography," *Journal of Chromatography A,* vol. 1081, pp. 92-98, Jul 2005.

[224] J. Kohr and H. Engelhardt, "Characterization of Quartz Capillaries for Capillary Electrophoresis," *Journal of Chromatography A,* vol. 652, pp. 309-316, Oct 1993.

[225] Z. E. Rassi and W. Nashabeh, "High Performance Capillary Electrophoresis of Carbohydrates and Glycconjugates," in *Carbohydrate Analysis-High Performance Liquid*

Chromatography and Capillary Electrophoresis, Z. E. Rassi, Ed. Amsterdam: Elsevier Science B.V., 1995, pp. 267-276.

[226] A. G. Diress and C. A. Lucy, "Electroosmotic Flow Reversal for the Determination of Inorganic Anions by Capillary Electrophoresis with Methanol-Water Buffers," *Journal of Chromatography A*, vol. 1027, pp. 185-191, Feb 2004.

[227] A. M. MacDonald and C. A. Lucy, "Highly efficient protein separations in capillary electrophoresis using a supported bilayer/diblock copolymer coating," *Journal of Chromatography A*, vol. 1130, pp. 265-271, Oct 2006.

[228] D. C. Harris, "Introduction to Analytical Separations," in *Quantitative Chemical Analysis*, J. Fiorillo, Ed. New York: Clancy Marshall, 2010, p. 552.

[229] Z. Krivacsy, A. Gelencser, J. Hlavay, G. Kiss, and Z. Sarvari, "Electrokinetic injection in capillary electrophoresis and its application to the analysis of inorganic compounds," *Journal of Chromatography A*, vol. 834, pp. 21-44, Feb 1999.

[230] B. Paull and M. King, "Quantitative capillary zone electrophoresis of inorganic anions," *Electrophoresis*, vol. 24, pp. 1892-1934, Jun 2003.

[231] X. H. Huang, M. J. Gordon, and R. N. Zare, "Bias in Quantitative Capillary Zone Electrophoresis Caused by Electrokinetic Sample Injection," *Analytical Chemistry*, vol. 60, pp. 375-377, Feb 15 1988.

[232] J. N. van der Moolen, H. F. M. Boelens, H. Poppe, and H. C. Smit, "Origin and correction of bias caused by sample injection and detection in capillary zone electrophoresis," *Journal of Chromatography A*, vol. 744, pp. 103-113, Sep 1996.

[233] Y. S. Fung and K. M. Lau, "Analysis of Organic Acids and Inorganic Anions in Beverage Drinks by Ccapillary Electrophoresis," *Electrophoresis,* vol. 24, pp. 3224-3232, Sep 2003.

[234] E. S. Yeung, "Indirect Detection Methods: Looking for What Is Not There," *Acc. Chem. Res.,* vol. 22, pp. 125-130, 1989.

[235] M. Macka and P. R. Haddad, "Determination of metal ions by capillary electrophoresis," *Electrophoresis,* vol. 18, pp. 2482-2501, Nov 1997.

[236] M. P. Harrold, M. J. Wojtusik, J. Riviello, and P. Henson, "Parameters Influencing Separation and Detection of Anions by Capillary Electrophoresis," *Journal of Chromatography,* vol. 640, pp. 463-471, Jun 1993.

[237] T. S. Wang and R. A. Hartwick, "Noise and Detection Limits of Indirect Absorption Detection in Capillary Zone Electrophoresis," *Journal of Chromatography,* vol. 607, pp. 119-125, Aug 1992.

[238] X. Xu, W. T. Kok, and H. Poppe, "Noise and baseline disturbances in indirect UV detection in capillary electrophoresis," *Journal of Chromatography A,* vol. 786, pp. 333-345, Oct 1997.

[239] H. Salimi-Moosavi, Y. T. Jiang, L. Lester, G. McKinnon, and D. J. Harrison, "A multireflection cell for enhanced absorbance detection in microchip-based capillary electrophoresis devices," *Electrophoresis,* vol. 21, pp. 1291-1299, Apr 2000.

[240] M. W. F. Nielen, "Quantitative Aspects of Indirect UV Detection in Capillary Zone Electrophoresis," *Journal of Chromatography,* vol. 588, pp. 321-326, Dec 1991.

[241] J. L. Beckers and P. Bocek, "Calibrationless quantitative analysis by indirect UV absorbance detection in capillary zone electrophoresis: The concept of the conversion factor," *Electrophoresis,* vol. 25, pp. 338-343, Jan 2004.

[242] P. E. Jackson and P. R. Haddad, "Optimization of Injection Technique in Capillary Ion Electrophoresis for the Determination of Trace-Level Anions in Environmental Samples," *Journal of Chromatography,* vol. 640, pp. 481-487, Jun 1993.

[243] C. W. Klampfl, "Analysis of Organic Acids and Inorganic Anions in Different Types of Beer Using Capillary Zone Electrophoresis," *Journal of Agricultural and Food Chemistry,* vol. 47, pp. 987-990, Mar 1999.

[244] M. C. Breadmore and P. R. Haddad, "Approaches to Enhancing the Sensitivity of Capillary Electrophoresis Methods for the Determination Inorganic and Small Organic Anions," *Electrophoresis,* vol. 22, pp. 2464-2489, Aug 2001.

[245] A. Weston, P. R. Brown, P. Jandik, W. R. Jones, and A. L. Heckenberg, "Factors Affecting the Separation of Inorganic Metal Cations by Capillary Electrophoresis," *Journal of Chromatography,* vol. 593, pp. 289-295, Feb 1992.

[246] A. Febo, C. Perrino, and I. Allegrini, "Measurement of nitrous acid in Milan, Italy, by DOAS and diffusion denuders," *Atmospheric Environment,* vol. 30, pp. 3599-3609, Nov 1996.

[247] R. B. Norton, "Measurements of Gas Phase Formic and Acetic Acids at the Mauna Loa, Obsevatory, Hawaii during the Mauna Loa Observatory Photochemistry Experiment 1988," *Journal of Geophysical Research-Atmospheres,* vol. 97, pp. 10389-10393, Jun 1992.

[248] W. R. Cofer, V. G. Collins, and R. W. Talbot, "Improved Aqueous Scrubber for Collection of Soluble Atmospheric Trace Gases," *Environmental Science & Technology,* vol. 19, pp. 557-560, 1985.

[249] R. S. Spaulding, R. W. Talbot, and M. J. Charles, "Optimization of a mist chamber (cofer scrubber) for sampling water-soluble organics in air," *Environmental Science & Technology,* vol. 36, pp. 1798-1808, Apr 15 2002.

[250] W. C. Keene, J. R. Maben, A. A. P. Pszenny, and J. N. Galloway, "Measurement Technique for Inorganic Chlorine Gases in the Marine Boundary-layer," *Environmental Science & Technology,* vol. 27, pp. 866-874, May 1993.

[251] W. C. Keene and D. L. Savoie, "The pH of Deliquesced Sea-salt Aerosol in Polluted Marine Air," *Geophysical Research Letters,* vol. 25, pp. 2181-2184, Jun 1998.

[252] W. J. Stratton and S. E. Lindberg, "Use of A Refluxing Mist Chamber for Measurement of Gas-phase Mercury(II) Species in the Atmosphere," *Water Air and Soil Pollution,* vol. 80, pp. 1269-1278, Feb 1995.

[253] R. W. Talbot, J. E. Dibb, E. M. Scheuer, D. R. Blake, N. J. Blake, G. L. Gregory, G. W. Sachse, J. D. Bradshaw, S. T. Sandholm, and H. B. Singh, "Influence of Biomass Combustion Emissions on the Distribution of Acidic Trace Gases over the Southern Pacific Basin during Austral Springtime," *Journal of Geophysical Research-Atmospheres,* vol. 104, pp. 5623-5634, Mar 1999.

[254] H. Destaillats and M. J. Charles, "Henry's law constants of carbonyl-pentafluorobenzyl hydroxylamine (PFBHA) derivatives in aqueous solution," *Journal of Chemical and Engineering Data,* vol. 47, pp. 1481-1487, Nov-Dec 2002.

[255] R. W. Talbot, E. M. Scheuer, B. L. Lefer, and W. T. Luke, "Measurements of sulfur dioxide during GASIE with the mist chamber technique," *Journal of Geophysical Research-Atmospheres,* vol. 102, pp. 16273-16278, Jul 1997.

[256] B. L. Lefer, R. W. Talbot, and J. W. Munger, "Nitric Acid and Ammonia at A Rural Northeastern US Site," *Journal of Geophysical Research-Atmospheres,* vol. 104, pp. 1645-1661, Jan 1999.

[257] M. S. Landis, R. K. Stevens, F. Schaedlich, and E. M. Prestbo, "Development and characterization of an annular denuder methodology for the measurement of divalent inorganic reactive gaseous mercury in ambient air," *Environmental Science & Technology,* vol. 36, pp. 3000-3009, Jul 2002.

[258] W. C. Keene, R. W. Talbot, M. O. Andreae, K. Beecher, H. Berresheim, M. Castro, J. C. Farmer, J. N. Galloway, M. R. Hoffmann, S. M. Li, J. R. Maben, J. W. Munger, R. B. Norton, A. P. Pszenny, H. Puxbaum, H. Westberg, and W. Winiwarter, "An Intercomparison of Measurement Systems for Vapor and Particulate Phase Concentrations of Formic and Acetic Acids," *Journal of Geophysical Research-Atmospheres,* vol. 94, pp. 6457-6471, May 1989.

[259] T. Morikami, S. Tanaka, Y. Hashimoto, T. Inomata, and Y. Hanaoka, "An Automatic System for the Measurement of Carboxylic Acids (HCOOH, CH_3COOH) in the Urban Atmosphere by Combination of An Aqueous Mist Chamber and Ion Exclusion Chromatography," *Analytical Sciences,* vol. 7, p. 1033, 1991.

[260] W. J. Stratton, S. E. Lindberg, and C. J. Perry, "Atmospheric mercury speciation: Laboratory and field evaluation of a mist chamber method for measuring reactive gaseous mercury," *Environmental Science & Technology,* vol. 35, pp. 170-177, Jan 2001.

[261] R. W. Talbot, J. E. Dibb, B. L. Lefer, E. M. Scheuer, J. D. Bradshaw, S. T. Sandholm, S. Smyth, D. R. Blake, N. J. Blake, G. W. Sachse, J. E. Collins, and G. L. Gregory, "Large-Scale Distributions of Tropospheric Nitric, Formic, and Acetic Acids Over the Western Pacific Basin during Wintertime," *Journal of Geophysical Research-Atmospheres,* vol. 102, pp. 28303-28313, Dec 1997.

[262] J. J. Schultztokos, S. Tanaka, T. Morikami, H. Shigetani, and Y. Hashimoto, "Gaesous Formic and Acetic Acids in the Atmosphere of Yokohama, Japan," *Journal of Atmospheric Chemistry,* vol. 14, pp. 85-94, Apr 1992.

[263] R. S. Parmar, G. S. Satsangi, A. Lakhani, S. S. Srivastava, and S. Prakash, "Simultaneous Measurements of Ammonia and Nitric Acid in Ambient Air at Agra (27 degrees 10 ' N and 78 degrees 05 ' E) (India)," *Atmospheric Environment,* vol. 35, pp. 5979-5988, Dec 2001.

[264] G. F. Knoll, "Radiation Detection and Measurement," Hoboken: John Wiley & Sons. Inc., 2010.

[265] J. R. Taylor, *An Introduction to Error Analysis: the Study of Uncertainties in Physical Measurements-2nd edition*. Sausalito, CA: University Science Books, 1997.

[266] Y. N. Lee and X. L. Zhou, "Method for the Determination of Some Soluble Atmospheric Carbonyl Compounds," *Environmental Science & Technology,* vol. 27, pp. 749-756, Apr 1993.

[267] L. R. Williams and D. M. Golden, "Solubility of HCl in Sulfuric Acid at Stratospheric Temperatures," *Geophysical Research Letters,* vol. 20, pp. 2227-2230, Oct 1993.

[268] G. F. Zhang, A. David, and T. S. Wiedmann, "Performance of the Vibrating Membrane Aerosol Generation Device: Aeroneb Micropump Nebulizer (TM)," *Journal of Aerosol Medicine-Deposition Clearance and Effects in the Lung,* vol. 20, pp. 408-416, Win 2007.

[269] W. C. Keene, J. N. Galloway, and J. D. Holden, "Measurement of Weak Organic Acidity in Precipitation from Remote Areas of the World," *Journal of Geophysical Research-Oceans and Atmospheres,* vol. 88, pp. 5122-5130, 1983.

[270] B. J. Finlayson-Pitts and J. N. Pitts, *Chemistry of the upper and lower atmosphere*. San Diego: Academic Press, 2000.

[271] G. F. Zhang, S. Slanina, C. B. Boring, P. A. C. Jongejan, and P. K. Dasgupta, "Continuous Wet Denuder Measurements of Atmospheric Nitric and Nitrous Acids during the 1999 Atlanta Supersite," *Atmospheric Environment,* vol. 37, pp. 1351-1364, Mar 2003.

[272] D. R. Benson, A. Markovich, M. Al-Refai, and S. H. Lee, "A Chemical Ionization Mass Spectrometer for ambient measurements of Ammonia," *Atmospheric Measurement Techniques,* vol. 3, pp. 1075-1087, 2010.

[273] L. Gronberg, Y. Shen, and J. A. Jonsson, "Ion-chromatographic Determiantion of Carboxylic-acids in Air with Online Liquid Membrane Pretreatment," *Journal of Chromatography A,* vol. 655, pp. 207-215, Dec 1993.

[274] A. Rohrl and G. Lammel, "Determination of Malic Acid and Other C_4 Dicarboxylic Acids in Atmospheric Aerosol Samples," *Chemosphere,* vol. 46, pp. 1195-1199, Mar 2002.

[275] Y. Wang, G. S. Zhuang, S. Chen, Z. S. An, and A. H. Zheng, "Characteristics and Sources of Formic, Acetic and Oxalic Acids in $PM_{2.5}$ and PM_{10} Aerosols in Beijing, China," *Atmospheric Research,* vol. 84, pp. 169-181, Apr 2007.

[276] D. A. Hegg, S. Gao, and H. Jonsson, "Measurements of Selected Dicarboxylic Acids in Marine Cloud Water," *Atmospheric Research,* vol. 62, pp. 1-10, May 2002.

[277] H. Aufmhoff, M. Hanke, J. Uecker, H. Schlager, and F. Arnold, "An Ion Trap CIMS Instrument for Combined Measurements of Atmospheric OH and H2SO4: First Test Measurements above and Inside the Planetary Boundary Layer," *International Journal of Mass Spectrometry,* vol. 308, pp. 26-34, Nov 2011.

[278] A. Kurten, L. Rondo, S. Ehrhart, and J. Curtius, "Calibration of a Chemical Ionization Mass Spectrometer for the Measurement of Gaseous Sulfuric Acid," *Journal of Physical Chemistry A,* vol. 116, pp. 6375-6386, Jun 2012.

[279] V. Barwick, J. Langley, T. Mallet, B. Stein, and K. Webb, "Best Practice Guide for Generating Mass Spectra," in *Best Practice Guide for Generating Mass Spectra* Teddington, Middlesex: LGC, 2006.

[280] J. Brito and A. Zahn, "An Unheated Permeation Device for Calibrating Atmospheric VOC Measurements," *Atmospheric Measurement Techniques,* vol. 4, pp. 2143-2152, 2011.

[281] C. Jost, "Calibration with Permeation Devices: Is There A Pressure Dependence of the Permeation Rates?," *Atmospheric Environment,* vol. 38, pp. 3535-3538, Jul 2004.

[282] O. Abida, L. H. Mielke, and H. D. Osthoff, "Observation of Gas-Phase Peroxynitrous and Peroxynitric Acid during the Photolysis of Nitrate in Acidified Frozen Solutions," *Chemical Physics Letters,* vol. 511, pp. 187-192, Aug 2011.

[283] K. Kita, Y. Morino, Y. Kondo, Y. Komazaki, N. Takegawa, Y. Miyazaki, J. Hirokawa, S. Tanaka, T. L. Thompson, R. S. Gao, and D. W. Fahey, "A chemical ionization mass spectrometer for ground-based measurements of nitric acid," *Journal of Atmospheric and Oceanic Technology,* vol. 23, pp. 1104-1113, Aug 2006.

[284] T. Jurkat, C. Voigt, F. Arnold, H. Schlager, H. Aufmhoff, J. Schmale, J. Schneider, M. Lichtenstern, and A. Dornbrack, "Airborne Stratospheric ITCIMS Measurements of SO2, HCl, and HNO3 in the Aged Plume of Volcano Kasatochi," *Journal of Geophysical Research-Atmospheres,* vol. 115, p. 14, Nov 2010.

[285] M. A. Zondlo, R. L. Mauldin, E. Kosciuch, C. A. Cantrell, and F. L. Eisele, "Development and Characterization of an Airborne-Based Instrument Used to Measure Nitric Acid during the NASA Transport and Chemical Evolution over the Pacific Field Experiment," *Journal of Geophysical Research-Atmospheres,* vol. 108, p. 18, Sep 2003.

[286] S. A. Shamsi, N. D. Danielson, and I. M. Warner, "Flavin Mononucleotide for Indirect Laser-Induced Fluorescence Detection of Anions Separated by Capillary Electrophoresis," *Journal of Chromatography A,* vol. 835, pp. 159-168, Mar 1999.

[287] T. Soga, Y. Ueno, H. Naraoka, K. Matsuda, M. Tomita, and T. Nishioka, "Pressure-Assisted Capillary Electrophoresis Electrospray Ionization Mass Spectrometry for Analysis of Multivalent Anions," *Analytical Chemistry,* vol. 74, pp. 6224-6229, Dec 2002.

[288] H. Lord and J. Pawliszyn, "Evolution of Solid-Phase Microextraction Technology," *Journal of Chromatography A,* vol. 885, pp. 153-193, Jul 2000.

[289] Z. Q. Xu, T. Doi, A. R. Timerbaev, and T. Hirokawa, "Sensitive Determination of Anions in Saliva Using Capillary Electrophoresis after Transient Isotachophoretic Preconcentration," *Talanta,* vol. 77, pp. 278-281, Oct 2008.

[290] M. C. Breadmore and J. P. Quirino, "100,000-Fold Concentration of Anions in Capillary Zone Electrophoresis Using Electroosmotic Flow Controlled Counterflow Isotachophoretic Stacking under Field Amplified Conditions," *Analytical Chemistry,* vol. 80, pp. 6373-6381, Aug 2008.

[291] J. P. Quirino and S. Terabe, "Sample Stacking of Fast-Moving Anions in Capillary Zone Electrophoresis with pH-Suppressed Electroosmotic Flow," *Journal of Chromatography A,* vol. 850, pp. 339-344, Jul 1999.

[292] D. J. Rose and J. W. Jorgenson, "Characterization and Automation of Sample Introduction Methods for Capillary Zone Electrophoresis," *Analytical Chemistry,* vol. 60, pp. 642-648, Apr 1988.

[293] V. Dolnik, S. R. Liu, and S. Jovanovich, "Capillary Electrophoresis on Microchip," *Electrophoresis,* vol. 21, pp. 41-54, Jan 2000.